

# **Correlation of Mesozoic Strata in Northern Vancouver Island to West Coast Sedimentary Basins**

**by  
Alec Sproule**

B.Sc. (Geology), University of Texas of the Permian Basin, 2018

A.A. (Liberal Arts and Sciences), Potomac State College of West Virginia  
University, 2016

Thesis Submitted in Partial Fulfillment of the  
Requirements for the Degree of  
Master of Science

in the  
Department of Earth Sciences  
Faculty of Science

© Alec Sproule 2024  
SIMON FRASER UNIVERSITY  
Summer 2024

Copyright in this work is held by the author. Please ensure that any reproduction or re-use is done in accordance with the relevant national copyright legislation.

## **Declaration of Committee**

**Name:** Alec Sproule

**Degree:** Master of Science

**Title:** Correlation of Mesozoic strata in Northern  
Vancouver Island to West Coast Sedimentary  
Basins

**Committee:**

**Chair: Reid Staples**  
Lecturer, Earth Sciences

**Shahin E. Dashtgard**  
Supervisor  
Professor, Earth Sciences

**James A. MacEachern**  
Committee Member  
Professor, Earth Sciences

**H. Daniel Gibson**  
Committee Member  
Professor, Earth Sciences

**Jennifer M. Galloway**  
Examiner  
Researcher  
Geological Survey Canada

## **Abstract**

Mesozoic sedimentary strata exposed throughout Northern Vancouver Island (NVI), British Columbia, Canada records periods of deposition from the Triassic to the Paleogene. Sections of these strata have been correlated to west coast sedimentary basins based on lithological and sparse biostratigraphic evidence found therein. However, the ages of many outcrops remain poorly constrained. This study utilises multiple datasets; palynology, biostratigraphy, and detrital zircon geochronology to assign and refine ages assigned to seven stratigraphic intervals across Northern Vancouver Island. A new chronostratigraphic chart for Northern Vancouver Island is presented and Mesozoic and younger strata are correlated to contemporaneous strata within and below Canada's other west coast sedimentary basins. From these data, it is determined that NVI strata record deposition in both the Queen Charlotte Basin, and the Georgia Basin at different times.

**Keywords:** Sedimentology; Biostratigraphy; Palynology; Geochronology; Queen Charlotte Basin; Georgia Basin

## **Dedication**

This thesis is dedicated to three people without whom I would not be in a position to begin and complete this work, nor would I be the person I am today. My parents, David and Meredith Sproule who instilled in me from a young age the importance of education and of always trying to learn and grow, in all parts of my life. They fostered my curiosity and later my passion for science, which has taken me all over the world and allowed me to study my longest held passion. My grandmother, Mary O'Donoghue who encouraged me, and sacrificed so much, to help me chase my dream of studying rocks. She isn't here to see the completion of this work, but I like to think she would be proud of how far I have come.

## Acknowledgements

The work presented in this thesis is the outcome of the hard work and dedication of a significant number of people who I would like to thank for their time, passion, and effort. Firstly, Dr. Shahin Dashtgard, my supervisor, without whom this work would not have been possible. Throughout the process of writing this thesis, Shahin has been a patient, insightful and supportive mentor, allowing me to conduct this work in a way that developed my fieldwork, research, writing, and presentation skills. His passion and dedication as a geologist has been inspiring to work with and Shahin has set the bar for what it means to be a dedicated and driven scientist. I will always remain grateful for the opportunities Shahin has provided for me to start my life in Canada, develop further through my research and education, and follow my passion for geology to the furthest extent.

Next, I would like to thank Dr. James MacEachern, who's expertise has been an invaluable resource during the completion of this work. James has provided insight and perspective into aspects of this project without which, many of the interpretations and conclusions I have drawn would not have been possible. I have had my eyes opened to the wonderful world of ichnology and its many uses interpreting aspects of deposition and paleogeography. James' detail driven approach has improved my ability to focus on precision and accuracy in field work, lab work, and writing. I would like to thank him for his patience in analysing every fieldwork photo with possible trace fossils, and for his work helping to edit my thesis.

I would also like to thank Dr. H Daniel Gibson, who's expertise in structural geology and knowledge of the development of the Canadian Cordillera have shown me ways in which small elements of a project can have much bigger picture implications than I was aware of. Spending time in the field with Dan, and through working in his lab, I have been able to develop interpretive skills and techniques which have helped me to be sure that my work is thorough and robust. Dan also provided the skills and materials for processing detrital zircon samples, which have been instrumental in completing this work.

The work in this thesis would not have been possible without Gwyneth CathylBickford. Gwyneth, from the very beginning of this project has shared her

expertise on Nanaimo group, and North Vancouver Island sedimentary strata. From outcrop locations, and historical data which would otherwise have been unknown to me, to her expertise on coal geology, Gwyneth has been a fundamental part of ensuring that all avenues of investigation could be completed for this work.

I would like to thank the Quatsino First Nation for their support in completing this project and for access to their lands and facilities. Much of this work would not have been possible without access to their time, resources and knowledge during the challenging times that COVID-19 presented. Thanks to James Redford, Quatsino First Nation Lands Manager for taking the time to allow me to utilise the lands and facilities.

I owe much of the successful completion of this work to Chuqiao Huang. Throughout this project, Chu has been a fieldwork assistant, housemate, colleague, confidant, editor, and friend. From helping me to identify sedimentary structures on miserable, cold, windy days on beaches in the remote northern Vancouver Island, to providing me with feedback on parts of my writing, this project would have been impossible without him. Chu also provided much of the geochronologic data for this project and has allowed me to use his knowledge and expertise to process and interpret the data and results which form the backbone of much of this work. Chu's insights and dedication to his work have inspired me to become a better research scientist, and I would like to thank him for his time, effort, and camaraderie.

I would like to extend my thanks to all the SFU Earth Sciences staff who have helped me in innumerable ways during this project. Tarja Vaisanen, Matt Plotnikoff, Elilan Ganesathas, Alyssa Hamilton-Messenger and Lorena Munoz have assisted me in everything from applying for and maintaining my visa, to microscope photography, to preparing and loading vehicles for fieldwork. The Earth Sciences department at SFU is staffed by incredible people who do an amazing amount of work both in the open and behind the scenes. I would like to thank Mike Ranger, who supplied the Applecore software through James MacEachern, which was used in this thesis. I would also like to thank all of my friends and colleagues at SFU for their feedback and support throughout my time here. Thank you to Amy Hsieh, Kristian Giroto, Maziyar Nazemi, Eric Schmidtke, Rob Rondeau, and Kevin Cameron to name but a few.

Finally, I would like to thank my fiancé, the most important rock in my life, Cleo Bisanz. Without you I would not have had the ability or the perseverance to complete this work. This project has taken longer than I had first planned and throughout, you have been supportive, both financially and emotionally, you have gone above and beyond what anybody could reasonably have asked, and you have carried us through these last few years. You kept me up during some low periods and you have shown me what it takes to work hard for the things that matter. With you by my side, I feel like I can do anything, and this thesis is a testament to that.

# Table of Contents

Declaration of Committee.....	ii
Abstract.....	iii
Dedication.....	iv
Acknowledgements.....	v
Table of Contents.....	viii
List of Tables.....	x
Chapter 1. Introduction.....	1
1.1. West-Coast Basins – Geography and Ages.....	2
1.2. Lithostratigraphy and genetic stratigraphy of Canada’s west-coast sedimentary basins.....	5
1.2.1. Queen Charlotte Basin.....	5
1.2.2. Georgia Basin.....	9
1.2.3. Northern Vancouver Island (NVI).....	15
1.3. Biostratigraphy of Canada’s west-coast sedimentary basins.....	16
1.3.1. Macrofossil biostratigraphy.....	16
1.3.2. Microfossil biostratigraphy.....	19
1.4. Chronostratigraphy.....	21
1.5. Research Goals/Questions.....	27
1.6. Study Area and Methods.....	27
Chapter 2. Methods and Data.....	30
2.1. Introduction.....	30
2.2. Palynology.....	31
2.3. Detrital Zircon.....	33
2.4. Mesozoic Data Comparison for North Vancouver Island Strata.....	38
2.4.1. Triassic Strata.....	38
2.4.2. Jurassic Strata.....	42
2.4.3. Lower Cretaceous Strata.....	45
2.4.4. Upper Cretaceous and Younger Strata.....	48
Chapter 3. Discussion.....	75
3.1. Assessment and Discussion of Dating Techniques.....	75
3.1.1. Parsons Bay Formation.....	75
3.1.2. Hashamu Creek Strata.....	79
3.1.3. Lower Cretaceous Strata.....	80
3.1.4. Upper Cretaceous and Younger Strata.....	82
Fort Rupert Beach.....	83
Suquash Coal Mine.....	84
Orca Gravel Loader.....	86
Port McNeill.....	87
3.2. Relation of NVI strata to West-Coast Sedimentary Basins.....	88
3.3. Suquash Outcrop Area Stratal Architecture.....	91
Chapter 4. Conclusions.....	96
4.1. Do Northern Vancouver Island Mesozoic Strata Lying Stratigraphically Below the Suquash Outcrop Area Reflect a History of Sedimentation Within One or More Sedimentary Basins?.....	96



4.2. What is the Depositional History of Upper Cretaceous to Danian Strata in the Suquash Outcrop Area, and do those Strata Share a Basin Evolutionary History with Either the Georgia Basin or the Queen Charlotte Basin? .....	99
4.3. Future Work .....	102
References .....	104
Appendix A. Logged Outcrop Sections.....	113

## List of Tables

Table 1.1	Maximum depositional ages of samples analyzed by Dorsey (2019). Ages are calculated using the Y3Zo approach ..... 22
Table 2.1.	Palynology results from northern Vancouver Island (data from Galloway et al., 2023). Table contents include sample name used in this study; GSC curation number; stratigraphic unit assignment based on the presently established lithostratigraphy; lithology and stratigraphic height (where available); palynological and dinocyst ages, and comments. .... 34
Table 2.2.	Detrital zircon data from this study and from Huang (pers. comm., 2024). Ages recorded by the table are given as Youngest Grain Cluster with 1 $\sigma$ overlap (YGC1 $\sigma$ ), and Youngest Grain Cluster with 2 $\sigma$ overlap (YSG2 $\sigma$ ). The total number of zircon in each sample as well as the number of grains used to calculate YGC1 $\sigma$ and YSG2 $\sigma$ MDAs are indicated by “(n=#)” after each age. All ages are presented in mega-annum (Ma) and uncertainties are presented at the 2-sigma level. .... 36
Table 2.3.	Outcrop locations where measured sections were described at Fort Rupert Beach (FRB). Table includes outcrop location data, bedding orientation, and the location and stratigraphic position of samples taken within each section. A map of outcrop locations relative to one other and to Vancouver Island is shown in Figure 2.12. .... 51
Table 2.4.	List of measured outcrop sections and samples from the Suquash Coal Mine (SQM) site. Location data as well as bedding orientations for outcrop sections are included. Sample data include location as well as stratigraphic height within the relevant measured section. .... 55
Table 2.5.	List of measured outcrop sections and samples from the Orca Gravel Loader (OGL) site. Location data as well as bedding orientations for outcrop sections are included. Sample data include location as well as stratigraphic height within the relevant measured section. .... 66
Table 2.6.	List of measured outcrop sections and samples from the Port McNeil (PMO) site. Location data as well as bedding orientations for outcrop sections are included. Sample data include location as well as stratigraphic height within the relevant measured section. .... 71

# Chapter 1.

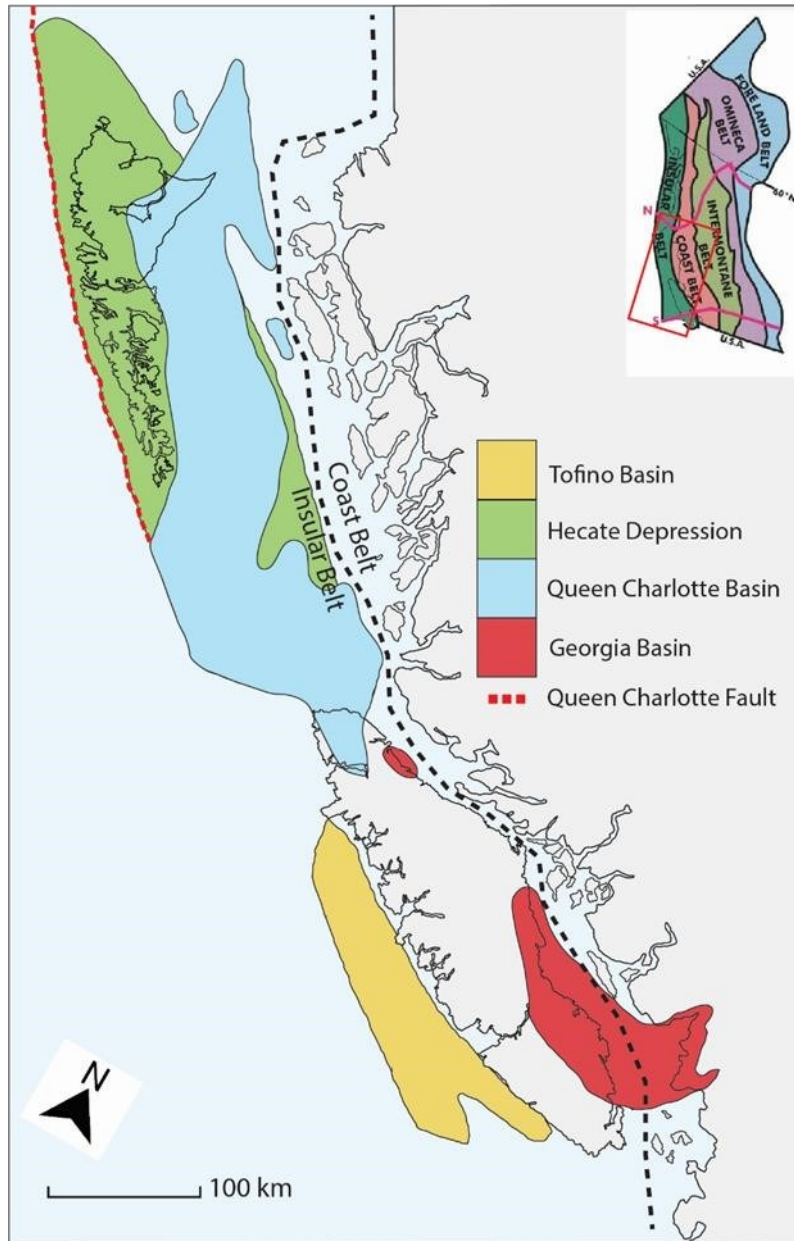
## Introduction

Canada's west coast hosts several sedimentary basins, including the Georgia Basin (GB), Queen Charlotte Basin (QCB), Tofino Basin, and Hecate Depression (Figure 1.1). The areal extent of these basins is poorly constrained, however, and in northern Vancouver Island sedimentary strata have been ascribed to both the GB and QCB. The GB, QCB and intervening strata are the focus of this study, with the aim of determining the spatial and temporal relationships between sedimentary units in northern Vancouver Island and those in both the GB and QCB. The strata of the Suquash Sub-Basin (Upper Cretaceous, northern Vancouver Island) have been related to the evolution of the GB, but no model has been developed showing a direct relationship. Alternatively, these strata may comprise part of the QCB; strata attributed to the QCB have been identified stratigraphically below the Suquash Sub-Basin. Strata equivalent in age to those below the Suquash OA in NVI also occur below the GB. Resolving the relation of northern Vancouver Island strata to the GB and QCB is the focus of this thesis.

The ages of strata assessed herein are derived from detrital zircon geochronology and palynology. These ages are compared to stratal ages presented in the detailed genetic stratigraphic framework developed recently for the GB (Huang et al. 2019; Kent et al. 2018; Giroto et al. 2024) and to the lithostratigraphic framework and biostratigraphic ages available for the QCB (Haggart et al. 2009; Shellnutt & Dostal 2019; Alberts et al. 2021). Through these comparisons, I aim to constrain the geographic extent of two of Canada's west-coast basins, which in turn will enable comparisons of time-equivalent strata therein. Finally, by evaluating the Lower Cretaceous strata of the Longarm Formation (Ludvigsen & Beard 1994; Lowe et al. 2002; Nixon & Orr 2010) and older strata of northern Vancouver Island, this study aims to reconcile the depositional histories and geographical displacements of the GB and QCB throughout the Mesozoic. This will allow for a greater understanding of the depositional history of the North American west coast, and the long-lived and varied sedimentary basins hosted along it.

## 1.1. West-Coast Basins – Geography and Ages

The Canadian Cordillera extends over 1.6 million km<sup>2</sup>, from northernmost Yukon to Canada's southern border and up to 1000 km east from the subduction and transform plate boundaries along the western North American continental margin to the Cordilleran deformation front within Alberta, British Columbia, Yukon and Northwest Territories. The Canadian Cordillera comprises 5 geomorphological belts that each exhibit a distinct geological character and tectonic history. Within the western Canadian Cordillera are a series of sedimentary basins, and these basins mainly overlie the Insular Belt (also known as the Insular Superterrane) and partly overlie the Coast Belt (Figure 1.1). From Middle Jurassic to Early Cretaceous time, the Insular Belt accreted to the western margin of North America. This belt comprises allochthonous terranes with a shared tectonic history (Monger et al. 1982). Prior to, and following accretion of the Insular belts onto the North American Craton, eastward subduction of material below the Insular Belt resulted in the formation of the Coast Plutonic Complex (CPC) (Monger et al. 1982; Gehrels et al. 2009). From Late Cretaceous to possibly Eocene time the Insular Belt and parts of the Coast Belt, including the CPC, translated northward to their present positions, due to north oblique convergence between the North America craton and the oceanic plates within the ancestral Pacific basin (Monger et al. 1982; Monger and Price 2002). The total amount of northward translation remains hotly debated (e.g., Irving et al., 1995; Cowan et al., 1997; Mahoney et al., 1999, 2021; Housen et al., 1999; Butler et al., 2001; Wylde et al., 2006; Matthews et al., 2017).



**Figure 1.1** Map of Canada's west coast, showing the approximate extents of the Georgia Basin, Queen Charlotte Basin, Hecate Depression, and Tofino Basin (after Wheeler et al. 1996 and Huang et al. 2019). The black dashed line demarcates the boundary between the Coast Belt and Insular Belt of the Canadian Cordillera. Figure modified, and insert map from Monger and Price (2002).

The Coast Belt contains Late Paleozoic through to Tertiary plutonic rocks and sedimentary strata with moderate- to high-grade metamorphism and a complex Late

Mesozoic–Early Cenozoic deformation history (Monger et al. 1982; Monger & Price 2002). The Insular Belt is composed of: 1) Paleozoic to Mesozoic volcanics and related sedimentary strata derived from primarily island arc settings; 2) Late Mesozoic to Tertiary clastics derived from the weathering of the Coast Belt; and 3) Middle Mesozoic to Holocene accretionary complexes (Monger et al. 1982; Monger & Price 2002). The Insular Belt has undergone periods of deformation beginning in the Paleozoic, with significant deformation occurring mainly from the Late Cretaceous to Holocene. Paleozoic- through to Tertiary-aged granitic intrusions also penetrate the Insular Belt (Monger et al. 1982).

The southern Insular Belt forms the basement over which the QCB and GB are situated. Wrangellia terrane comprises a large portion of the southern Insular Belt and is composed of Paleozoic to Jurassic volcanics and Triassic tholeiitic basalt flows overlain by Jurassic carbonates (Monger et al. 1982; Monger & Price 2002). The QCB and GB represent long-lasting sedimentary basins that presumably received sediment from exposures of underlying Wrangellia and from more distal sources, including the Coast Belt and rocks residing farther east (Monger et al. 1982; Mustard 1994; Mahoney et al. 1999; Huang et al. 2019; Mahoney et al. 2021).

The Queen Charlotte Basin extends over approximately 40,000 km<sup>2</sup> and comprises Late Triassic to Neogene units deposited on Wrangellia. The QCB is located ~300 km northwest of the GB (Figure 1.1) and sedimentary strata in the QCB outcrop on Haida Gwaii and possibly on northern Vancouver Island marking its southern extent (Bustin 1997; Haggart et al. 2009). The QCB is approximately 400 km long and over 100 km wide at its widest point. It is bounded to the west by the transform Queen Charlotte Fault and to the east by the Coast Belt of the Canadian Cordillera (Figure 1.1; Bustin 1997). The basin encompasses many of the islands of Haida Gwaii along its northern extent, and much of the Queen Charlotte Strait.

The Georgia Basin is situated south of the QCB and overlies the boundary between the Coast and Insular belts within the southwestern Canadian Cordillera. It is commonly referred to as a forearc basin (Mustard 1994; Bain & Hubbard 2016; Matthews et al. 2017; Coutts et al. 2019; Kent et al. 2020) based on its position between the CPC to the east and the Cascadia subduction zone to the west. Georgia Basin sedimentary strata crop out primarily across eastern Vancouver Island and along the mainland on

either side of the Canada-US border. Georgia Basin strata unconformably overlie basement rocks in all areas (Huang et al. 2019). The GB has been divided into 5 sub-basins: Comox, Nanaimo, Suquash, Chuckanut and Whatcom; however, these subbasins are better described as outcrop areas (Giroto et al. 2024) and will be referred to as such herein. The strata hosted within the Comox, Nanaimo, and Suquash outcrop areas are Cretaceous in age and Tertiary age in the Chuckanut and Whatcom OAs (Muller & Jeletzky 1970; Bickford and Kenyon 1988; Kent et al. 2020).

## **1.2. Lithostratigraphy and genetic stratigraphy of Canada's west-coast sedimentary basins**

### **1.2.1. Queen Charlotte Basin**

Early evaluations of the geology of the Queen Charlotte Islands (now Haida Gwaii) were undertaken to map the distribution of significant mineral and coal deposits, and then to assess the hydrocarbon potential of sedimentary strata throughout the QCB (Stacey 1975; Bustin 1997). The development of a lithostratigraphic framework for QCB strata (Figure 1.2) has been ongoing since Richardson (1878) first described three distinct “coal-bearing units” on Graham Island (Haggart 1987). No genetic stratigraphic framework exists for the basin.

The basement of the Mesozoic succession on Haida Gwaii is the spatially extensive Karmutsen Formation (Fm), which comprises several stages of Upper Triassic flood basalt represented by multiple massive basaltic flows, pillow lavas and brecciated intervals, capped by minor argillite and limestone (Haggart et al. 2009; Shellnutt & Dostal 2019; Alberts et al. 2021). Conformably overlying the Karmutsen Fm is the Late Triassic to Early Jurassic Kunga Group, which comprises both clastic and shelf carbonate units. These are divided into the Sadler Limestone, Peril Fm, which comprises thinly bedded limestone; and the Sandilands Fm, which is composed of thinly bedded siltstone, sandstone, and minor tuff (Lewis et al. 1991; Haggart et al. 2009; Shellnutt & Dostal 2019) The Sadler Limestone and Peril Fm are inferred to be time-equivalent to the Quatsino and Parson Bay formations on northern Vancouver Island (Jeletzky 1976; Lewis et al. 1991).

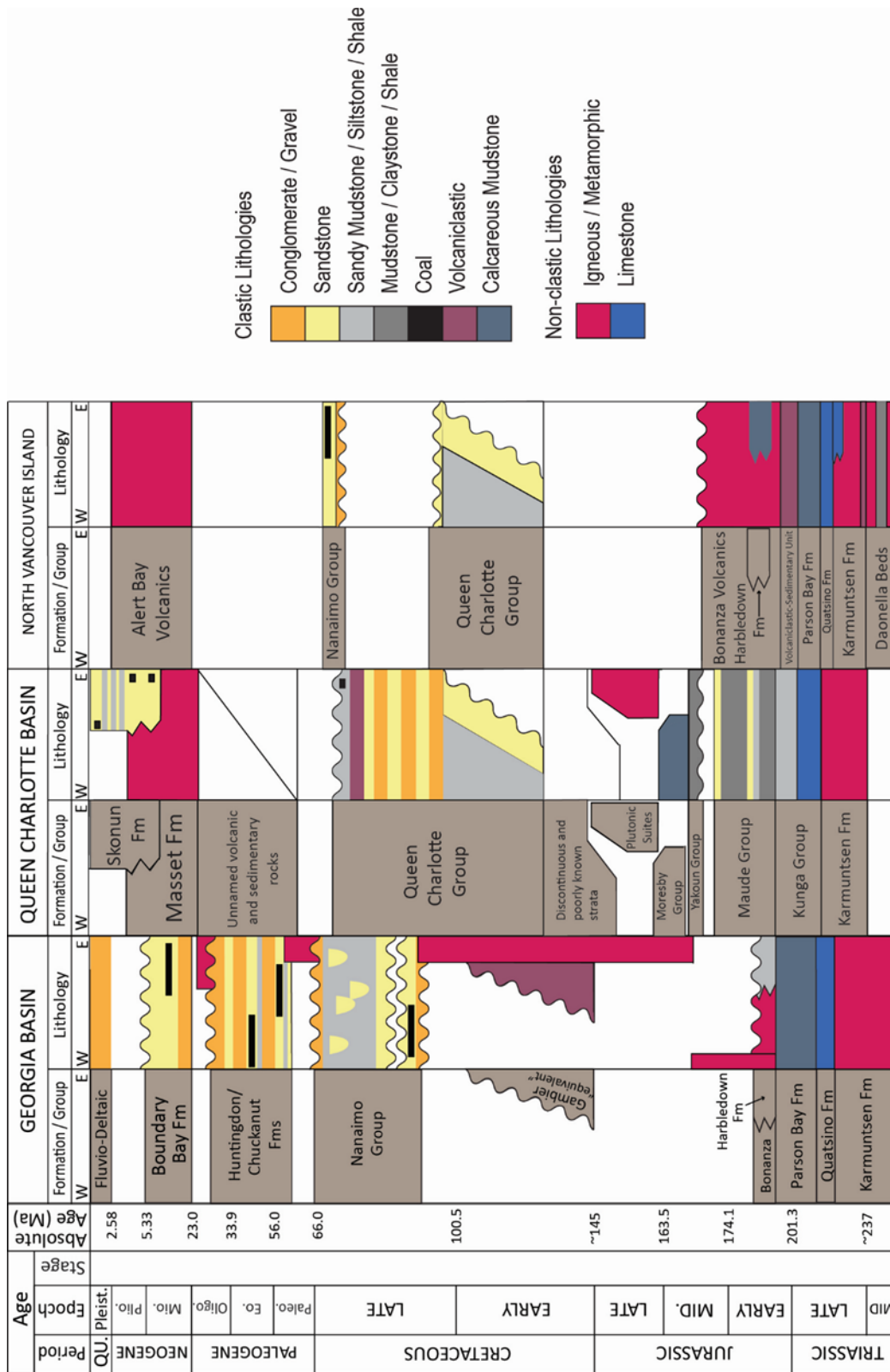
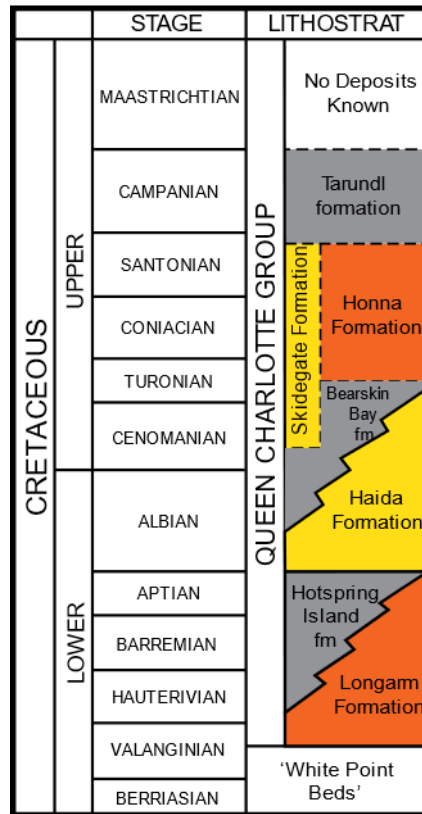


Figure 1.2 Generalised chronostratigraphy of the Georgia Basin, Queen Charlotte Basin, and northern Vancouver Island. Georgia Basin chronostratigraphy is modified after Hannigan et al. (2001); Queen



**Charlotte Basin chronostratigraphy is modified after Haggart et al. (2009) and Dalby et al. (2009); and northern Vancouver Island chronostratigraphy is modified after Muller and Jeletzky (1970), Nixon et al. (1992, 2011), and Nixon and Orr (2010).**

Conformably overlying the Kunga Group is the Maude Group, which comprises four formations: dark shale of the Ghost Creek Fm; sandstone, siltstone, and shale of the Fannin Fm; grey shale and mudstone of the Whiteaves Fm; and fossiliferous sandstone of the Phantom Creek Fm (Lewis et al. 1991; Haggart et al. 2009; Shellnutt & Dostal 2019). Above the Kunga and Maude Groups are the Middle Jurassic Yakoun and Moresby groups and are separated from these older units by an angular unconformity (Lewis et al. 1991). The Yakoun Group comprises intermediate calc-alkalic volcanic rocks and volcanically sourced conglomerate, sandstone, and siltstone. A biostratigraphic hiatus appears to be present between the Yakoun and Moresby groups (Cameron & Tipper 1985) with the latter comprising sandstone, conglomerate, and shale sourced from the underlying Yakoun Group (Lewis et al. 1991).



**Figure 1.3 Lithostratigraphy for the Queen Charlotte Group (after Dalby et al. 2009). Colours represent the dominant lithology: conglomerate (orange), sandstone (yellow), and siltstone/mudstone/shale (grey).**

The Queen Charlotte Group comprises the Cretaceous sedimentary fill of the QCB and ranges in age from Valanginian to Maastrichtian (Haggart 1987; Haggart et al. 2009; Dalby et al. 2009). The Queen Charlotte Group is interpreted to record near continuous deposition in a forearc basin that was open to the proto-Pacific Ocean throughout the Cretaceous (Haggart 1991; Haggart et al. 2009; Dalby et al. 2009). The basin fill is divided into the formally defined coarse-clastic strata of the Longarm, Haida, Skidegate, and Honna formations, and the fine-grained strata of the informally defined Hot Spring Island, Bearskin Bay, and Tarundl formations (Figure 1.3). Together, these units record a basin-wide transgressive succession where coarse-clastic strata thin to the west (Haggart 1991; Lewis et al. 1991).

The Longarm Fm is the basal unit of the Queen Charlotte Group and unconformably overlies various poorly known sedimentary units and plutonic rocks of

Late Jurassic age (Vellutini & Bustin 1990). The Longarm Fm is Valanginian to Aptian in age and is up to 1,275 m thick (Nixon & Orr 2010). It consists of basal conglomerate and coarse-grained sandstone that fines upwards into a mudstone interpreted to have been deposited on the shelf. The shelf mudstones are assigned to the informally designated Hotspring Island fm (Hauterivian–Aptian; Dalby et al. 2009). The Albian- to Turonian-aged Haida Fm also consists of basal conglomerate and coarse-grained sandstone, but fines upwards into siltstone, mudstone, and shale. The fine-grained strata above the Haida Fm were initially designated as the Haida Shale Member but are now assigned to the informal Bearskin Bay fm (Dalby et al. 2009). Overlying the Bearskin Bay Fm are turbiditic and distal fan strata of the Skidegate Fm, which accumulated during the Cenomanian to early Santonian. The upper Skidegate Fm was deposited contemporaneously with submarine fan and fan-delta deposits of the Honna Fm, and together these strata are interpreted to represent progradation of turbidite systems into the QCB (Dalby et al. 2009). The youngest unit of the Queen Charlotte Group within the QCB is the informally designated Tarundl Fm. The Tarundl Fm is composed of shelf mudstone that was deposited from the upper Santonian to upper Campanian (Dalby et al. 2009). Locally, basal conglomerates in the Longarm and Haida formations mark the beginning of transgressive packages (Lewis et al. 1991).

### **1.2.2. Georgia Basin**

The Nanaimo Group represents the mainly Late Cretaceous depositional phase of the Georgia Basin and comprises mainly Turonian- to Maastrichtian-aged sedimentary strata (Mustard 1994). The Georgia Basin has been the focus of study and exploration for the past 150 years due to the presence of large coal seams throughout the various outcrop areas (Bickford and Kenyon 1988; England 1989) and its potential for hydrocarbon production (England 1989). Early workers in the Georgia Basin defined three distinct sub-basins and categorized Nanaimo Group strata therein by lithology (Figure 1.4 ; Clapp 1914; Clapp & Cooke 1917; Williams 1924; Usher 1952). Later workers separated Nanaimo strata into two coeval basins within which the lower Nanaimo Group comprises braided fluvial, coastal plain and paralic deposits (McGugan 1979; England 1989), as well as the marine mudstone of the Haslam Fm. Overlying this is the upper Nanaimo Group, which is characterised by long-lasting and spatially broad, deep-water, slope-channel and submarine-fan deposits (Pacht 1980; Katnick and

Mustard 2003; Bain & Hubbard 2016; Englert et al. 2018; Coutts et al. 2020; Giroto et al. in press). The upper Nanaimo Group represents the fill of a single widespread depocenter, whose formation was possibly facilitated by changing obliquity in the subduction angle of the Kula Plate to the east that resulted in deepening of the GB and amalgamation of the Comox and Nanaimo sub-Basins (outcrop areas; England and Bustin 1998; Coutts et al. 2020).

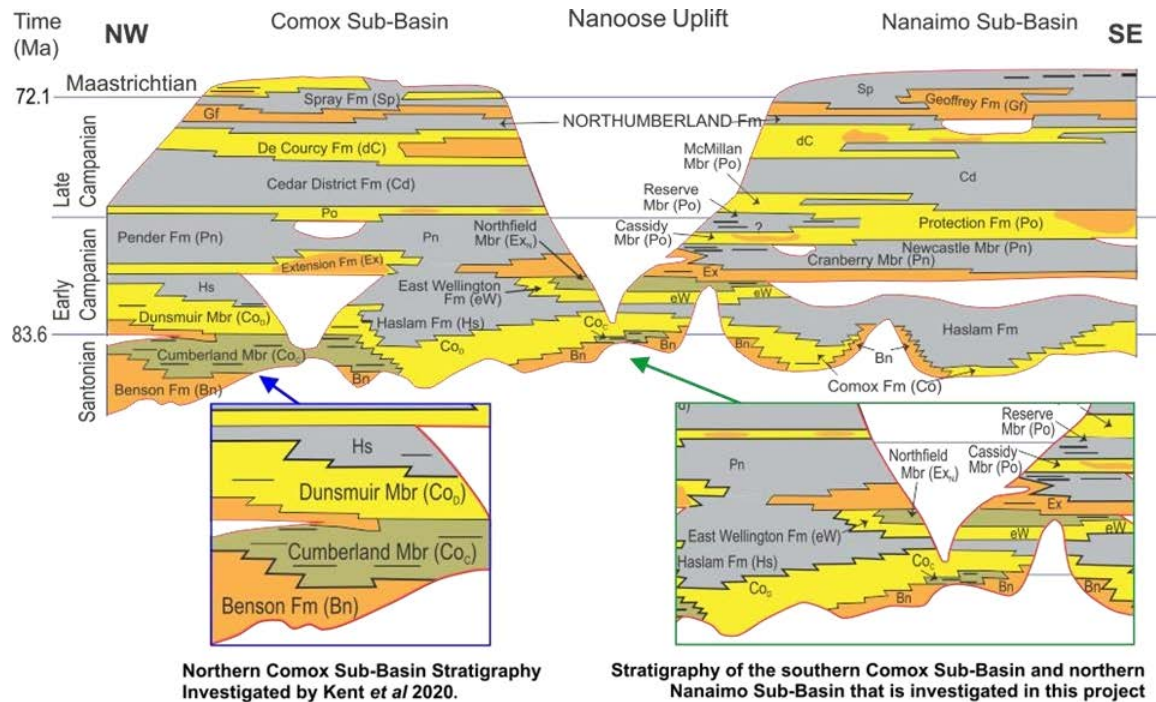
Prior to development of the genetic stratigraphic framework for the lower Nanaimo Group (Kent et al. 2020; Giroto et al. 2024), the accepted lithostratigraphic scheme correlated lithologic units based on their positions relative to the basal nonconformity and to the coarse-grained units within the succession (Muller and Jeletzky 1970; Bickford and Kenyon 1988; Kent et al. 2020; Giroto et al. in press). Unfortunately, the lithostratigraphic scheme does not account for the greater than 500 m of relief on the nonconformity (Hamblin 2012; Jones et al. 2018; Kent et al. 2020), nor does it account for the marked diachroneity of the depositional units (Bickford and Kenyon 1988). Consequently, Huang et al. 2019 identified multiple instances where strata of similar lithology but high temporal variance were correlated together. Bickford and Kenyon (1988) generated a schematic basin-wide stratigraphic model (Figure 1.5) using coal seams as datums in order to constrain correlations of lithostratigraphic units across topographic highs both within and between outcrop areas of the GB. Their model accounts for relief generated by topographic variance in each of the Comox and Nanaimo outcrop areas and considers structural features such as the Nanoose Uplift by using a combination of lithologic and geophysical data.

Pre-1970 nomenclature				Post-1970 nomenclature								
Early Studies - Evolving Nomenclature				Two Basins, Two Nomenclatures				One Basin, One Nomenclature				
Nanaimo Basin Clapp (1914), Buckham (1947), Usher (1952)		Cowichan Basin Richardson (1873, 1873, 1878) Clapp (1912, 1914)		Comox Basin Williams (1924), Mackenzie (1922) Usher (1952)		Nanaimo Basin England (1989) McGugan (1990)		Comox Basin England (1989) McGugan (1990)		Nanaimo Basin Muller & Jeletzky (1970) Ward (1978), Mustard (1984), and later		
Gabriola	Gabriola			St. John	Hornby	Gabriola	Gabriola	Hornby	Hornby	Gabriola	Gabriola	
North-umberland	North-umberland			Tribune	Spray	Mayne	North-umberland	Spray	Spray	Spray	Spray	
				Hornby	Geoffrey	Galiano		Geoffrey	Upper Lambert	Geoffrey	Geoffrey	
				Lambert	Lambert	North-umberland		Lambert		North-umberland	North-umberland	
De Courcy	De Courcy			Denman	Denman	De Courcy	De Courcy	Denman		De Courcy	De Courcy	
Cedar District	Cedar District	Duncan	Trent River	Trent River	Trent River	Cedar District	Cedar District	Trent River	Trent River	Extension-Protection	Cedar District	Cedar District
Protection	Protection					Protection	Protection				Protection	
Newcastle	Ganges					Protection	Newcastle				Protection	
Cranberry						Pender	Cranberry				Pender	
Extension	Extension					Extension	Extension				Extension	
E. Willington						Extension	Extension				Extension	Extension
Haslam	Haslam	Haslam	Comox	Comox	Haslam	Haslam	Comox	Comox	Lower Trent River	Haslam	Haslam	
Benson	Benson	Benson			Comox	Benson			Benson	Comox	Dunsmuir Benson	Comox

**Figure 1.4 Evolution of the lithostratigraphic nomenclature for Nanaimo Group strata in the Georgia Basin from 1914 to 1990. The various schemes show the change from the early, multiple basin interpretation to the unified basin interpretation. The one basin interpretation has recently been revised to reflect the stratigraphic complexities inherent in the lower Nanaimo Group. The colours in the right-hand column reflect the dominant lithologies of each formation (conglomerate (orange), sandstone (yellow), and siltstone/mudstone/shale (grey)); modified from Huang (2018) after Mustard 1994).**

Recent research has reinterpreted the stratigraphic framework for the lower Nanaimo Group throughout most of the GB using genetic stratigraphy (Figs. 1.6 and 1.7; Kent et al. 2020; Giroto et al. 2024) and by constraining correlations using detrital zircon maximum depositional ages and macrofossil biostratigraphy (Haggart et al. 2005; Haggart & Graham 2018; Huang et al. 2019, 2022). The resulting model shows there were initially two depocenters that correlate roughly to the Comox and Nanaimo outcrop areas, and these contain lower Nanaimo Group strata. The two depocenters are separated by the shale basin between Parksville and Comox (Huang et al. 2022; Giroto et al. 2024), whereas the separation between the Nanaimo and Comox OAs is the Nanoose Uplift. The two depocenters of lower Nanaimo Group strata merged through a

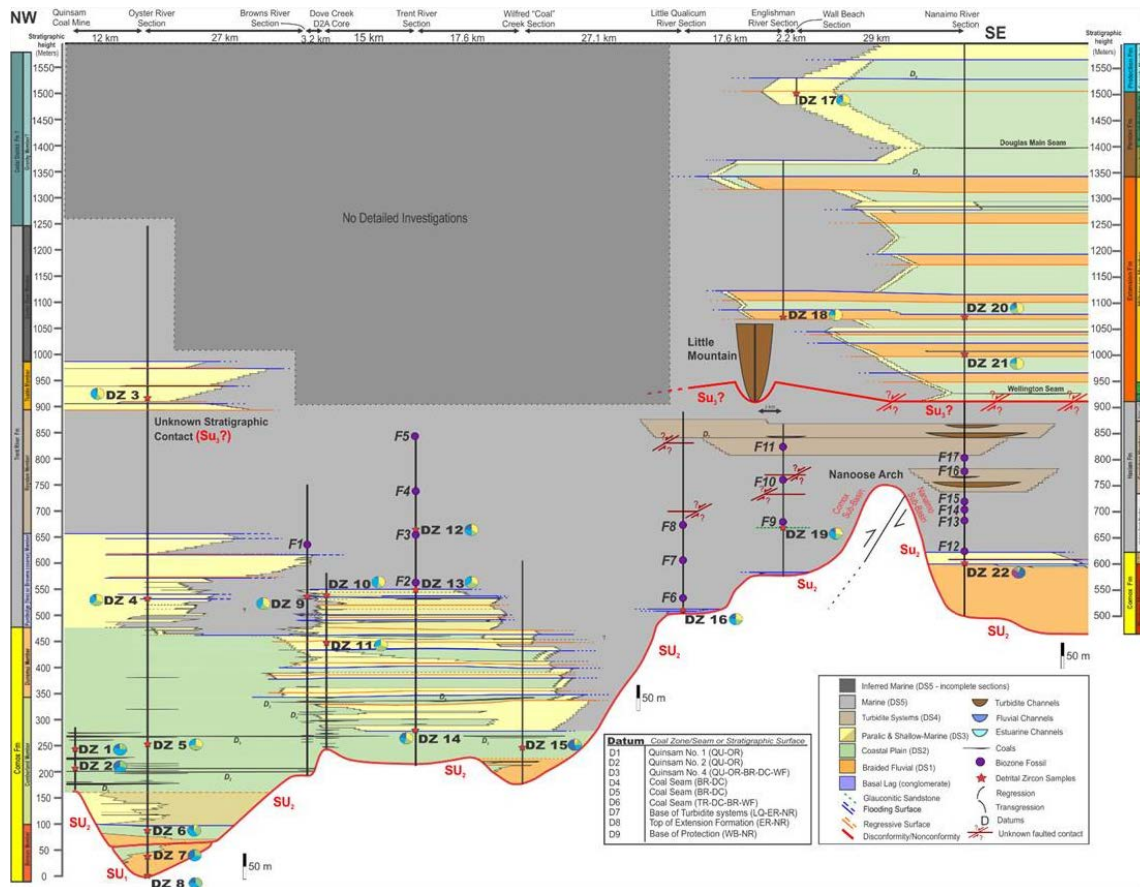
basin-wide transgression following deposition of the Protection Fm, and basin-wide deposition of the upper Nanaimo Group followed after that.



**Figure 1.5** Schematic reconstruction of the Nanaimo Group lithostratigraphy (S. Dashtgard, pers. comm. 2021; and adapted from Bickford & Kenyon 1988). The blue box shows the strata of the northern Comox SB upon which the T–R framework of Kent *et al.* (2020) is based. The green box shows the strata investigated by Girotto *et al.* (2024) and shown in Figure 1.6. The coloured polygons indicate the dominant lithology of each stratigraphic unit, including conglomerate (orange); sandstone (yellow); siltstone/mudstone/shale (grey); and terrestrial mudstones, siltstones and coals (greenish-brown). Age boundaries are based on International Commission on Stratigraphy time scale (Cohen *et al.* 2021)

The oldest formally recognized unit of the Nanaimo Group is the Comox Fm, which consists of a basal conglomerate unit (Benson Member; England 1989, CathylBickford 1991) and an upper sandstone unit (England and Bustin 1998; Hamblin 2012). Above this sits the Haslam Fm, which is composed of mainly shale and siltstone with minor sandstone (Clapp 1914; England and Bustin 1998). Above the Haslam Fm is the Extension Fm, which consists of conglomerate and sandstone with minor coal measures

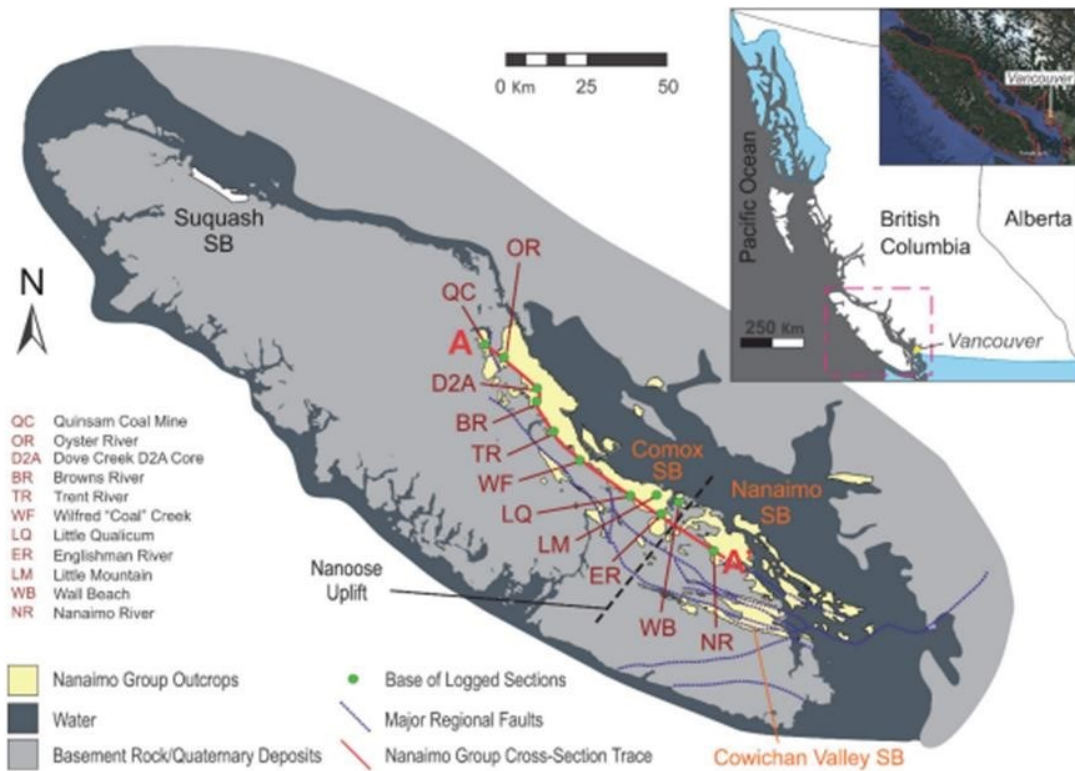
(Bickford and Kenyon 1988; England and Bustin 1998). Above the Extension Fm is the Pender Fm, which consists of fine-grained sandstone, shale and siltstone (Ward 1978; England and Bustin 1998). The Protection Fm overlies the Pender Fm and consists of thick sandstone. Thick coal seams in the Extension, Pender, and Protection formations occur in the Nanaimo area (Figure 1.5; Clapp 1914; England and Bustin 1998; Giroto et al. 2024). The Protection Fm defines the top of the lower Nanaimo Group.



**Figure 1.6** Cross section of lower Nanaimo Group strata from NW to SE and through the Comox and Nanaimo outcrop areas (Giroto et al. 2024 with data from Kent et al. 2020). The line of section is shown in Figure 1.7. The genetic stratigraphic framework is based on facies interpretations as well as spatial and temporal correlations of strata. Unit ages are constrained by detrital zircon ages and biostratigraphy (Huang et al. 2019; 2022).

The upper Nanaimo Group comprises deep-marine clastic strata (Pacht 1980; Katnick and Mustard 2003; Bain and Hubbard 2016; Coutts et al. 2020; Mahoney et al.

2021). The oldest unit of the upper Nanaimo Group is the Cedar District Fm (Clapp 1914) which consists of thin-bedded shale, siltstone, and fine-grained sandstone (England and Bustin 1998). Above this are thick-bedded sandstone strata with minor siltstone and conglomerate of the De Courcy Fm (Clapp 1914), which is interpreted as high-energy, deep-water deposits (England and Bustin 1998; Hamblin 2012). The Northumberland Fm (Muller and Jeletzky 1970) succeeds the De Courcy and is composed of mainly mudstone and siltstone with minor very fine-grained sandstone interbeds (England and Bustin 1998; Hamblin 2012). Overlying the Northumberland Fm is the Geoffrey Fm, which consists of thick-bedded, coarse-grained sandstone with coarser units ranging up to boulder conglomerate (Hamblin 2012). The Geoffrey Fm is overlain by the Spray Fm, which comprises siltstone and mudstone with minor sandstone. Finally, the youngest formation of the Nanaimo Group is the Gabriola Fm (Clapp 1914) composed of thin-bedded, coarse-grained sandstone with minor conglomerate (England and Bustin 1998; Hamblin 2012; Coutts et al. 2020; Mahoney et al. 2021).



**Figure 1.7** Map view of Nanaimo Group outcrops (yellow polygons) as well as measured sections and core locations used to build cross-section A–A' shown in Figure 1.6 (from Giroto et al. 2024).



The strata of the upper Nanaimo Group have been studied extensively in outcrops on Hornby and Denman Islands, where they extend vertically and laterally for 10s to 1000s of metres (Katnick and mustard 2003; Bain and Hubbard, 2016; Mahoney et al. 2021). Recent evaluation of these strata suggests the upper Nanaimo Group records long-lived submarine slope-channel systems with associated areas of sediment bypass. Deposition in submarine channel systems resulted in the layering and interfingering of coarse- and fine-grained units (Bain and Hubbard 2016; Mahoney et al. 2021). The ages of units and timing of events within the upper Nanaimo Group have been constrained with biostratigraphy (Muller and Jeletzky 1970; Haggart et al. 2005, 2009; Haggart and Graham 2018) and maximum depositional ages derived from detrital zircon geochronology (Matthews et al. 2017; Coutts 2020; Mahoney et al. 2021).

### **1.2.3. Northern Vancouver Island (NVI)**

Mesozoic strata of northern Vancouver Island (NVI) comprise a range of lithologies that record the mobile and accretionary history of the terranes in this area. NVI strata are delineated by major units, faults, and plutons (Nixon et al. 2011). Vancouver Island, situated in the Wrangellia Terrane, is overlain unconformably to the east by Cretaceous–Eocene rocks of the Coast Belt and to the west is adjoined by the ongoing subduction complex involving the Wrangellia, Pacific Rim, and Crescent terranes (Wheeler and McFeely 1991; Nixon et al. 1992; Nixon et al. 1993).

The base of the Mesozoic strata in NVI comprises Triassic units including the Daonella Beds, Karmutsen Fm, Quatsino Limestone, and Parsons Bay Fm (figure 1.2). The Daonella beds comprise a 100–800 m thick interval of shale and metasediment with abundant basaltic sills. Overlying the Daonella beds is the regionally extensive and up to 6000m thick Karmutsen Fm (Figure 1.2). The Karmutsen Fm comprises pillow basalts and volcanic breccias and is capped with up to 3 km of massive basalt flows (Nixon et al. 1993; Nixon 2010). Above the Karmutsen Fm is the Quatsino Limestone, which is a regionally restricted, Late Triassic coarse-grained bioclastic limestone, and the Parsons Bay Fm, which comprises argillaceous limestone, carbonaceous mudstone and shale.

The Parsons Bay Fm is only preserved in fault blocks near the west coast of Vancouver Island (Nixon et al. 1993; Nixon 2010). The Triassic units of NVI are collectively ascribed to the Vancouver Group. Overlying Triassic strata on NVI are Jurassic units, including the Harbledown Fm and the Bonanza Volcanics (Figure 1.2). The Harbledown Fm consists of up to 500 m of calcareous siltstone. The overlying Bonanza Volcanics are more than 1000 m thick and consist predominantly of subaerially accumulated tuffs and basaltic to rhyolitic-tuff flows with interbedded clastics and limestones (Nixon et al. 1993; Nixon 2010). The Bonanza Volcanics continue temporally before, contemporaneously to, and following the end of deposition of the Harbledown Fm. An angular unconformity separates Jurassic strata from the Cretaceous Queen Charlotte Group in NVI.

Cretaceous sedimentary strata include rocks ascribed to both the Queen Charlotte Group and the Nanaimo Group. The Queen Charlotte Group includes the Longarm Fm (see Section 1.2.1) and up to 1000 m of variable, unassigned siliciclastic units situated on the west coast of Vancouver Island within Quatsino Sound and Holberg Inlet (Nixon et al. 1992; Nixon and Orr 2010). Conglomerate, sandstone, shale, siltstone, and coal within the Suquash OA have been broadly assigned to the Nanaimo Group and are the youngest of the Mesozoic strata in NVI (Nixon et al. 1992). Younger strata in NVI include mainly the Neogene Alert Bay volcanics, which consist of basaltic to calcitic lavas and tuffs interbedded with conglomerate and cross-cut by coeval dykes and plutonic rocks (Nixon et al. 1993).

## **1.3. Biostratigraphy of Canada's west-coast sedimentary basins**

### **1.3.1. Macrofossil biostratigraphy**

The macrofossil assemblages of Cretaceous strata in Haida Gwaii are diverse and abundant, and correspondingly have become a standard reference for correlation of Cretaceous macrofossil assemblages across the northeastern Pacific region (Dalby et al. 2009). Several studies have developed molluscan teilzones, which are employed to correlate sedimentary strata between the QCB, GB, and other Mesozoic sedimentary basins around the Pacific (Haggart 1991, 1994; Haggart et al. 2009, Huang et al. 2022).

Molluscan teilzones are defined by the first and last appearance of any given taxa within the local stratigraphy (Huang et al. 2022) and are assigned ages based on comparison to: 1) biostratigraphic successions throughout the Pacific basin (Muller and Jeletzky 1970; Haggart and Graham 2018); 2) foraminiferal and dino-cyst biostratigraphy (Sliter 1973; McGugan 1979; McLachlan et al. 2018, 2019); and 3) magnetostratigraphy (Ward et al. 2012). The current molluscan biozonation used for the Queen Charlotte Group (Figure 1.8) is undergoing revision to better define and constrain ages with teilzones for Cretaceous strata in the northeastern Pacific region (e.g., proposed *Nostoceras hornbyense* zone of Haggart et al. 2009).

In the Georgia Basin, biostratigraphic evaluation of the Nanaimo Group has focussed primarily on identifying and defining molluscan biozones. Usher (1952) proposed the first biostratigraphic zonation of the Nanaimo Group, which consists of four biozones based on ammonite assemblages. These zones correlate to Cretaceous (Santonian to Maastrichtian) ages. Usher's (1952) scheme was expanded by Muller and Jeletzky (1970) to include an additional four biostratigraphic zones, all of which are based on ammonite and inoceramid assemblages. Further additions were made by Haggart (1991, 1994) and Haggart et al. (2005), who identified Turonian assemblages overlying the basal nonconformity in the southern Georgia Basin (Haggart et al. 2005). The most recent change to the macrofossil biostratigraphic scheme is the addition of the crinoidal *Marsupites testudinarius* biozone, the end of which marks the SantonianCampanian boundary (Figure 1.9; Haggart and Graham 2018).

		STAGE	LITHOSTRAT	MOLLUSC ZONE	
CRETACEOUS	UPPER	MAASTRICHTIAN	No Deposits Known	No Fossils Known	
		CAMPANIAN	Tarundi formation	<i>Pachydiscus suciaensis</i> No Fossils Known	
		SANTONIAN	Skidegate Formation	Honna Formation	<i>Eupachydiscus haradai</i> <i>Sphenoceras cf. orientalis</i> <i>Plesiotexanites sp.</i>
		CONIACIAN			<i>Peroniceras sp.</i>
		TURONIAN			No Fossils Known
		CENOMANIAN	Bearskin Bay fm		<i>Mytiloides ex gr. labiatus</i> <i>I. aff. incebratus</i>
	LOWER	ALBIAN	Haida Formation		<i>D. (P.) japonicum</i> <i>Turritites sp.</i> <i>Mortonicerias-D. (P.) dawsoni</i>
					<i>C. (Grycia?) perezianum</i> <i>Brewericeras huienense</i> <i>Leconteites sp.</i>
		APTIAN	Hotspring Island fm	Longarm Formation	<i>Tropasum sp.</i> <i>Lytoceras (Gabbrioceras) sp.</i> <i>Shasticroceras sp.</i> <i>Shastoceras sp.</i>
		BARREMIAN			<i>Inoceramus colonicus</i> <i>I. cf. paraketzovi</i> <i>Simbirskites spp.</i> <i>Buchie crassicolis</i>
		HAUTERIVIAN			
		VALANGINIAN			
		BERRIASIAN	'White Point Beds'		No Fossils Known

**Figure 1.8** Lithostratigraphic and biostratigraphic successions of the Queen Charlotte Group in the Queen Charlotte Basin (after Dalby 2009 with data from Haggart 2004 and others). Colours indicate dominant lithology, including conglomerate (orange); sandstone (yellow); siltstone/mudstone/shale (grey).

Mesozoic sedimentary strata in NVI have been ascribed to both the Queen Charlotte Group (Queen Charlotte Basin) and the Nanaimo Group, based on molluscan fossils (Georgia Basin; Muller and Jeletzky 1970; Mustard 1994; Ludvigsen and Beard 1997; Nixon and Orr 2010). Molluscan fossils common to the Longarm Fm have been identified in the northwestern part of Vancouver Island (Muller and Jeletzky 1970; Ludvigsen and Beard 1997), and these data are used to extend the QCB to NVI (Figure 1.1). Conversely, Maastrichtian to Campanian molluscan fossils in the Suquash OA have been ascribed to the Georgia Basin, suggesting that these strata are geographically linked to the southern Georgia Basin (Usher 1952; Muller and Jeletzky 1970; Haggart et al. 2005).

### 1.3.2. Microfossil biostratigraphy

In the Queen Charlotte Basin, Dalby et al. (2009) identified Albian and Cenomanian foraminifera in the first extensive study of its type of the Queen Charlotte Group. The study included 267 samples from the Albian to Cenomanian Haida and Bearskin Bay formations, in which 57 species of both planktic and benthic foraminifera were identified. The intention of the study was to build and expand upon the ammonite- and bivalve-based biostratigraphic framework for the region (Dalby et al. 2009). Recent work studying radiolarians (Haggart et al. 1993; Carter et al. 2006) has shown promise in also using micro-biostratigraphy as a correlative tool in the region.

The Dalby et al. (2009) study has wider implications in Canadian Cordilleran geology and in framing part of the tectonic history of the terranes containing the westcoast sedimentary basins. Sixty percent of foraminiferal species (both planktic and benthic) within the QCB correlate temporally to species in strata of northern Alaska, suggesting that the northward translation of Wrangellia occurred prior to the middle Cretaceous. If this were the case, it challenges paleomagnetic interpretations of the timing of its accretion to the Western Canadian margin (Dalby et al. 2009) and proposes a new timeline for the movement of the Insular Terrane relative to the western margin of North America. Paleomagnetic and biostratigraphic studies have shown evidence that the terranes of the Insular Belt were situated at tropical latitudes in the Middle Triassic (Monger and Ross 1971; Ward et al. 1997; Enkin et al. 2001), but constraints on the timing of both the northward and initial southward translation of these terranes remain a point of contention (Baja BC controversy; see Monger et al. 1982; Garver and Brandon 1994; Irving et al. 1995; Enkin et al. 2001; Gehrels et al. 2009).

Micropaleontological studies of the Nanaimo Group in the Georgia Basin have focussed primarily on foraminifera (McGugan 1962, 1979, 1981, 1982; Sliter 1973). The current foraminiferal biozonation scheme defines 5 planktic and 5 benthic foram biozones (Figure 1.9; McGugan 1979) and no major changes in the proposed foraminiferal biozonation scheme have taken place since its initial inception. Planktic foraminifera in the Nanaimo Group are dominated by species of the genus *Globotruncana*, and species boundaries are correlated to biostratigraphic regimes within similar settings in the US Gulf Coast and to Upper Cretaceous strata in Europe (McGugan 1979). Benthic foraminifera present a higher diversity within the Nanaimo

Group (Sliter 1973; McGugan 1979). Several genera of benthic foraminifera are used as biozone markers (Figure 1.9), and like planktic forms, have been correlated to other known Cretaceous Basins within the Pacific realm to constrain biozonation (McGugan 1979).

SERIES	STAGE	Ma	LITHOSTRATIGRAPHY Haggart et. al. (2011)	BIOSTRATIGRAPHY (MACRO)			BIOSTRAT. (MICRO)			
				Jeletzky (1970) and Ward (1978)	Haggart (1989); Haggart et. al (2005, 2011)	Haggart & Graham (2018)	Sliter (1973) McGugan (1979)			
							PLANKTIC	BENTHIC		
UPPER CRETACEOUS	Maast.	72.1	Gabriola Fm.	No fauna known	No fauna known	No fauna known	<i>Globotruncana confusa</i>	<i>Bolivina decurrens</i> - <i>Gavelinella velascoensis</i>		
			Spray Fm.		<i>Baculites</i> sp.	<i>Baculites</i> sp.				
			Geoffrey Fm.		No fauna known	No fauna known				
	Campanian	U	72.1	Northumberland Fm.	<i>Pachydiscus suciaensis</i>	<i>Nostoceras hornbyense</i>	<i>N. hornbyense</i>	<i>G. churchi</i>	<i>Gyrogonoides nitidus</i> - <i>G. stephensoni</i>	
				De Courcy Fm.		<i>P. suciaensis</i>	<i>P. suciaensis</i>			
				Cedar District Fm.		<i>Metaplac. cf. pacificum</i>	<i>M. cf. pacificum</i>			
		L	84.2	84.2	Protection Fm.	<i>Hoplitoplacenticeras vancouverense</i>	<i>H. vancouverense</i>	<i>M. cf. pacificum</i>	<i>G. stuartiformis</i>	<i>Stensioina Pommerana</i>
					Pender Fm.	<i>Baculites chicoensis</i>	<i>B. chicoensis</i>	<i>S. chicoense</i>		
					Extension Fm.	<i>Inoceramus schmidti</i>	<i>Sphenoceramus ex gr. schmidti</i>	<i>Pseudo. umbulazi</i>		
	Santonian	U	86.3	Haslam Fm.	<i>Bostrychoceras elongatum</i>		<i>Marsupites testudinarius</i>	<i>G. elevata</i>	<i>Margulinopsis austinana</i> - <i>G. birdi</i>	
				Comox Fm. (Marine)		<i>Eubostrychoceras elongatum</i>	<i>E. elongatum</i>			
				Comox Fm. (non-marine, age inferred)		No marine fauna known	No marine fauna known			No marine fauna known

**Figure 1.9 Evolution of molluscan and foraminiferal biozonation of Nanaimo Group strata (modified from McGugan 1979 and Haggart and Graham 2018). Dominant lithologies are shown as: conglomerate (orange); sandstone (yellow); siltstone/mudstone/shale (grey).**

Palynological studies within the Georgia Basin comprise early work done by Bell (1957) who examined pollen and spores collected from the Comox Formation which were determined to be between Santonian and Maastrichtian age. Many species identified were interpreted to be unique to the Nanaimo Group. This added to an interpretation that the floral province was unique on North America's west coast and that a barrier existed between the paleocontinent and late Cretaceous depocenters now hosted on Vancouver Island (Galloway et al. 2023). This unique biotic province is reaffirmed through later study by Rouse et al. (1970) who studied Upper Cretaceous and Paleogene rocks in BC and Alberta. Upper Cretaceous coastal assemblages were dominated by ferns, herbaceous angiosperms, and *Proteacidites*, which contrasted with assemblages in Alberta that contained different fern spores, pollen from likely herbaceous angiosperms, and *Aquilapollenites*. These differences were used to infer the presence of two floristic provinces.

Within the Suquash outcrop area, Muller et al. (1973) collected samples from near the Keogh River (GCS Plant Location 8026) and these samples were examined by W. S. Hopkins. Similar to previous identifications by Bell (1957), these samples were assigned to the then Suquash Formation and were given a Campanian or Maastrichtian age.

Recent work has been completed by McLachlan et al. (2018, 2019, 2021), McLachlan and Pospelova (2021) and McLachlan (2021) who describe dinocyst populations in both the Campanian Northumberland Fm of the Nanaimo Group and the Late Cretaceous – Early Paleogene Oyster Bay Fm. Both intervals are situated in the Comox outcrop area. McLachlan et al. (2018) identified well-preserved Campanian dinocysts on Hornby Island which include the first appearance of chronostratigraphic indicator taxa, and McLachlan and Pospelova (2021) were able to identify a conformable succession within the Oyster Bay Fm spanning the Cretaceous – Paleogene boundary based on dinocysts. This is the first place this boundary is recognised in west coast sedimentary successions.

## **1.4. Chronostratigraphy**

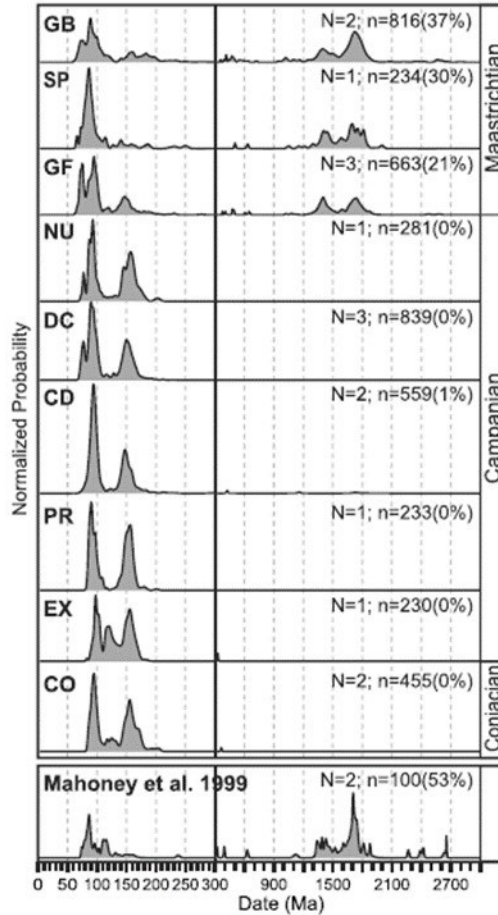
A geochronological study was undertaken in the QCB by Dorsey (unpublished MSc thesis, 2019) who collected and processed DZ samples from Mesozoic exposures across Haida Gwaii and compared calculated DZ maximum depositional ages (MDAs) with the biostratigraphic framework for the QCB. Overall, detrital zircon MDAs were comparable to biostratigraphic ages; however, a few small deviations between DZ and biostratigraphic ages were noted, which may be attributable to the conservative methods employed in calculating MDAs (Dorsey 2019; Coutts et al. 2019). The ages of the samples from Dorsey's study were determined using the youngest three grain (Y3Zo) approach (Table 1.1).

Sample Number	Formation	Stage	Date and Uncertainty (Ma)
1	Longarm	Aptian	119.6 +/- 2.2
2	Longarm	Aptian	118.3 +/- 2.0
3	Haida	Albian	103.6 +/- 2.8
4	Haida	Albian	103.6 +/- 1.8
5	Haida	Albian	100.7 +/- 1.8
6	Haida	Albian	98.3 +/- 1.7
7	Skidegate	Turonian	90.8 +/- 1.3
8	Skidegate	Turonian	90.5 +/- 1.4
9	Skidegate	Turonian	90.1 +/- 2.2
10	Honna	Turonian	89.7 +/- 1.5
11	Honna	Coniacian	87.6 +/- 1.3
12	Tarundl	Campanian	83.1 +/- 1.2
13	Unnamed Volcanics	Rupelian	28.0 +/- 0.5

**Table 1.1 Maximum depositional ages of samples analyzed by Dorsey (2019). Ages are calculated using the Y3Zo approach**

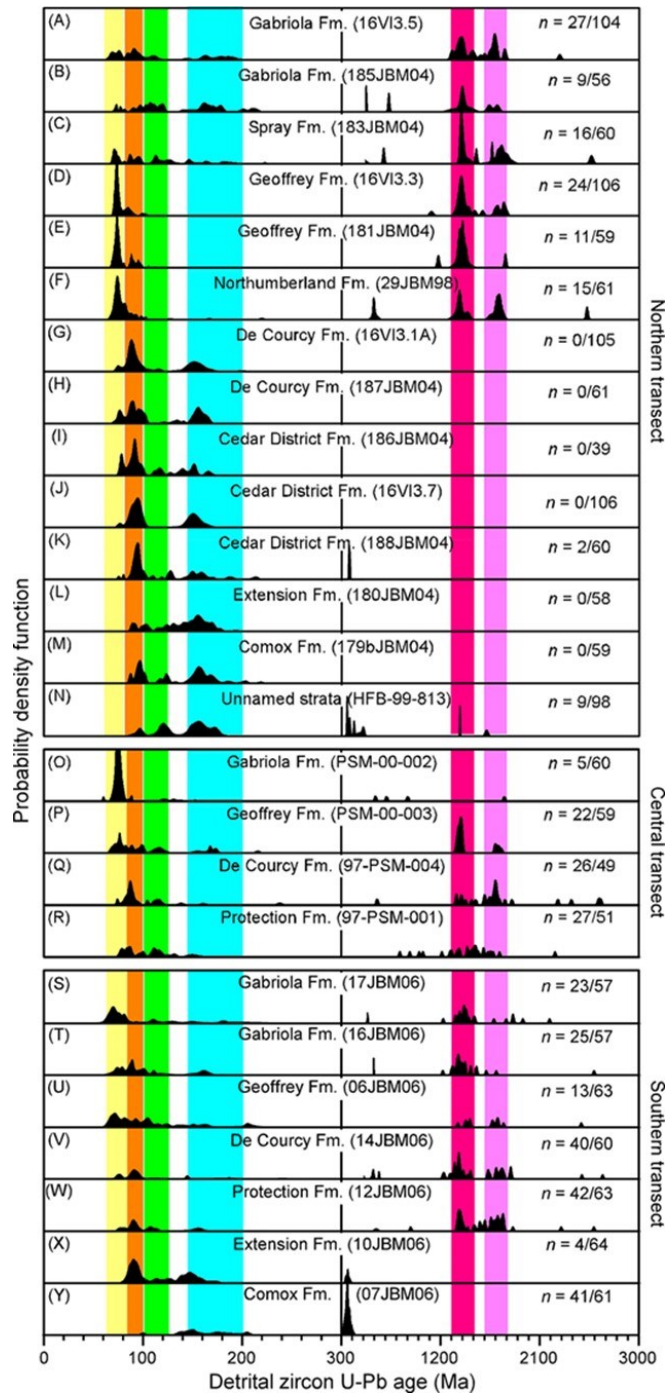
The only *in situ* radiometric age from Late Cretaceous strata in the Georgia Basin is derived from a tonstein along the Iron River in the northern Comox OA. It is assigned to the Dunsmuir Member of the Comox Formation and has a U-Pb age of 82.5 +/- 1 Ma (Kenyon et al. 1992; Huang et al. 2022). Other studies have attempted to ascribe provenance and estimate true depositional ages (TDAs) of sedimentary strata in the Georgia Basin, based on maximum depositional ages (MDAs) calculated from detrital zircon (Matthews et al. 2017; Huang et al. 2019, 2022; Mahoney et al., 2021). Matthews et al. (2017) utilised high-n (n > 200) detrital zircon samples to calculate MDAs for Nanaimo Group strata and the normalised probability density plots for each formation are shown in Figure 1.10.





**Figure 1.10 Normalized probability density plots for Nanaimo Group samples from Matthews et al. (2017). Formation abbreviations are CO – Comox, EX- Extension, PR- Protection, CD- Cedar District, DC- DeCourcy, NU-Northumberland, GF- Geoffrey, SP- Spray, GB- Gabriola.**

A similar study, also utilising high-n detrital zircon samples, Argon-Argon muscovite dating, and Hafnium isotope analyses, was undertaken by Mahoney et al. (2021), expanding this dataset further and providing additional geochronological ages for Nanaimo Group strata. This study concluded that the Nanaimo Group records patterns of subsidence, structural deformation, and exhumation within the southern Canadian Cordillera (Mahoney et al. 2021). This study was also able to constrain sediment source regions throughout the deposition of Nanaimo Group strata through a multi-proxy approach to geochronology (Mahoney et al. 2021). The normalised probability density plots for the DZ data from this study are shown in Figure 1.11.



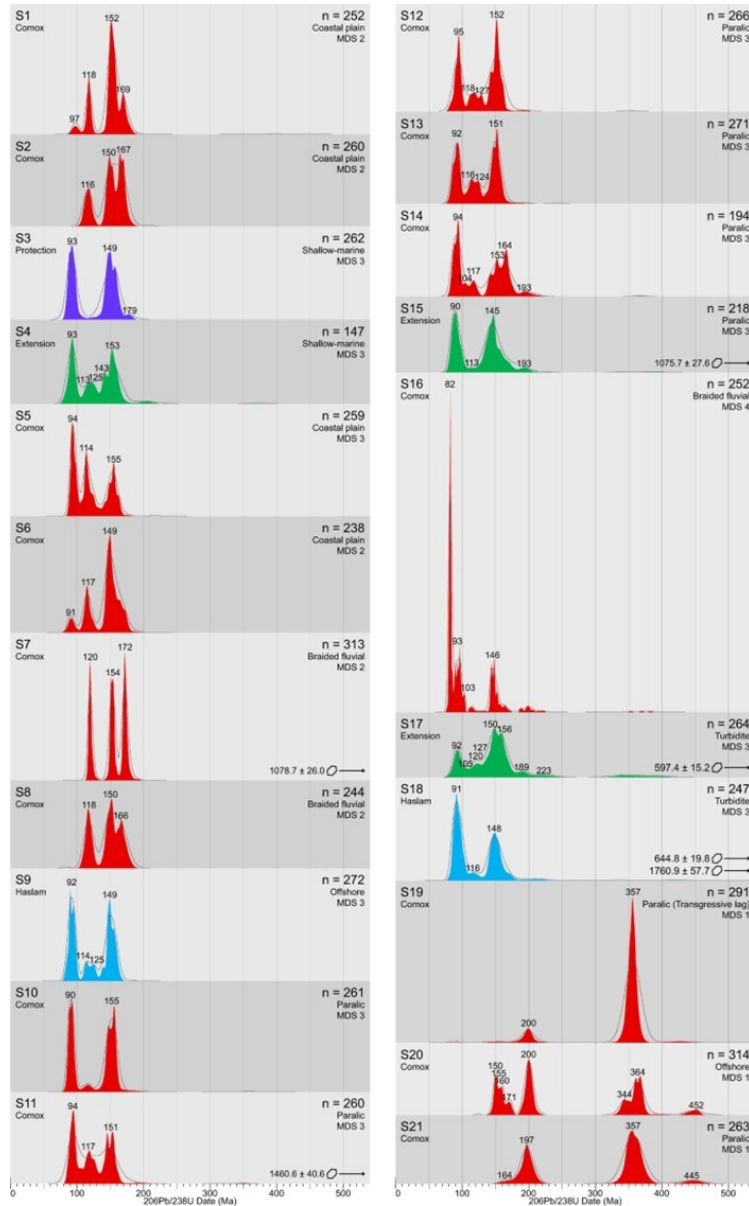
**Figure 1.11** Normalized probability density plots of DZ data from Mahoney et al. (2021), showing U-Pb age distributions of Nanaimo Group samples. On the right  $n = x/a$  where  $x$  represents the number of samples which returned an age >300ma and  $a$  represents the number of analyses performed per sample.

Huang et al. (2019) explored the use of DZ data in re-assessing the evolution and stratigraphy of the GB and how MDAs derived from DZ geochronology could be applied more broadly to refine basin-scale frameworks in convergent-margin basins. MDAs calculated from the study reflect the diachroneity of the lower Nanaimo Group (see Section 1.2.2) and suggest a more complex early basin evolution than has been described using lithostratigraphic studies within the basin (Figure 1.12). While Huang et al. (2019) shows that detrital zircon geochronological data are less suited for making bedset-scale interpretations within a basin, it is shown to be a useful tool in assessing basin-wide architecture when supported by both facies analyses and biostratigraphy.

Huang et al. (2022) compiled datasets related to the chronostratigraphy of the Georgia Basin including biostratigraphy and DZ geochronology. These datasets were compiled as a case study to show that integrated methodology analyses can be used to resolve the basin evolution and chronostratigraphy of convergent margin sedimentary basins (Huang et al. 2022). These datasets spanned the spatial and temporal extent of the Lower Nanaimo Group. Through this study, Huang et al. (2022) demonstrated that in the Georgia Basin, biostratigraphic age constraints on strata are superior estimates of true depositional ages (TDAs) compared to MDAs derived from DZ. While DZ MDAs approximated TDAs closely in some cases, this was dependent on the basin-wide distribution of near-depositional age DZ. The controlling factors identified for the distribution near-depositional age DZ include the local depositional environment as well as the distribution of coeval magmatism in the hinterland of the basin (Huang et al. 2022). They concluded, however, that where near-depositional age DZ exist, YGC2 $\sigma$  MDAs are universally more accurate when approximating TDAs than are any other analytical methods.

The discussion in the previous paragraph includes the use of MLA analysis, which incorporates every age derived from a sample into the calculated MDA (Vermeesch, 2021). For samples with multiple peaks of ages or an extended old tail on the spectrum of ages, MLA may overestimate the true depositional age. Further, it is argued by Copeland (2020) that zircon ages cannot be grouped into discrete age components without further geochemical justification, eliminating the risk of analysing grains which have re-crystallised or experienced lead-loss skewing towards an underestimated MDA. Given a lack of constraint on the potential spectra within samples

in the Suquash OA, as well as the known correlation of the YGC2 $\sigma$  MDA analysis with biostratigraphic ages determined in both the GB and the QCB, it was decided to continue with that analysis for this study.



**Figure 1.12 Normalized detrital zircon spectra from Huang et al. (2019), displayed for samples taken from the Comox (red), Haslam (blue), Extension (green), and Protection (purple) formations. The n values as well as the interpreted depositional environment are shown for each sample. Samples are arranged from northwest to southeast, and in each sample significant age modes (in which grains represent more than 3% of the sample) are labelled (from Huang et al. 2019).**

## 1.5. Research Goals/Questions

The main objective of this thesis is to explore the spatial and temporal relations between strata exposed in northern Vancouver Island to strata in both the Georgia Basin and the Queen Charlotte Basin. This thesis also aims to compare depositional ages assigned to strata by comparing DZ datasets to the presently assigned biostratigraphic ages. The results of this study address 2 main questions:

- 1) *Do Mesozoic strata of NVI that are stratigraphically below the Suquash outcrop area reflect a history of sedimentation within one or more of the west-coast sedimentary basins?*
- 2) *What is the depositional history of Upper Cretaceous to Danian strata in the Suquash outcrop area, and do those strata share a basin evolutionary history with either the Georgia Basin or Queen Charlotte Basin?*

## 1.6. Study Area and Methods

The study area encompasses outcrops of Mesozoic and Paleocene strata in northern Vancouver Island, B.C. (Figures 1.1 and 1.13). Late Cretaceous strata in the Suquash OA (Figure 1.13) were interpreted previously as Nanaimo Group (Muller and Jeletzky 1970; Nixon et al. 2011), and these strata crop out along the northeastern coastline between Port Hardy and Port McNeill. Four sites are examined in this area, including shoreline exposures at the site of the former Suquash Coal Mine (B in Figure 1.13), the shoreline at the Orca Gravel ship loader, sites adjacent to Port McNeill (C in Figure 1.13), and outcrop sections along the shoreline at the beach near Fort Rupert (F in Figure 1.13). Early Cretaceous strata in the study area comprise the Longarm Fm and equivalents (Ludvigsen and Beard 1997; Nixon et al. 2010), which crop out approximately 8 km north of Holberg along the Strandby River (D in Figure 1.13).

Older Mesozoic strata include Triassic sedimentary strata cropping out at the Goodspeed Fossil Beds (G in Figure 1.13; Ludvigsen and Beard 1997) and Jurassic strata in Holberg inlet exposed along Hashamu Creek (E in Figure 1.13; Muller et al. 1974). In more recent studies, the strata along Hashamu Creek have been assigned a Lower Cretaceous age (Nixon et al. 2011).

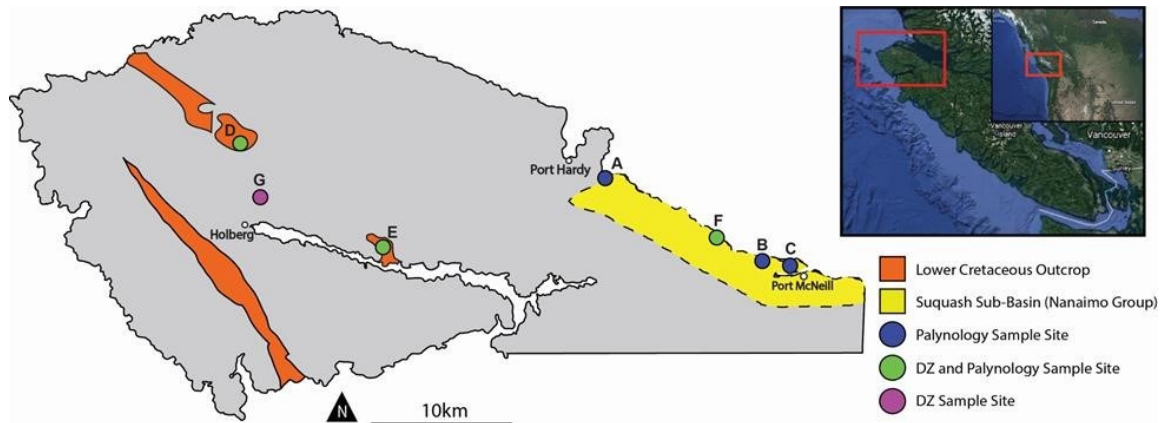
Descriptions and strip logs have been made for measured sections of the Nanaimo Group in the Suquash OA, as well as other strata from sites in NVI (Figure 1.12). For each of these sections, the lithology, sedimentology, and ichnology are described at the decimetre-scale, and where possible, molluscan fossils were photographed to determine depositional ages using molluscan biozones. Detrital zircon samples (taken from sites D, E, F, G in Figure 1.13) are used to calculate MDAs using several methods. DZ MDAs are compared to depositional ages derived from palynological samples from NVI (Sites A, B, C, D, E, F in Figure 1.13).

Micropaleontological samples consist of 100 g of rock taken preferentially from fine-grained marine units within identified sections. Samples were sent for processing and identification by Dr. Jennifer Galloway, Dr. Sandy McLachlan, and Dr. Manuel Bringué at the Geological Survey of Canada (GSC) in Calgary, Alberta. These data are published in Galloway et al. (2023).

Detrital zircon samples consist of approximately 2 kg of rock collected from sandstone-dominated intervals within the Nanaimo Group and Mesozoic strata. DZ samples processed at Simon Fraser University by the author and Chuqiao Huang where they were ground into powder through mechanical crushing, disc milling and Wilfey table separation. Zircon grains were separated from the powder by means of Franz magnetic separation and heavy liquid separation. Zircon grains were then mounted and analyzed using Laser Ablation – Inductively Coupled Plasma – Mass Spectrometry (LA-ICP-MS) at the Geo- and Thermochronology Lab at the University of Calgary by Will Matthews. The resulting DZ ages are used to calculate MDAs (Huang, pers. Comm. 2021)

To maximize the likelihood of calculating MDAs that closely approximate TDAs, only samples with a high number of zircon grains were analyzed (Vermeesch 2004; Coutts 2019). Specifically, studies using a range of potential sample sizes have demonstrated that any sediment source present in a sample will be represented 95% of the time (within two standard deviations) if greater than 117 grains are analyzed (Vermeesch 2004; Huang et al. 2022). If a sample has a large population of neardepositional age grains, and ages derived from those grains are acquired using low uncertainty methods such as those outlined below, then the MDA established from that sample will most closely represent the TDA (Vermeesch 2004). Two low-uncertainty methods of analysing age spectra include the use of the weighted averages of the Y3Zo

and YGC  $2\sigma$  (Coutts 2019). The Y3Zo method determines MDAs based on a weighted average of the youngest three grains that overlap within an uncertainty of two standard deviations ( $2\sigma$ ). The YGC  $2\sigma$  method determines the MDA from a weighted average of all DZ ages that overlap within  $2\sigma$ . Based on the work of Huang et al. (2022), the YGC  $2\sigma$  method shows the closest correlation to biostratigraphically defined ages, and hence, this method is used in this study to determine MDAs. Maximum depositional ages calculated using Y3Zo and YGC  $2\sigma$  are presented herein, and YGC  $2\sigma$  ages are presented alongside biostratigraphic ages to constrain unit ages within the study area.



**Figure 1.13** A map of Cretaceous outcrops and sample sites within the proposed study area. The inset maps show the position of the study area relative to Vancouver Island and North America (Courtesy of Google Earth). Outcrop positions are derived from the BCGS (Nixon et al. 2011 and Ludvigsen & Beard 1997). Blue dots mark palynological sample sites (A, B, C). Sites from which both palynological and detrital zircon data are derived are marked in green (D, E, F), and sites which were sampled for detrital zircon only are marked in purple (G). Larger regional towns are demarcated with white circles.



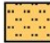









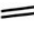



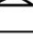










## Chapter 2. Methods and Data

### 2.1. Introduction

Chapter 2 presents palynology- and detrital zircon- (DZ) based ages, as well as sedimentological and ichnological data recorded from outcrop sections and cored intervals. Palynological data are from samples taken from Nanaimo Group-equivalent and older Mesozoic strata exposed on North Vancouver Island (NVI). Pollen and spore ages are compiled from Galloway et al. (2023) and aid in correlating strata between the Georgia Basin (GB), NVI, and the Queen Charlotte Basin (QCB). Detrital zircon data from NVI are used to calculate maximum depositional ages (MDAs; done collaboratively with Chuqiao Huang). MDAs are then compared with palynological ages and are used to place sampled strata into stratigraphic context with other sedimentary strata on Vancouver Island (e.g., Matthews et al. 2017; Huang et al. 2019, 2021; Mahoney et al. 2021).

Sedimentological and ichnological data were recorded from outcrop sections and cored intervals from NVI. Sedimentological datasets include lithology, grain size, sedimentary structures and lithological accessories. Ichnological datasets include bioturbation intensity (Bioturbation Index or BI; Reineck, 1963; Taylor and Goldring, 1993) and trace-fossil identifications to the ichnogenus level where possible. Lithologs of the major outcrop sections and core descriptions were compiled using AppleCORE. Some sections of strata described and sampled in this study lie outside the presently mapped limits of sedimentary strata in NVI. Inferences based on collected data have been made concerning the ages and extent of these strata. A full legend, which can be applied to all the measured sections presented in this thesis, is shown in Figure 2.1.



LEGEND		
<b>Lithology</b>		
 Sand/Sandstone	 Silty Sand	 Silt/Siltstone
 Sandy Silt	 Shale/ Mudstone	 Sandy Shale
 Clay/Claystone	 Coal	 Conglomerate
 Covered Section		
<b>Physical Structures</b>		
 Trough Cross-Strat.	 Planar Bedding/Laminae	 Low Angle Tabular Bedding
 Wavy Parallel Bedding	 Mud Drapes	 Mud Laminae
 Bar	SSD - Soft Sediment Deformation	 Current Ripple
<b>Lithologic Accessories</b>		
oooo - Pebbles/Granules	 Coal Lamina	Sid - Siderite
 Rip Up Clasts	---- - Coal Fragments	Carb - Carbonaceous or Macerated Plant Material
<b>Ichnofossils</b>		
√√ - Rootlets	Pl - Planolites	Di - Diplocraterion
Op - Ophiomorpha	Th - Thalassinoides	Ter - Teredolites
<b>Bioturbation</b>		
 Barren	 Sparse	 Low
 Moderate	 Abundant	 Intense
 Complete		

**Figure 2.1** A full legend for AppleCORE-generated measured sections and core descriptions for this thesis. Not all features shown above are present in every core or section.

## 2.2. Palynology

Palynology samples were analysed at Global GeoLabs Ltd. in Medicine Hat, Alberta. Samples were prepared using standard extraction techniques (Traverse, 2007) including: washing, acid digestion, oxidation with Schulze’s solution, staining with Safranin O, and final residue mounting with polyvinyl and liquid bioplastic. Identification of terrestrial palynomorphs was completed by Dr. Jennifer Galloway of the Geological Survey of Canada, and a qualitative approach was taken in processing these samples in order to determine a biostratigraphic age. Select preparations recommended by Dr. Galloway were further analyzed by Dr. Manuel Bringué of the Geological Survey of

Canada and Dr. Sandy McLachlan at the University of Minnesota Twin Cities for dinoflagellate cysts (dinocysts). Observations were made using a Zeiss M2 transmitted light microscope and associated camera system operated with Zen 3.5 software at 400x and 1000x magnification under oil immersion in brightfield, phase contrast, and differential interference contrast. Detailed palynological data are available in Galloway et al. (2023).

All samples analysed for palynology comprised 100–200 g of whole rock. Finegrained, shallow-marine and terrestrial strata were targeted to maximise potential for dinocyst, pollen, and spore preservation. In all cases, fresh rock surfaces were exposed prior to sampling to reduce the likelihood of modern pollen contamination. Within the study area, a total of 13 samples were taken: 9 samples from the Suquash Sub-Basin (samples labelled as SQM, FRB, OGL, and PMO; Table 2.1) and 4 from older Mesozoic strata (samples labelled as SBR and HCO; Table 2.1).

The preservation of pollen and spores range from exceptional to poor (Galloway et al., 2023). Of the 13 palynology samples, only five samples contained terrestrial pollen and spores that can be used to interpret depositional age. Of the seven that did not yield palynomorphs useful for determining depositional age: two were not analysed due to poor recovery from the samples (only a kerogen slide was produced for each); one sample was effectively barren; an age could not be determined for one sample; and three samples were first contaminated by modern pollen rain and an age could not be derived these three samples were reprocessed and found to be effectively barren. From the 13 samples submitted, four samples were analysed for dinocysts, six were not analysed for dinocysts due to poor recovery from the samples, and three were effectively barren. Table 2.1 displays the pollen, spores, fungal remains, and dinocysts identified in each sample and the interpreted depositional age.

Some ages reported from palynological analysis are shown as an oldest age with an “or younger” qualification. The “or younger” applies to samples that contain pollen and/or spore taxa that have modern/extant equivalent taxa (no last appearance datum). For example, *Alnipollenites* spp. exists today as *Alnus* (alder), but the first appearance of this pollen genera is in the Santonian. Samples that contain *Alnipollenites* spp., therefore, can range in age from the Santonian to present (Galloway et al., 2023; Galloway, pers. comm., 2024). Other samples contain species that have extant forms but these flora no

longer populate coastal BC (e.g. *Cyadopites* spp.; Galloway, pers. comm., 2024). The timing of the migration of these species away from coastal BC is not well constrained and hence, ages are given as an oldest age “or younger”.

Seventy-eight pollen and spore taxa and four non-pollen palynomorphs (excluding dinocysts) were observed. In general, Galloway et al. (2023) recommends that a more complete and systematic taxonomic approach be applied to these samples and suggests that new species or genera are likely present.

### **2.3. Detrital Zircon**

Five samples were collected in 2021 for DZ analysis, most taken from logged stratigraphic sections. An additional four samples were collected in 2023 (C. Huang, pers. comm., 2023). Detrital zircon samples comprise ~3 kg of sandstone taken from fresh surfaces at logged outcrop sections. Un-weathered surfaces were targeted to achieve maximum potential for zircon recovery. Mechanical separation of samples was conducted at Simon Fraser University. Samples were cleaned by hand and then placed in a solution of ~10% hydrogen peroxide (diluted from 50% by weight solution) to remove organic material. Bulk rock samples were converted into individual grains using a rock crusher and disk mill, and a heavy-minerals concentrate was generated using a Wilfey table. Magnetic minerals were removed using a rare earth magnet and a FrantzLB-1 magnetic barrier laboratory separator. A final heavy minerals concentrate was produced using heavy liquids separation with methylene iodide.

Epoxy mounting and LA-ICP-MS U-Th-Pb dating was conducted at the Calgary Geo- and Thermochronology Lab, University of Calgary, Alberta, Canada. Samples were ablated using an ASI Resochron™ 193 nm excimer laser ablation system, which incorporates a Laurin Technic M-50™ dual volume chamber. Isotopic signal intensities were measured using an Agilent 7700 quadrupole-ICP-MS. The ablation sequence employed a reference material-unknown bracketing procedure, with a measure of a FC1 zircon every 20 unknowns. Zircon reference materials FCT, Temora 2, 91500 and internal GSC reference 1242 from the Lac Flechette syenite were employed to validate the results and to assess uncertainties. Data reduction was facilitated by the lolite™ (V2.5) software package using the VizualAge data reduction scheme. Analyses with a probability of >1% discordance were eliminated from DZ datasets. Detailed analytical

procedures for the Calgary Geo- and Thermochronology Lab are available in Matthews et al. (2017). Raw LA-ICP-MS data were processed by C. Huang and the author using detritalPy to produce MDA plots. Maximum depositional age calculation methods included the calculation of the youngest grain cluster overlapping at  $1\sigma$  (YGC $1\sigma$ ) or  $2\sigma$  (YGC $2\sigma$ ; Table 2.2). The calculated ages are displayed with uncertainties which were calculated at the 2-sigma level. Probability density plots (PDPs) were also generated using detritalPy (Figure 2.2), which display analyses of grains within each sample grouped by age. These PDPs visually present the distribution of the ages within a population of grains for a sample (Vermeesch, 2021).

**Table 2.1. Palynology results from northern Vancouver Island (data from Galloway et al., 2023). Table contents include sample name used in this study; GSC curation number; stratigraphic unit assignment based on the presently established lithostratigraphy; lithology and stratigraphic height (where available); palynological and dinocyst ages, and comments.**

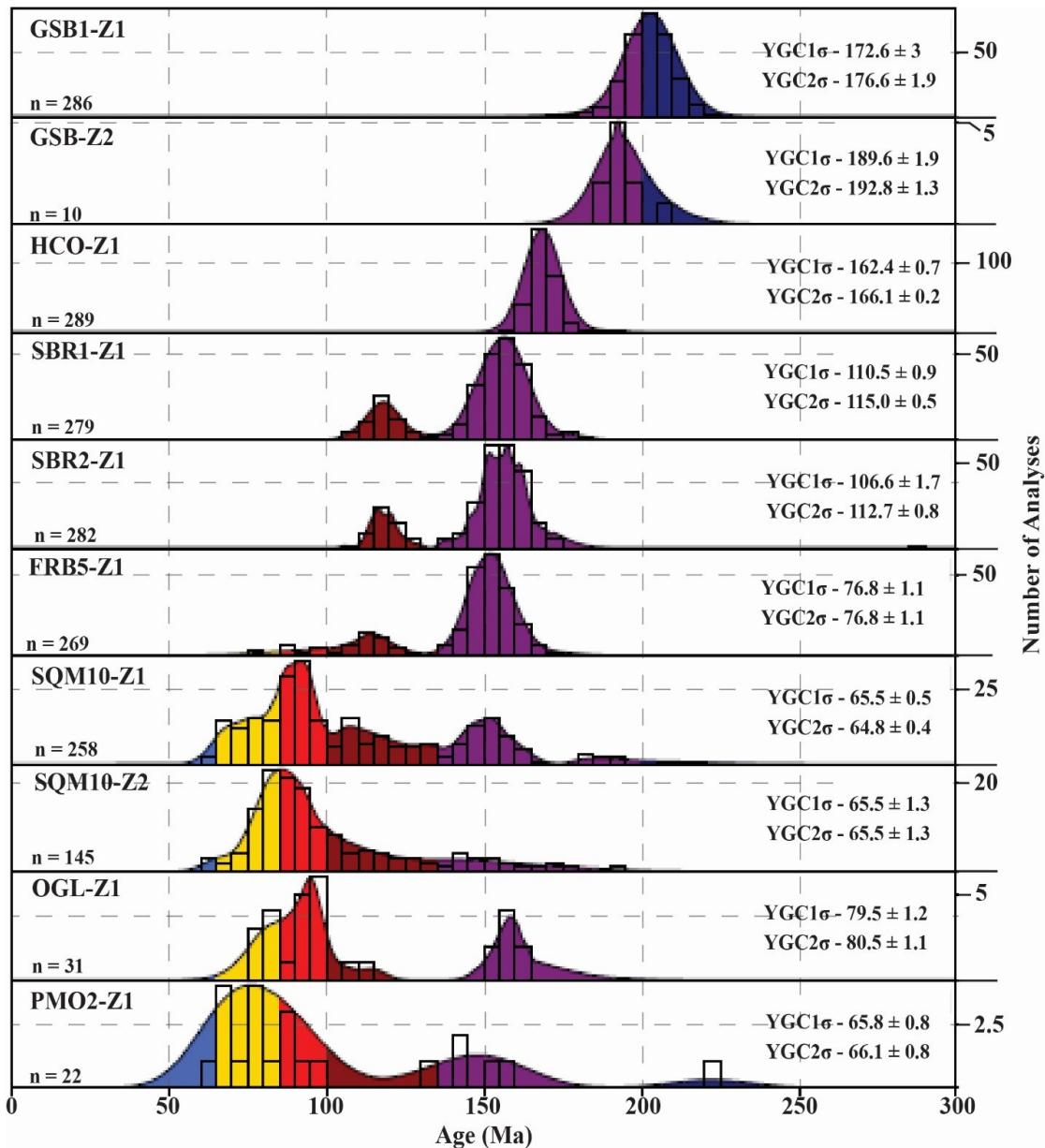
Sample name	GSC Curation number	Stratigraphic Unit	Locality	Lithology	Pollen / spore age/ comments	Dinocyst age/ comments
SBR1-P1	n/a	Longarm Formation Equivalents	50.719166° N 128.083888° W	Sandstone	Not analyzed	Not analyzed
SBR2-P1	n/a	Longarm Formation Equivalents	50.722765° N 128.082378° W	Sandstone	Not analyzed	Not analyzed
SQM10-P6	C-641973	Nanaimo Group Equivalents	50.645166° N 127.254293° W	Mudstone	Campanian or younger	Not analyzed
SQM1-P2	C-641974	Nanaimo Group Equivalents	50.645139° N 127.264809° W	Mudstone	early to middle Campanian or younger	Not analyzed

<b>SQM10-P2</b>	C-641975	Nanaimo Group Equivalents	50.636388° N 127.240555° W	Mudstone	Processed twice for palynology. Both samples yield middle Campanian or younger ages.	Isolated specimens, at least 7 dinocyst taxa; early Santonian–late Campanian
<b>SQM6-P1</b>	C-641976	Nanaimo Group Equivalents	50.642544° N 127.249342° W	Mudstone	Campanian or younger	Not analyzed
<b>SQM10-P1</b>	C-641977	Nanaimo Group Equivalents	50.6363888° N 127.240555° W	Sandstone	Campanian or younger	Not analyzed
<b>FRB7-P1</b>	C-641978	Nanaimo Group Equivalents	50.678966° N 127.357705° W	Sandstone	Effectively barren	late Berriasian to early Aptian
<b>OGL3-P1</b>	C-641979	Nanaimo Group Equivalents	50.608721° N 127.147182° W	Sandstone	Age not determined	late Barremianearly Cenomanian
<b>PMO1-P1</b>	C-641980	Nanaimo Group Equivalents	50.602999° N 127.086727° W	Mudstone	Santonian or younger	late Berriasianearly Aptian
<b>PMO2-P1</b>	C-641981	Nanaimo Group Equivalents	50.602593° N 127.092399° W	Sandstone	Contamination by modern pollen rain	Effectively barren of marine palynomorphs
<b>HCO4-P1</b>	C-641982	Longarm Formation Equivalents	50.612409° N 127.798439° W	Mudstone	Contamination by modern pollen rain	Effectively barren of marine palynomorphs

<b>HCO5-P1</b>	C-641983	Longarm Formation Equivalents	50.612409° N 127.798439° W	Mudstone	Kerogen slide only; contamination by modern pollen rain	Effectively barren of marine palynomorphs
----------------	----------	-------------------------------	-------------------------------	----------	---------------------------------------------------------	-------------------------------------------

**Table 2.2. Detrital zircon data from this study and from Huang (pers. comm., 2024). Ages recorded by the table are given as Youngest Grain Cluster with 1 $\sigma$  overlap (YGC1 $\sigma$ ), and Youngest Grain Cluster with 2 $\sigma$  overlap (YSG2 $\sigma$ ). The total number of zircon in each sample as well as the number of grains used to calculate YGC1 $\sigma$  and YSG2 $\sigma$  MDAs are indicated by “(n=#)” after each age. All ages are presented in mega-annum (Ma) and uncertainties are presented at the 2-sigma level.**

Sample	Location	No. of zircon		YGC1 $\sigma$ (Ma)	YGC2 $\sigma$ (Ma)
<i>This Study</i>					
GSB-Z1	50.67387° N, 127.99184° W	286		172.6 $\pm$ 3.03 (n= 2)	176.6 $\pm$ 1.9 (n= 6)
HCO-Z1	50.608304° N, 127.790132° W	289		162.4 $\pm$ 0.65 (n=18)	166.1 $\pm$ 0.2 (n=160)
SBR1-Z1	50.719166° N, 128.083888° W	279		110.5 $\pm$ 0.93 (n=9)	115.0 $\pm$ 0.5 (n=33)
SBR2-Z2	50.722765° N, 128.082378° W	282		106.6 $\pm$ 1.71 (n=2)	112.7 $\pm$ 0.8 (n=9)
SQM10-Z1	50.639166° N, 127.244166° W	258		65.5 $\pm$ 0.46 (n=6)	64.8 $\pm$ 0.4 (n=7)
<i>From C. Huang (pers. comm., 2024)</i>					
GSB-Z2	50.7384° N, 127.49185° W	10		189.6 $\pm$ 1.91 (n=4)	192.8 $\pm$ 1.3 (n=9)
OGL-Z1	50.60861° N, 127.14688° W	31		79.5 $\pm$ 1.24 (n=5)	80.5 $\pm$ 1.1 (n=8)
FRB5-Z1	50.68673° N, 127.36880° W	269		76.8 $\pm$ 1.15 (n=3)	76.8 $\pm$ 1.1 (n=3)
PMO2-Z1	50.60252° N, 127.08950° W	22		65.8 $\pm$ 0.81 (n=4)	66.1 $\pm$ 0.8 (n=5)
SQM10-Z2	50.63605° N, 127.23526° W	145		65.5 $\pm$ 1.3 (n=5)	65.5 $\pm$ 1.3 (n=6)



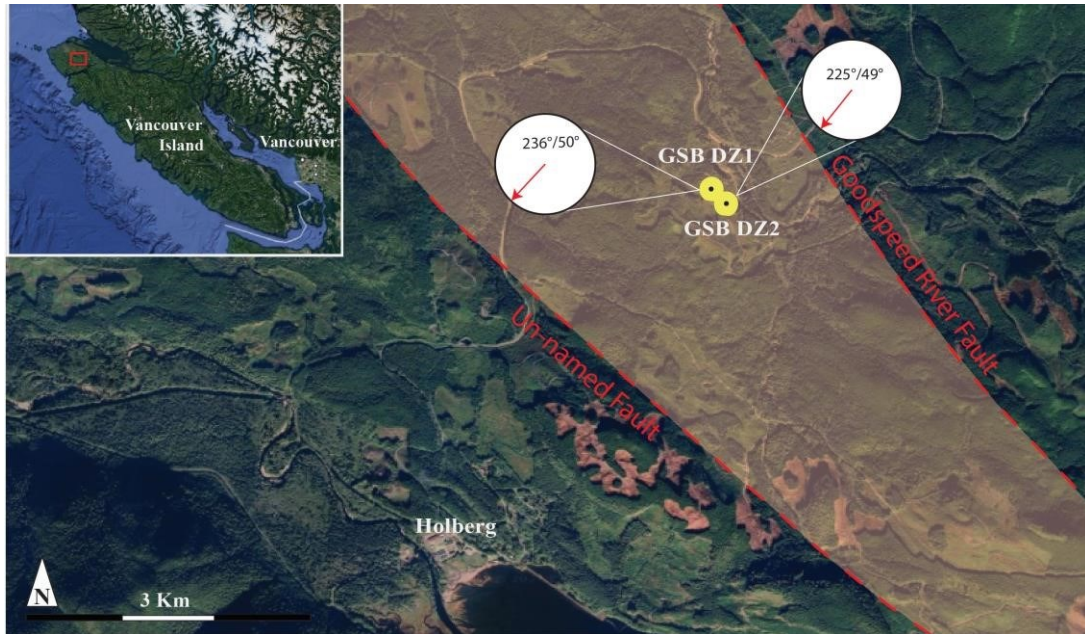
**Figure 2.2.** Probability Density Plots (PDPs) of DZ samples collected for this study and provided by Huang (pers. comm., 2023) generated using DetritalPy. Samples are organised as they appear in the text. Sample names and the number of grains analysed for each sample are shown on the left by (n = #). Two methods of deriving MDAs and their values are displayed on the right. Age distinctions are made by colour, with intervals at 0, 23, 65, 85, 100, 135, 200, and 300 Ma from left to right, corresponding with the colours: gray, royal blue, yellow, red, maroon, purple, and navy. Uncertainties are presented at the 2sigma level.

## 2.4. Mesozoic Data Comparison for North Vancouver Island Strata

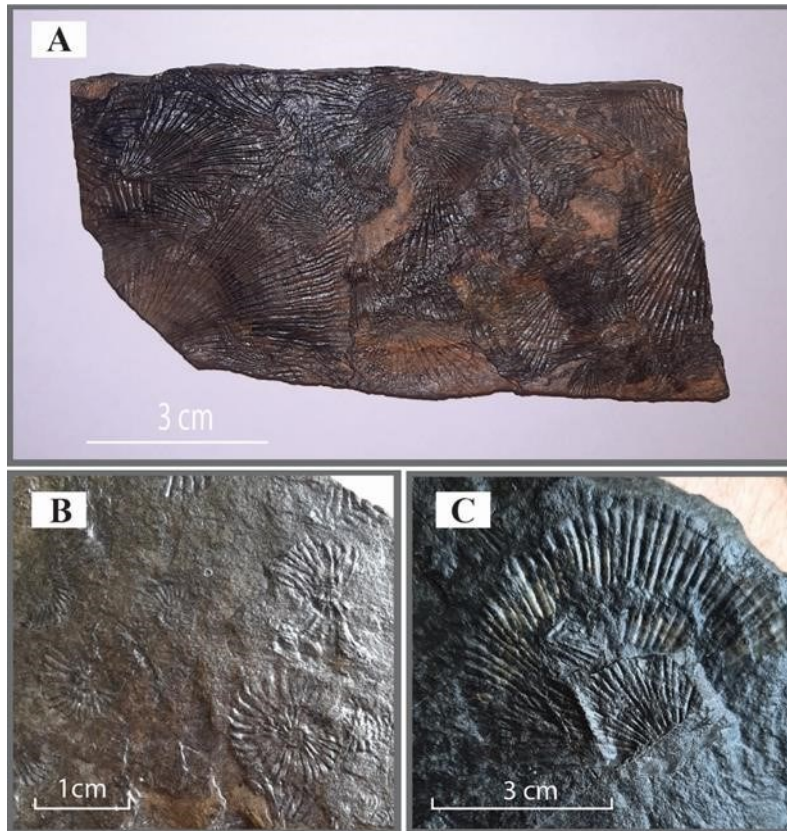
### 2.4.1. Triassic Strata

The Goodspeed Fossil Beds (GSB) are assigned to the Parson Bay Formation (Nixon et al., 2011) and are located approximately 35 km west of Port Hardy on the road to Holberg (Figure 2.3). The Parsons Bay Fm is the dominant Triassic sedimentary strata in NVI and comprises interbedded mudstone and sandstone. The GSB are a succession of high angle, fossiliferous beds. No measured section was generated for this outcrop. The GSB contain abundant *Halobia alaskana* (Figure 2.4A) and *Monotis subcircularis* paper clams (Figure 2.3C), as well as rarer ammonites such as *Choristeras suttonese* and *Sympocyclus gunningi* (?) (Figure 2.4B; Ludvigsen and Beard, 1997). Molluscan and cephalopod species identified in the GSB give a biostratigraphic range of early Carnian to mid-Rhaetian (~237–204 Ma). A single DZ sample (GSB-Z1) taken from sandstone beds in the lower part of the GSB section yields a YGC2 $\sigma$  MDA of  $178.6 \pm 1.9$  Ma (Toarcian; Figure 2.5). A second DZ sample, GSB-Z2, returned a YGC2 $\sigma$  MDA of  $192.8 \pm 1.3$  Ma (Sinemurian; Table 2.2). Sample GSB-Z2 was collected from the same strata that yielded the macrofossils in Figure 2.4 (location: 50.67384° N, 127.49185° W), whereas GSB-Z1 was acquired from strata that appear to be stratigraphically below those from which GSB-Z2 was taken. The exact stratigraphic relation between the strata from which GSB-Z1 and GSB-Z2 were derived remains unknown.

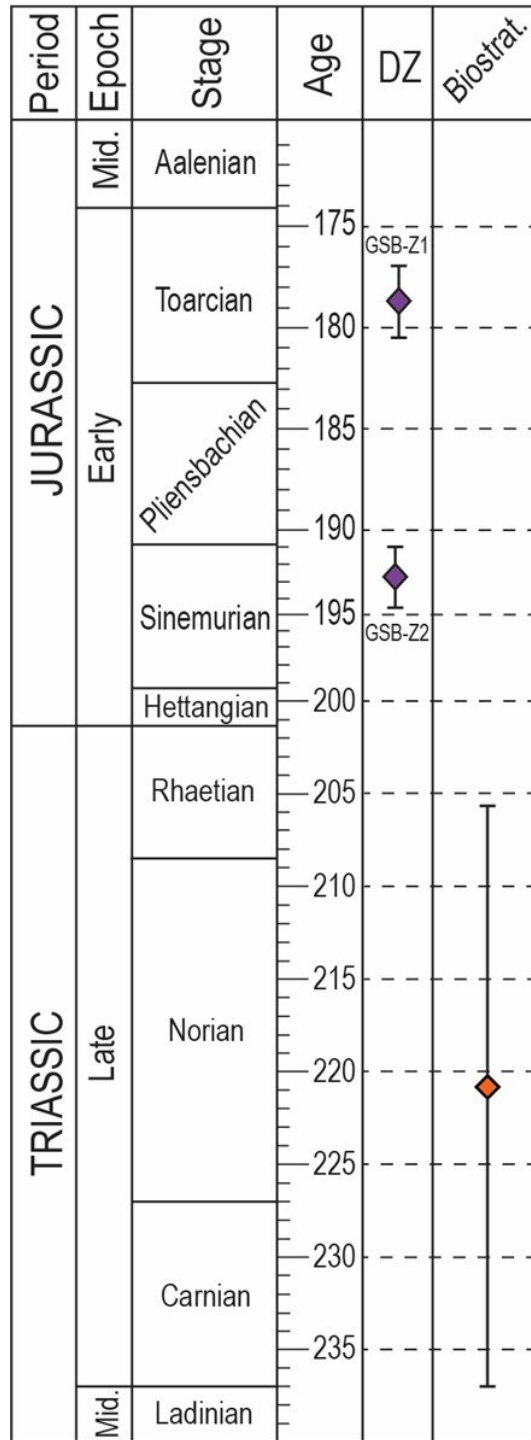




**Figure 2.3.** Map of the Goodspeed Fossil Beds (GSB) location (Courtesy of Google Earth). The inset map shows the position of the larger satellite image relative to Vancouver Island. DZ samples GSB-Z1, GSB-Z2, and the macrofossils depicted in Figure 2.4 derive from this site. The extent of the Triassic Parson Bay Formation is indicated by the semi-transparent orange polygon (after Nixon et al., 2011). These interpreted Triassic strata are bound to the east by the Goodspeed River Fault and to the west by a sub-parallel, unnamed fault.



**Figure 2.4** Photos of fossil samples from the Goodspeed Fossil Beds. A) Numerous *Halobia alaskana* with extensive iron staining. B) A death assemblage of the ammonite *Sympocyclus gunningi*(?). C) A partially pyritized example of the mollusc, *Monotis subcurcularis*. Identifications are based on comparison to photos in Ludvigsen and Beard (1997).



**Figure 2.5** Age data derived from the Triassic Goodspeed Fossil Beds. Purple represents  $YGC2\sigma$  MDAs with uncertainties from samples GSB-Z1 from this study and GSB-Z2 (Table 2.2). Orange represents the age range of first and last appearance of index taxa.

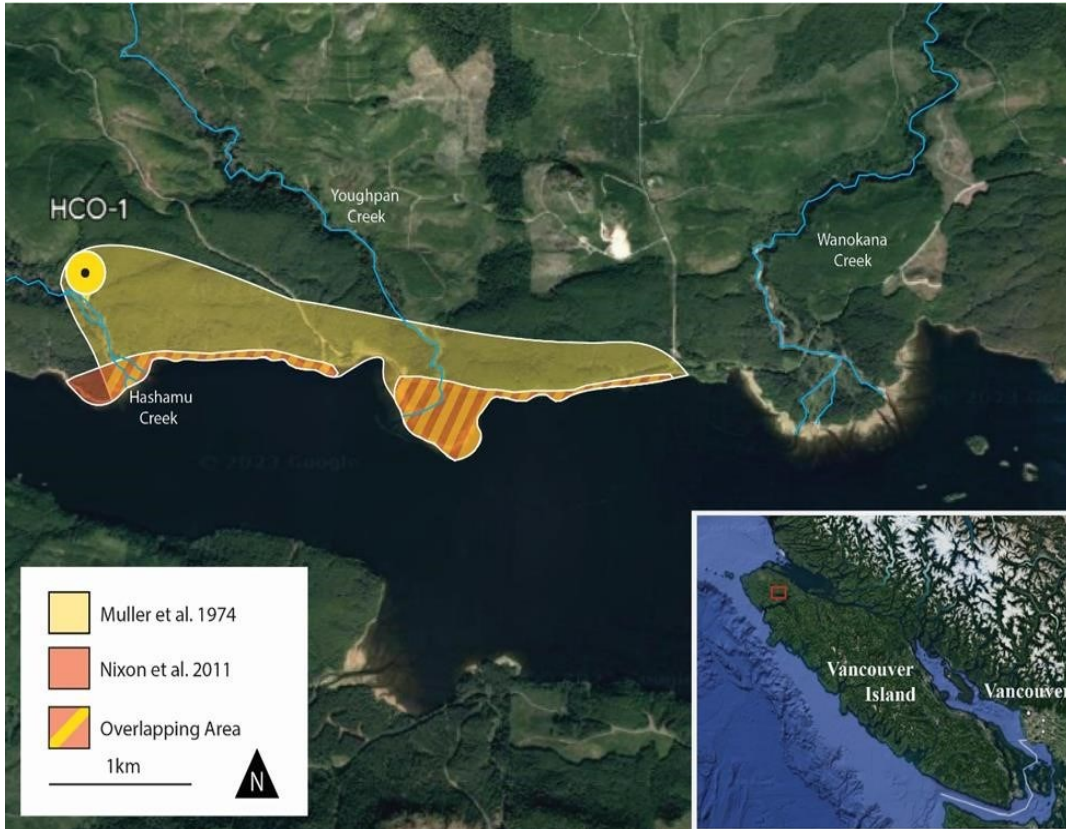
## 2.4.2. Jurassic Strata

Jurassic strata assessed in this study include intervals exposed along Hashamu Creek in Quatsino Sound (50.608304° N, 127.790132° W; Figure 2.6). The location and lithologies of these outcrops were provided by Gwyneth Cathyl-Huhn. The mouth of Hashamu Creek is located approximately 16 km west of Coal Harbour and is on the north shore of Holburg Inlet. Descriptions of this area were produced during previous field expeditions, including Crickmay (1928), Muller et al. (1974), and Nixon et al. (2011). The two latter studies assign different ages to the strata, based on macrofossils found therein.

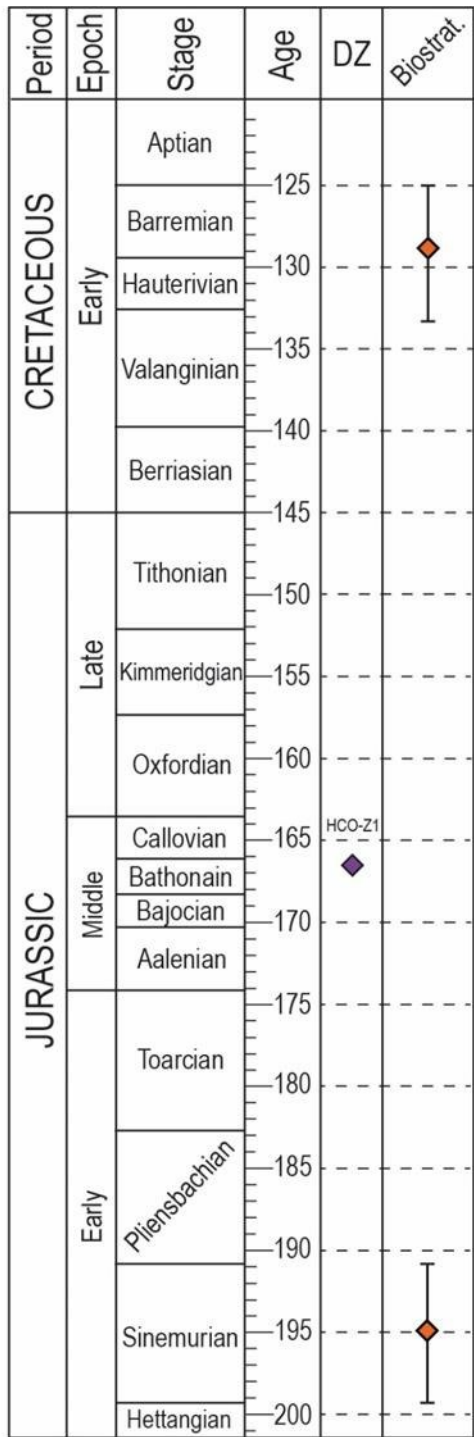
Crickmay (1928) described the strata as being predominantly argillite with minor beds that have a “green cherty quartzite appearance”. Muller et al. (1974) assigned the units to the Jurassic Harbledown Formation, but gave no detailed descriptions to support this. Instead, they interpreted the green, cherty beds described by Crickmay (1928) as being tuffaceous and probably containing the ammonite *Melanippites* (changed from *Melanhippites*), which was later renamed as *Paltechioceras* (Getty, 1973). *Paltechioceras* constrains the age of the Harbledown Formation as 199.3–190.8 Ma (Early to Late Sinemurian; Figure 2.7; Muller et al., 1974). Nixon et al. (2011) reinterpreted these strata based on updated biostratigraphic zonation to be Lower Cretaceous Longarm Formation equivalents and assigned a late Valanginian to early Barremian age (Figure 2.7).

A measured sections were not generated for the strata along Hashamu Creek, because the outcrop sections are short, difficult to access safely, and separated by numerous high angle faults and covered sections. Small sections of outcrop with similar characteristics (e.g., lithology, bed thickness, and the presence of minor coal seams) were present between the mouth of Hashamu Creek and the most upstream sections identified. The sedimentary strata along Hashamu Creek extend beyond the mapped area and were ascribed to Longarm Formation equivalents by Nixon et. al. (2011), suggesting that these strata have a greater extent than what has been mapped. Numerous high-angle faults crosscut the strata but the attitude of these faults could not be measured due to the lack of accessibility. Larger faults that separate exposed outcrop sections may also be present. Detrital zircon sample HCO-Z1 was taken from near the

mouth of Hashamu Creek (Table 2.2) and returned a YGC2 $\sigma$  MDA of  $166.1 \pm 0.2$  Ma (Bathonian to Callovian; Figure 2.7).



**Figure 2.6** Satellite image of the Hashamu Creek outcrop area and extent of previously mapped strata therein (Courtesy of Google Earth). The yellow polygon represents the extent of the strata interpreted as the Jurassic Harbledown Formation by Muller et al. (1974). The red polygon demarcates the extent of the same strata as mapped by Nixon et al. (2011), but interpreted as the Lower Cretaceous Longarm Fm. The contact with the surrounding geology from Nixon et al. (2011) is an inferred unconformity. Hashamu Creek and other significant creeks are highlighted in blue, and the location of DZ sample HCO-Z1 is shown.



**Figure 2.7** Age data deriving from Mesozoic strata of Hashamu Creek. Purple indicates the YGC2 $\sigma$  MDA with uncertainties derived from DZ sample HCO-Z1. Orange indicates biostratigraphic ages based on the first and last appearances of index taxa. The Sinemurian age is based on Muller et al. (1974) and the Valanginian to Barremian age is based on Nixon et al. (2011).

### 2.4.3. Lower Cretaceous Strata

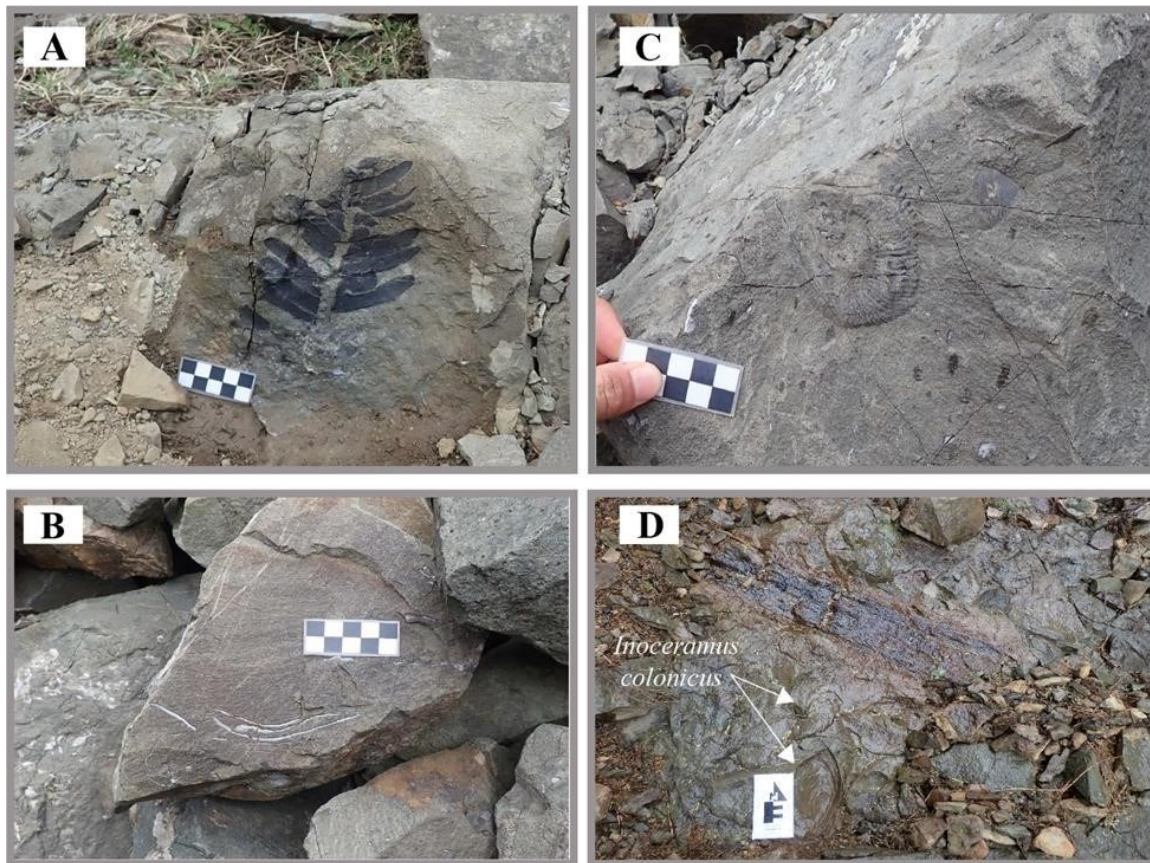
Lower Cretaceous strata in this study includes intervals exposed near Strandby River (Figure 2.8) that Muller and Jeletzky (1970) and Jeletzky (1976) describe as Valanginian- to Aptian-aged “Longarm Formation equivalents”. Two outcrop sections were assessed (SBR-1 and SBR-2; Figure 2.8). Longarm Formation-equivalent strata are bound to the southwest by the Strandby River Fault. The remaining boundaries of these strata are an inferred nonconformity over the Upper Triassic to Middle Jurassic Bonanza Group. Some of the bedrock geology for this part of NVI is inferred, based on published maps.



**Figure 2.8** Satellite imagery of outcrop locations of Longarm Formation equivalents near Strandby River (Courtesy of Google Earth). The grey polygon represents the mapped extent of Lower Cretaceous strata in this area (Nixon et al., 2011). All contacts for this polygon are inferred nonconformities with the exception of the Strandby River Fault, which is represented by the dashed red line.

The first outcrop, SBR-1 ( $50.719335^{\circ}$  N,  $128.083958^{\circ}$  W), is exposed in a quarry pit used for road construction. The outcrop in the quarry is isolated and its association with nearby strata is unknown. Additionally, strata in the pit are poorly bedded and showed no easily recognizable surfaces for measuring bedding dips or producing a measured section. The strata in the pit comprise mainly lower fine- to lower mediumgrained, well sorted, grey sandstone, and contain *Inoceramus colonicus*(?) as

well as an unidentified ammonite with a morphology suggestive of being Early Cretaceous(?) (Haggart pers. comm., 2022 Figures 2.9B and C respectively) and a fern fossil that remains unidentified at this time (Figure 2.9A). The trace fossil *Ophiomorpha* isp., mudstone rip up clasts, and woody carbonaceous material are also present in SBR-1. DZ sample SBR1-Z1 (Table 2.2) and palynology sample SBR1-P1 were taken from this location.



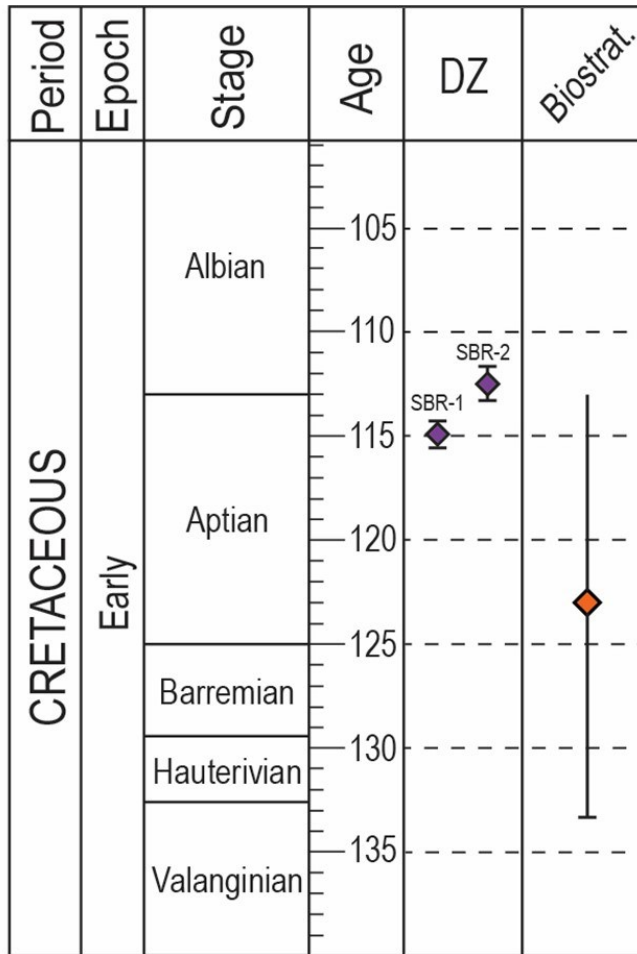
**Figure 2.9** Images from the two outcrops of Longarm Formation-equivalent strata along the Strandby River. A) Unidentified fern fossil from site SBR-1. The fern is presumably parallel to bedding but the bedding orientation remains uncertain. B) Unidentified ammonite from SBR1. The ammonite's morphology is suggestive of a Lower Cretaceous(?) origin (Haggart, pers. comm., 2022). C) *Inoceramus colonicus*(?) (Haggart pers. comm., 2022) in sandstone. D) Coalified tree limb and numerous *Inoceramus colonicus* (?) fossils in sandstone.

The second outcrop of Longarm Formation-equivalents, SBR-2 (50.722765° N, 128.082378° W; Figure 2.8), is situated in an area of inferred Lower Cretaceous strata.



SBR-2 also has poorly defined bedding and little or no lithological contrast; hence, no measured section was produced. This site has abundant *Inoceramus colonicus*(?) (Haggart, pers. comm., 2022) as well as carbonaceous detritus and coalified material (Figure 2.9D). Detrital zircon SBR2-Z2 (Table 2.2) was taken from this location.

Two YGC2 $\sigma$  MDAs were produced from the Strandby River DZ samples (Table 2.2, Figure 2.10). The MDAs establish an oldest age of  $115 \pm 0.46$  Ma and  $112.7 \pm 0.8$  Ma for sites SBR-1 and 2, respectively (Figure 2.10). Given the close proximity of the two sites as well as the presence of *Inoceramus colonicus*(?) at both locations, the DZ and biostratigraphic age data establish that the two sites are probably conformable, with SBR-2 being slightly younger than SBR-1. Palynology samples taken from these sites returned no usable data for the purpose of dating strata or comparison to palynological data from equivalent strata in Haida Gwaii and southern/central Vancouver Island.



**Figure 2.10. Sedimentary strata ages and the methods of deriving them from Strandby River locations, NVI. Purple represents DZ YGC2 $\sigma$  MDAs and associated uncertainties. Orange represents the biostratigraphic age presented by Jeletzky (1976) and others (Haggart and Tipper, 1994; Nixon et al., 2011).**

#### 2.4.4. Upper Cretaceous and Younger Strata

Upper Cretaceous and younger strata include numerous outcrops exposed along the coast in the Port Hardy-Port McNeill area (Figure 2.11), NVI. These strata are interpreted and mapped by Nixon et al. (2011) as being Campanian to ?Maastrichtian in age and locally comprise medium- to coarse-grained sandstone, pebble to cobble conglomerate, siltstone, and minor coal with rare, more laterally continuous coal beds. Several outcrop areas were identified, logged, and sampled in this study, including (from NW to SE): Fort Rupert Beach (FRB), Suquash Mine (SQM); Orca Gravel Loader (OGL), and Port McNeill Outcrops (PMO; Figure 2.11). The biostratigraphic ages for these strata are based on macrofossil identification at outcrop sites along and adjacent

to the Keogh River (Muller and Jeletzky, 1970). This study first identified placenticeratid fossil material that attributed these strata to the Upper Campanian *Metaplacenticeras cf. pacificum* zone (Haggart and Graham, 2018; Figure 1.9). Macrofossil evidence from subsequent study of this area (Ward, 1978; Nixon et al., 2011; Haggart and Graham, 2018) has extended the biostratigraphic extent of Suquash OA strata from the Campanian to ?Maastrichtian. All strata in the Port Hardy-Port McNeill area are mapped and presented as residing within this age range in Nixon et al. (2011).



**Figure 2.11. Map showing the location of outcrop areas within the Suquash SubBasin, including Fort Rupert Beach (FRB), Suquash Mine (SQM), Orca Gravel Loader (OGL), and Port McNeill Outcrops (PMO). The grey area depicts the mapped extent of the Suquash Sub-Basin (Nixon et al., 2011). The red and yellow dashed lines show the inferred contacts of the Suquash Sub-Basin with surrounding bedrock.**

At Fort Rupert Beach (FRB), several measured sections were generated (Appendix A; Figure 2.11), including FRB 3, 4, 6.5, and 7/7A (Table 2.3). Outcrops at FRB are laterally discontinuous and show significant weathering and cover by intertidal sediment, plants and extant sea life. This generally obscures identifiable sedimentological and ichnological features. The exposed strata of FRB also appear to form a NE-plunging, shallowly dipping syncline, where the most southeasterly outcrops

FRB-6.5 and 7 form one limb of the syncline and the most northerly outcrops, FRB-3, 4, and 5, form the other limb (Fig. 2.12). This structure was also noted by Muller and Jeletzky (1970).



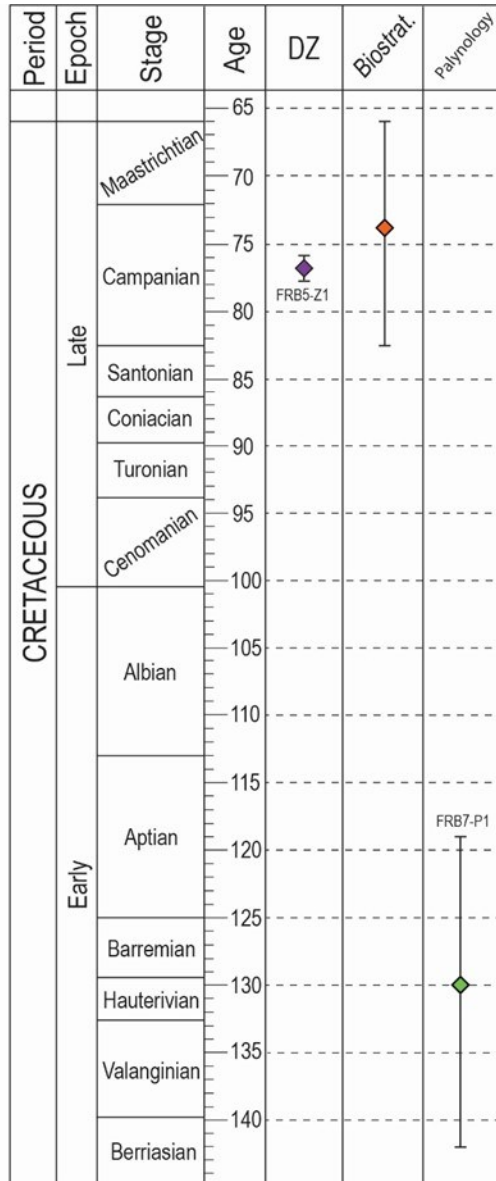
**Figure 2.12. Aerial map of Fort Rupert Beach (FRB) site with outcrop locations highlighted. Dip, and dip direction, for each outcrop is shown in white circles and the axis of the apparent dipping syncline is shown between FRB5 and FRB 6.5. Inset map shows Figure 2.11 with FRB outcrop locations highlighted and relative position on Vancouver Island.**

Biostratigraphic sampling from strata nearby the FRB outcrop sections by Muller and Jeletzky (1970) revealed fossil material which attributed these strata to the *Metaplacenticeras cf. pacificum* zone of the Upper Campanian. No fossil evidence was identified in these strata for the use of biostratigraphic dating, nor were the original outcrop sections described by Muller and Jeletzky able to be located. Sampling in the FRB sections was limited to measured section FRB-7/7A where a palynology sample (FRB-FS1) was taken. FRB7-P1 was effectively barren of pollen and spores, but dinocysts present in the sample returned an age of Late Berriasian to Early Aptian (Table

2.1). A DZ sample from these strata (FRA-Z1; Table 2.2) returned a YGC2 $\sigma$  age of 76.8  $\pm$  1.2 Ma (Campanian; C. Huang, pers. comm., 2024) The location of FRB5-Z1 (50.68673° N, 127.36880° W) corresponds most closely to outcrop location FRB 5 (no measured section; Figure 2.12). A direct age comparison for data collected from these outcrops is shown in Figure 2.12.

**Table 2.3. Outcrop locations where measured sections were described at Fort Rupert Beach (FRB). Table includes outcrop location data, bedding orientation, and the location and stratigraphic position of samples taken within each section. A map of outcrop locations relative to one other and to Vancouver Island is shown in Figure 2.12.**

Outcrop Name	Section Height (m)	Dip/ Dip Direction	Base of Section	Sample / Section Height	Sample Location
Fort Rupert 3	1	13°/092°	50.689556° N, 127.375806° W	N/A	N/A
Fort Rupert 4	2.25	13°/052°	50.688806° N, 127.371056° W	N/A	N/A
Fort Rupert 5	3	7°/141°	50.686861° N, 127.368972° W	FRB5-Z1	50.686861° N, 127.368972° W
Fort Rupert 6.5	7.5	11°/345°	50.685861° N, 127.366694° W	N/A	N/A
Fort Rupert 7/7A	16.9	11°/357°	50.682194° N, 127.357694° W	FRB7-P1: 1 m	50.682194° N, 127.357694° W



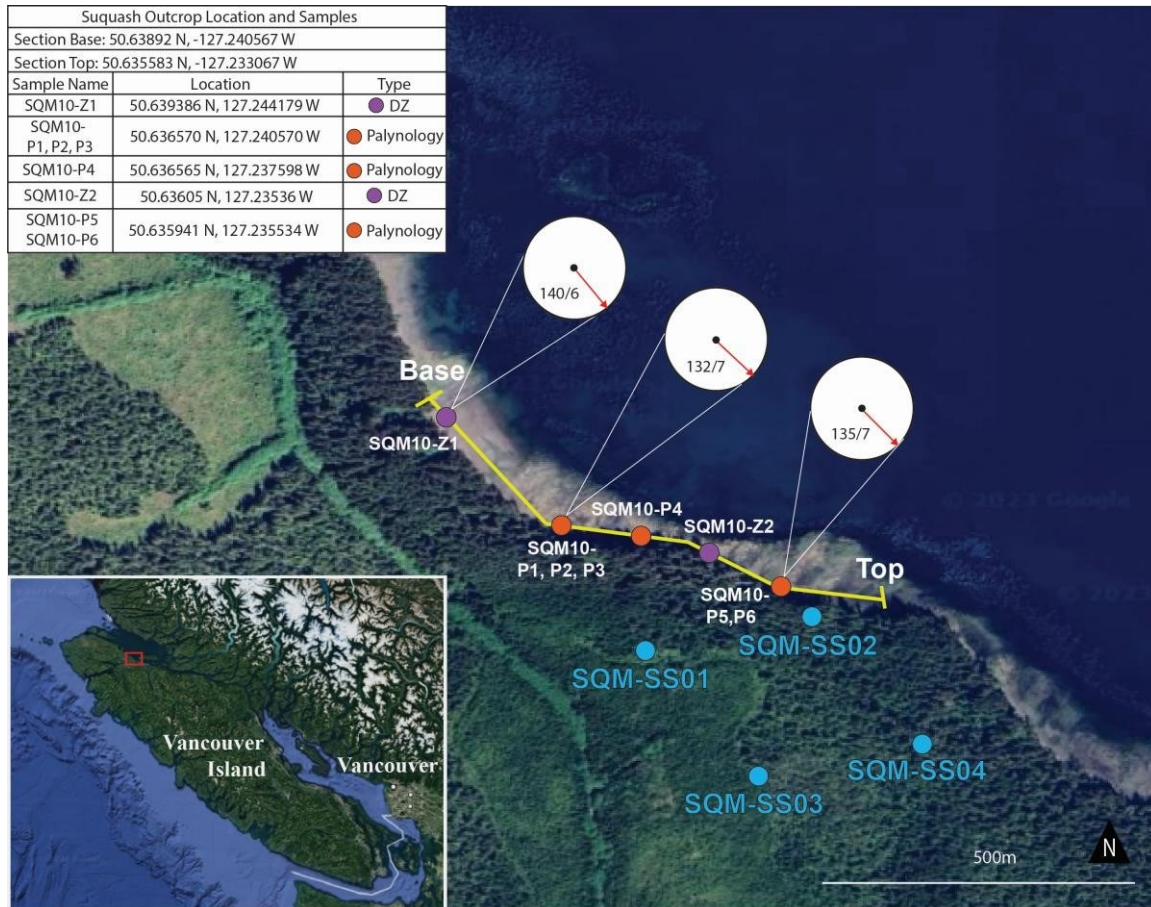
**Figure 2.13 . The age of sedimentary strata at Fort Rupert Beach and the methods used to derive them. Purple represents DZ YGC2 $\sigma$  MDAs along with uncertainties for sample FRA-Z1 (C. Huang, pers. comm., 2024; Table 2.2). Orange represents biostratigraphic ages based on work by Nixon et al. (2011), and green represents palynological ages based on pollen, spores, and dinocysts presented in Galloway et al. (2023) (Table 2.1).**

Suquash Sub-Basin strata were also logged at the Suquash Coal Mine (SQM) site (Figure 2.14), and these strata represent the most significant and continuous outcrops in the sub-basin. More than a dozen outcrop sections were identified, and 10 samples were collected for palynology and/or geochronology (Table 2.3). The most significant and most-sampled section, SQM-10, is compiled into a graphic litholog with a

full description of lithology, sedimentary structures, lithologic accessories, bioturbation index, and trace fossils (Figure 2.15).

Significant portions of measured section SQM-10 contain trace fossils indicative of marine influence, including *Ophiomorpha* (Op; Figure 2.16B), Planolites (Pl), and Thalassinoides (Th). Mudstone-dominated and coal-bearing strata that contain rootlets and are burrowed at the top with Thalassinoides from the overlying unit (Figure 2.16A) are interpreted as recording deposition in a terrestrial, near-coast setting. These inferred terrestrial strata were sampled for palynology and include samples SQM10-P1, SQM10-P2, SQM10-P3, SQM10-P4, SQM10-P5, and SQM10-P6 (Tables 2.1 and 2.4). Thick, coarse-grained sandstone intervals overlie the inferred terrestrial mud beds and coals. The sandstone intervals are mainly trough-cross stratified (Figure 2.17A, B), may constitute potential channel bars (Figure 2.18A, B), and contain a low abundance and diversity of trace fossils (Figure 2.15).

Electra Gold Company drilled four exploratory wells in the Suquash Coal Mine property in 2008. The physical cores have been destroyed since, but written descriptions of the lithology were recorded and are digitised for this study. The locations of these wells relative to one other and the SQM-10 measured section are shown in Figure 2.14. Although little detail is recorded in the Electra Gold descriptions, they offer insights into the subsurface lithology. For the purpose of this thesis, and for simplicity, these wells have been renamed as: SQM-SS01, SQM-SS02, SQM-SS03, and SQM-SS04, wherein SS indicates subsurface. Graphic lithologs of the three shallower wells (SQM-SS01, SS02, and SS03) are shown in Figure 2.19. The fourth well (SQM-SS04; Figure 2.20) is significantly deeper and penetrates the entire sedimentary sequence at the site, reaching the contact with the Karmutsen Formation basement.

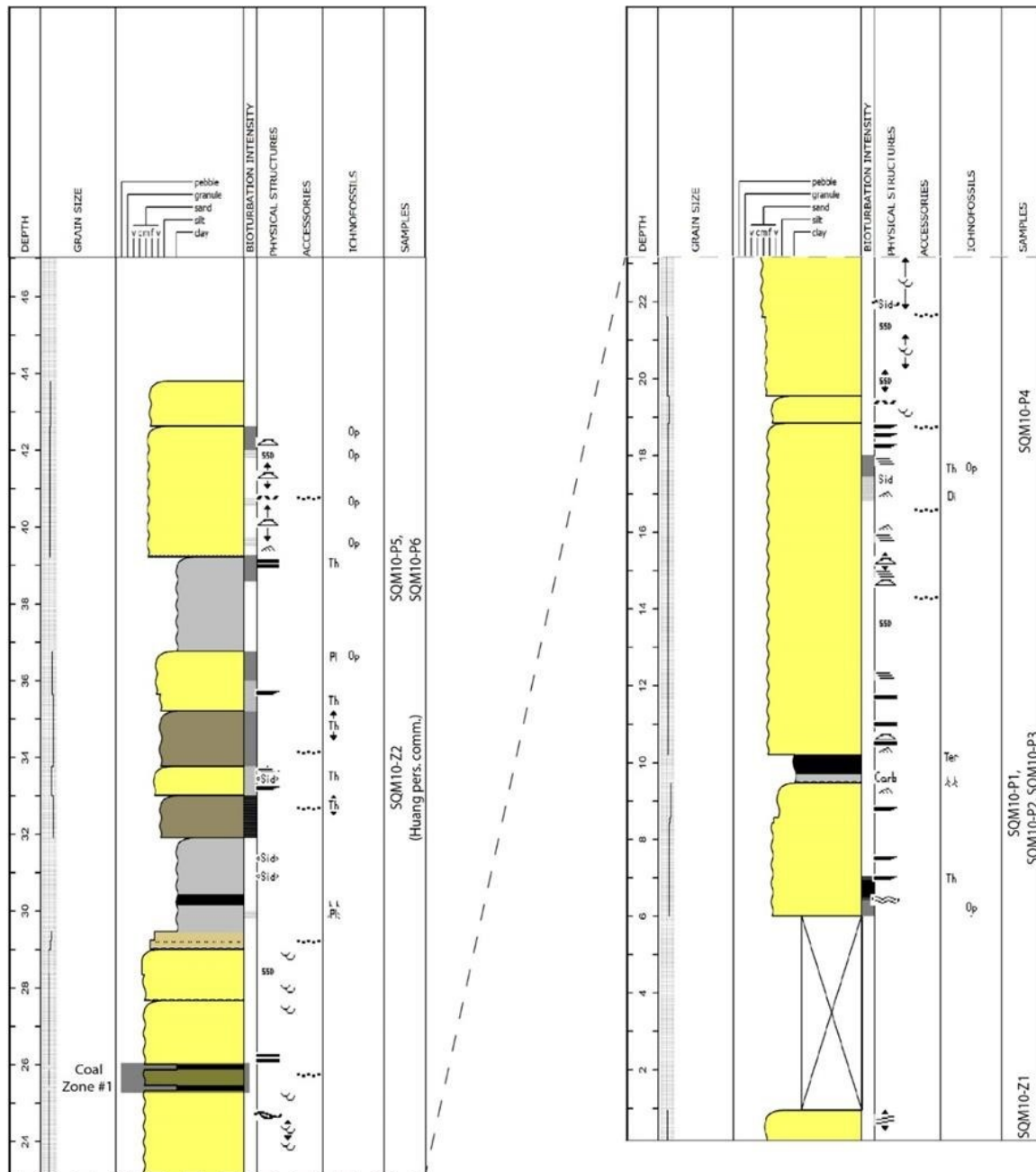


**Figure 2.14** Aerial map of the Suquash Mine Site (Courtesy of Google Earth), including measured section SQM-10 (yellow line), wellbores drilled by Electra Gold Company in 2008 (Blue sites labelled SQM-SS#), palynology sample locations (orange circles), and detrital zircon sample locations (purple circles). Measured dip, and dip direction are shown in the white circles.

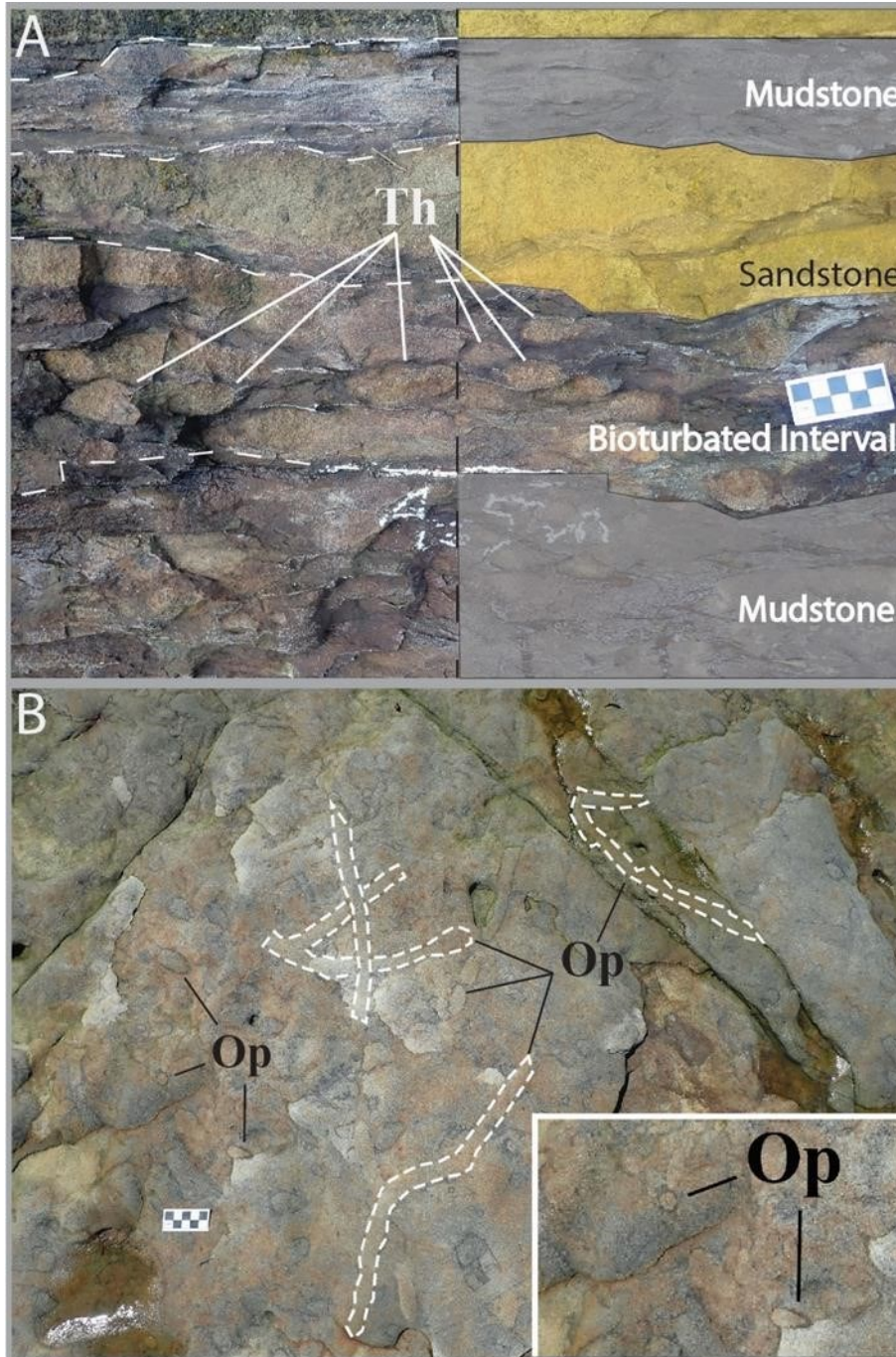


**Table 2.4. List of measured outcrop sections and samples from the Suquash Coal Mine (SQM) site. Location data as well as bedding orientations for outcrop sections are included. Sample data include location as well as stratigraphic height within the relevant measured section.**

Outcrop Name	Section Height (m)	Dip/Dip Direction	Base of Section	Sample/ Section Height	Sample Location
SQM-1	2.5	3□/252□	50.645083° N, 127.255056° W	SQM1-P1: 70 cm	50.645167° N, 127.254306° W
				SQM1-P2: 1.5 m	50.645139° N, 127.254806° W
SQM-5	10.75	11□/218□	50.641972° N, 127.249833° W	N/A	N/A
SQM-6	22.55	13□/131□	50.641972° N, 127.249833° W	SQM6-P1: 4.75 m	50.642556° N, 127.249333° W
SQM-10	43.75	6□/140□ measured at base.	50.638722° N, 127.24375° W	SQM10-Z1: 40 cm	50.638722° N, 127.24375° W
				SQM10-P1, SQM10-P2 & SQM10-P3: 9.6 m	50.636583° N, 127.240583° W
		SQM10-P4: 19.3 m		50.636556° N, 127.237611° W	
		SQM10-P5 & SQM10-P6: 38.6 m		50.635944° N 127.235528° W	
		7□/132□ measured at 24 m			



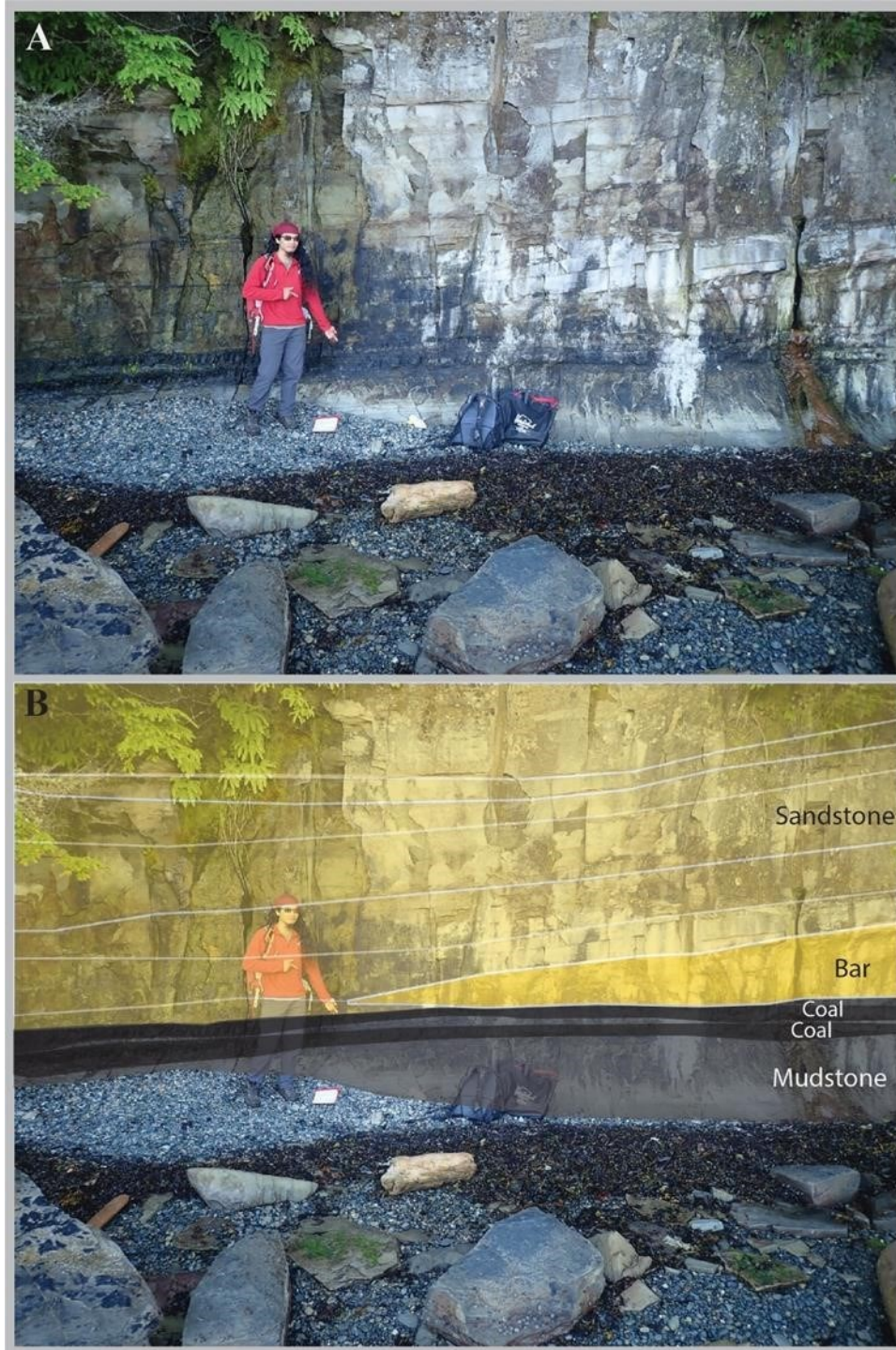
**Figure 2.15. Outcrop measured section SQM-10. Stratigraphic heights of DZ samples SQM10-Z1, SQM10-Z2 and palynology samples SQM10-P1, P2, P3, P4, P5, and P6 are indicated. Coal zone 1 (CZ 1) is highlighted with the grey rectangle and serves as one of several datums in subsurface correlations. The base of the measured section is at 50.638722 N, 127.24375 W, and the top of the section is at 50.635583 N, 127.233056 W. The location of the measured section is shown in Figure 2.14 and the legend for this measured section is in Figure 2.1, depths are shown in meters.**



**Figure 2.16. Trace fossils in measured section SQM-10. Scale bar increments are 1 cm. A) Mudstone interval in which the top has been extensively burrowed with *Thalassinoides* (Th) that extend from the overlying unit. B) Plan view to oblique exposure of a sandstone bed pervasively bioturbated with *Ophiomorpha* (Op and white outlines) inset image is zoomed to highlight pelleted margins.**



**Figure 2.17. A) Outcrop at SQM-10 showing a thick sandstone interval overlying a mudstone interval and B) with an interpretation of the section. The sandstone bed displays trough cross-stratification and migration of what are interpreted as stacked bars within a fluvial or estuarine channel, which crosscuts the underlying coastal plain. These beds overlie what is interpreted as terrestrial mudstone, and the sandstone interval extends from 38–43 m in SQM-10 (Figure 2.15). C. Huang (1.75 m in height) for scale.**



**Figure 2.18. A) Channel-related structures present in measured section SQM-10, and B) with an interpretation of the section. The sandstone bed overlies mudstone and coal beds and is situated between 26 and 30 m in SQM-10 (Figure 2.15). The section is interpreted to record deposition in a terrestrial, near-coast setting. C. Huang (1.75 m in height) for scale.**

Ages for the strata in SQM-10 are derived from palynological and DZ samples taken from multiple positions along the outcrop (Figure 2.14). Palynology samples (Table 2.1) taken from SQM-10 return ages ranging from Early Campanian to Maastrichtian (or younger), which aligns with the biostratigraphically established Campanian to ?Maastrichtian age assigned by Nixon et al. (2011). Detrital zircon sample SQM10-Z1 was taken at the base of SQM-10 from a clean sandstone with minimal weathering and high preservation potential for zircon grains. That sample returned a YGC2 $\sigma$  MDA of  $64.8 \pm 0.4$  Ma and establishes an earliest Paleogene (Danian) age for the strata (Table 2.2). A second sample, SQM10-Z2, was collected from SQM-10 at approximately 33.5 m stratigraphic height (Figure 2.13) and returned a YGC2 $\sigma$  MDA of  $65.5 \pm 1.3$  Ma (C. Huang, pers. comm., 2024; Table 2.2), which is also early Danian. A comparison of age data from this site is shown in Figure 2.21.

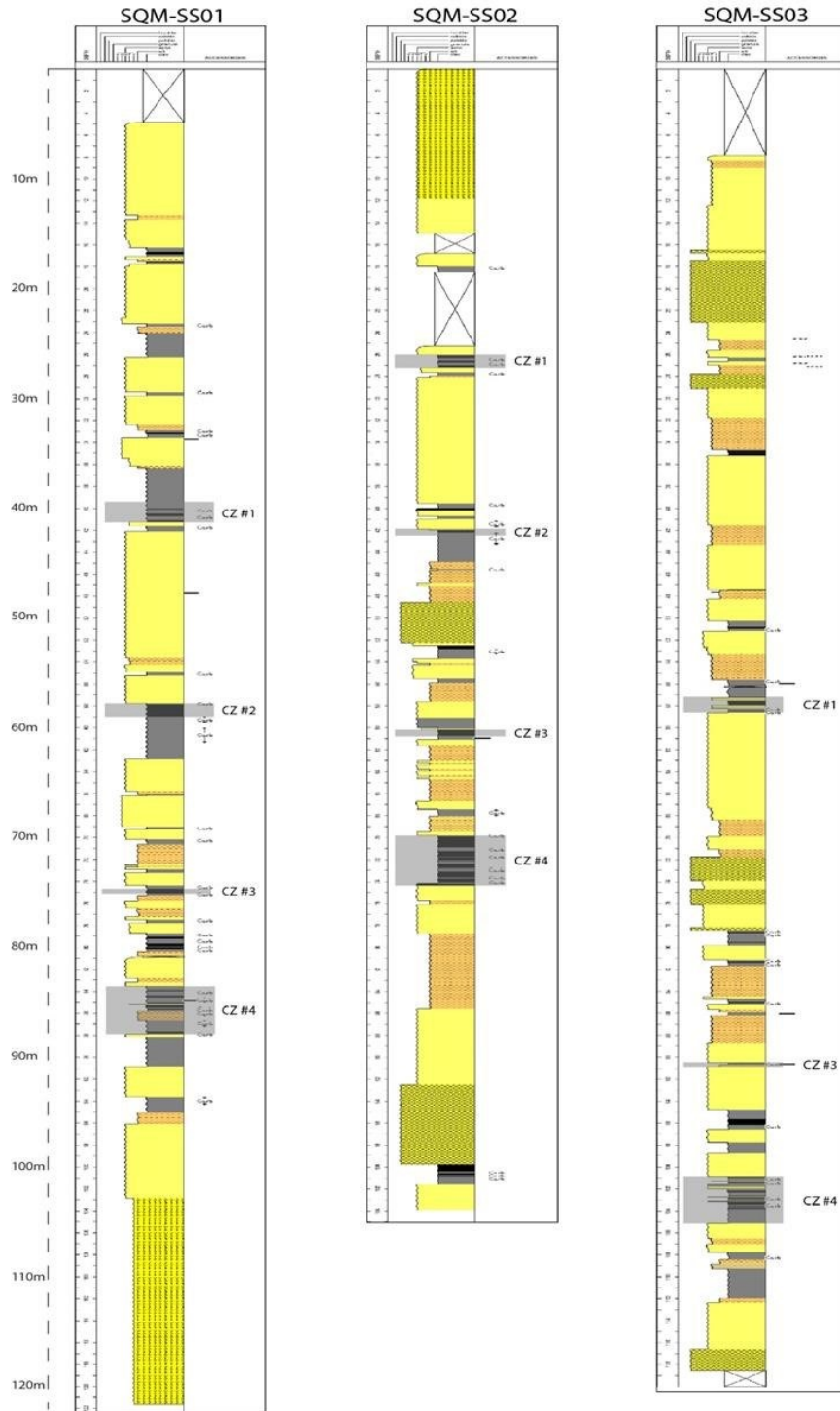
Correlation of strata in the SQM-SS wells to measured section SQM-10 is achieved using coal zones as datums (Figure 2.22). Four Coal Zones (CZ1–CZ4) are chosen as datums, with the top of CZ4 being the primary datum for correlating strata. CZ1 is used to correlate the outcrop SQM-10 section to the subsurface sections, and CZ2 and CZ3 are used to test the reliability of correlations made using CZ4 and CZ1. Note that numbered coal zones were identified by the Electra Gold Company, but that no supporting basis for correlating these zones between wells was given. Consequently, coal zones are renumbered based on stratigraphic correlations.

Coal Zone 4 is the most significant datum in terms of overall coal thickness (and therefore, inferred areal extent) and is present in all four wells (Figure 2.22). CZ4 represents several metres of fine-grained strata interbedded with coal beds of varying thickness. Coal Zone 1 is identified in measured section SQM-10 as two distinct coal beds within a series of stacked sandstone beds possessing trough cross-stratification. These same coal beds are identified in all four wells, enabling correlation of CZ1 from outcrop to subsurface. Coal Zone 2 is a significant coal in the lower part of measured section SQM-10 and is present in wells SQM-SS01 and SQM-SS02. CZ2 is sub-parallel to CZ1 and CZ4 but is not present in all wells. The relationship of CZ2 to adjacent strata in SQM-10 suggests that channel migration within the paleoenvironment may have removed CZ2 through erosion in SQM-SS03 and SQM-SS04. CZ3 is present in

SQMSS01, SQM-SS02, and SQM-SS03, but is situated below SQM-10 and is not present in

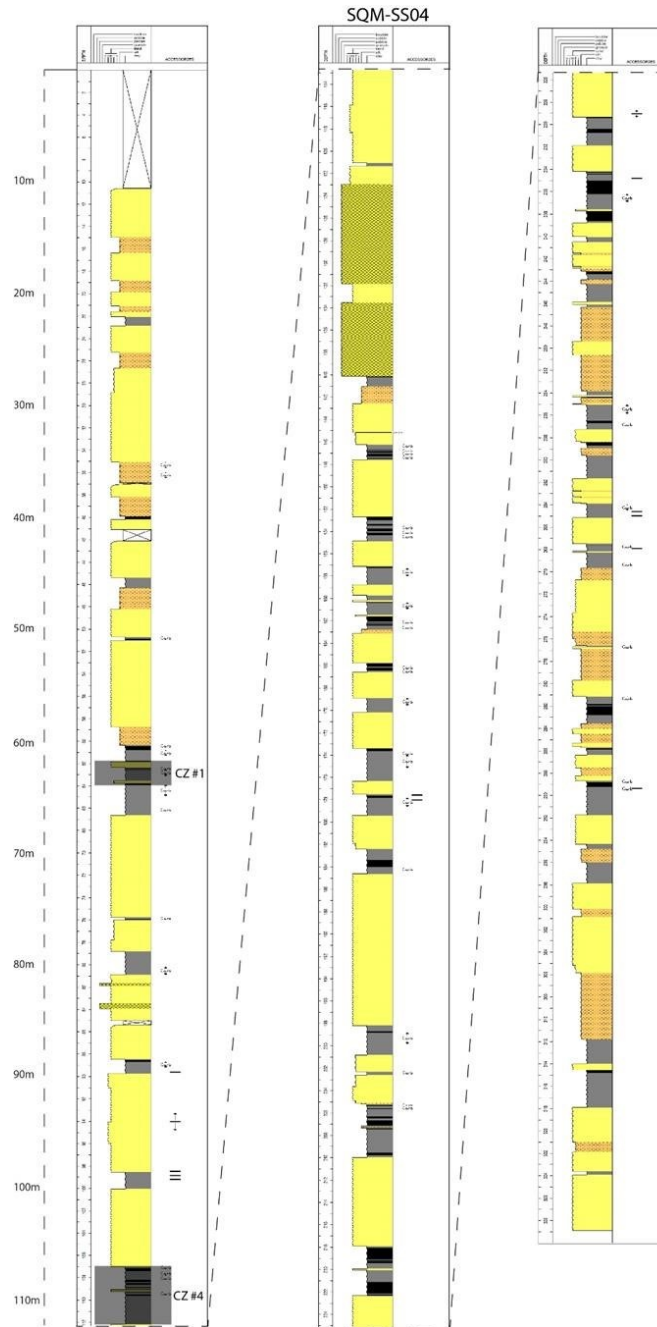
SQM-SS04. CZ3 is sub-parallel to CZ1 and CZ4 but appears to be a less regionally extensive coal interval. Alternatively, the presence of a large sand body at the stratigraphic height of CZ3 in SQM-SS04 may indicate its erosion by migrating channels within the depositional system. Many other minor coals are recorded in the SQM-SS wells. In some cases, these can be correlated between two wells but are not sufficiently regionally extensive to be considered as datums.

Interpretations of migrating channels have been made in SQM-10, based on stacked sequences of coarse-grained, trough cross-stratified sandstone (Figure 2.17), which are interpreted to mainly reflect migrating channel bars (Figure 2.18). These channel bars eroded into underlying mudstone and coal and removed previously deposited material. Where similar lithological relationships are observed in the subsurface logs, the removal of mudstone and coal is interpreted to have resulted from channel migration and erosion.



**Figure 2.19. Graphic lithologies of the SQM-SS01, SQM-SS02, and SQM-SS03 wells drilled in the Suquash Coal Mine site in 2008 by the Electra Gold Company. Coal zones (CZ #) that are used as orienting datums are highlighted in grey polygons. The legend for this figure is shown in Figure 2.1 and the location of the individual wells is shown in Figure 2.14.**





**Figure 2.20. Graphic litholog of the SQM-SS04. Coal zones are highlighted by grey polygons. The legend for this figure is shown in Figure 2.1 and the location of this well is shown in Figure 2.14. SQM-SS04 intersects the basement (Karmutsen Fm) at ~329 m depth.**

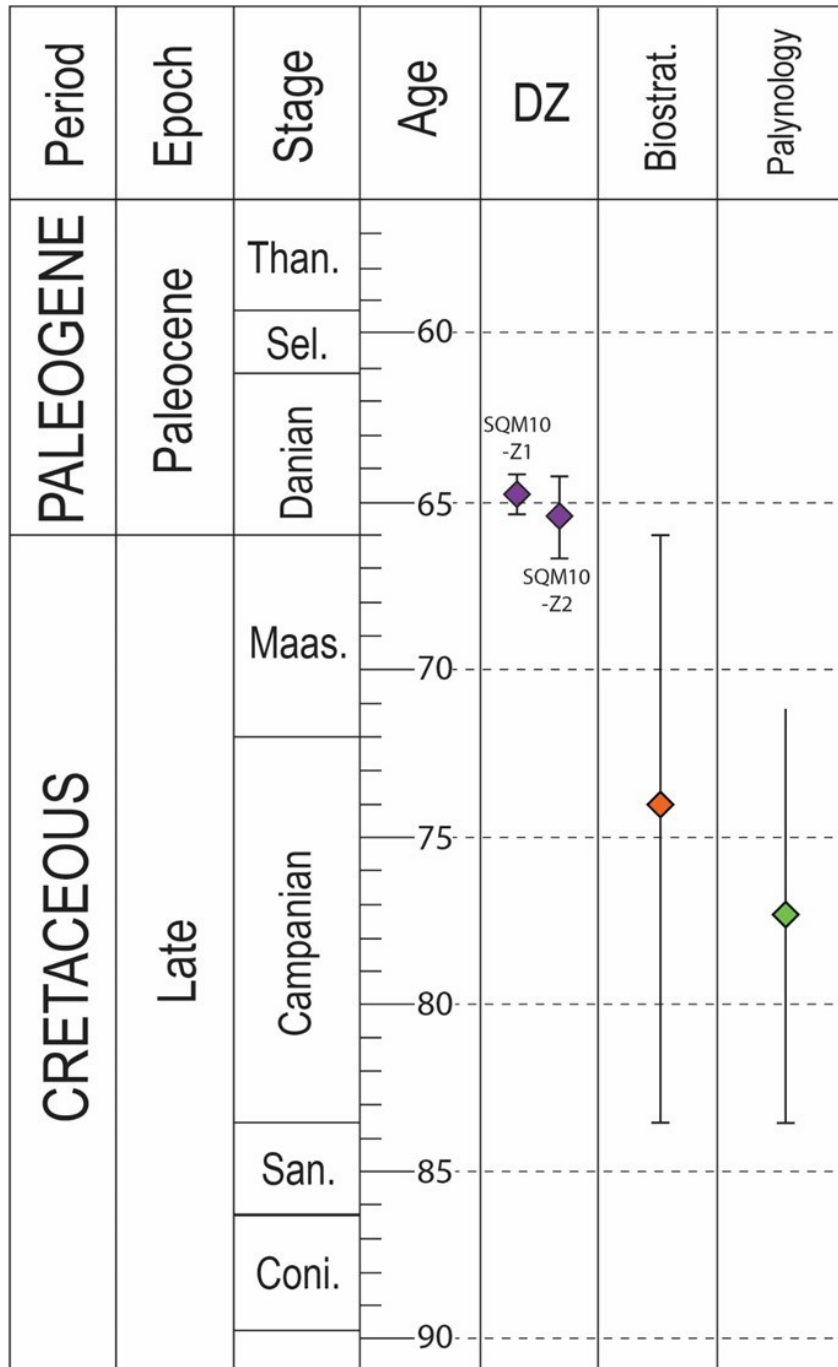
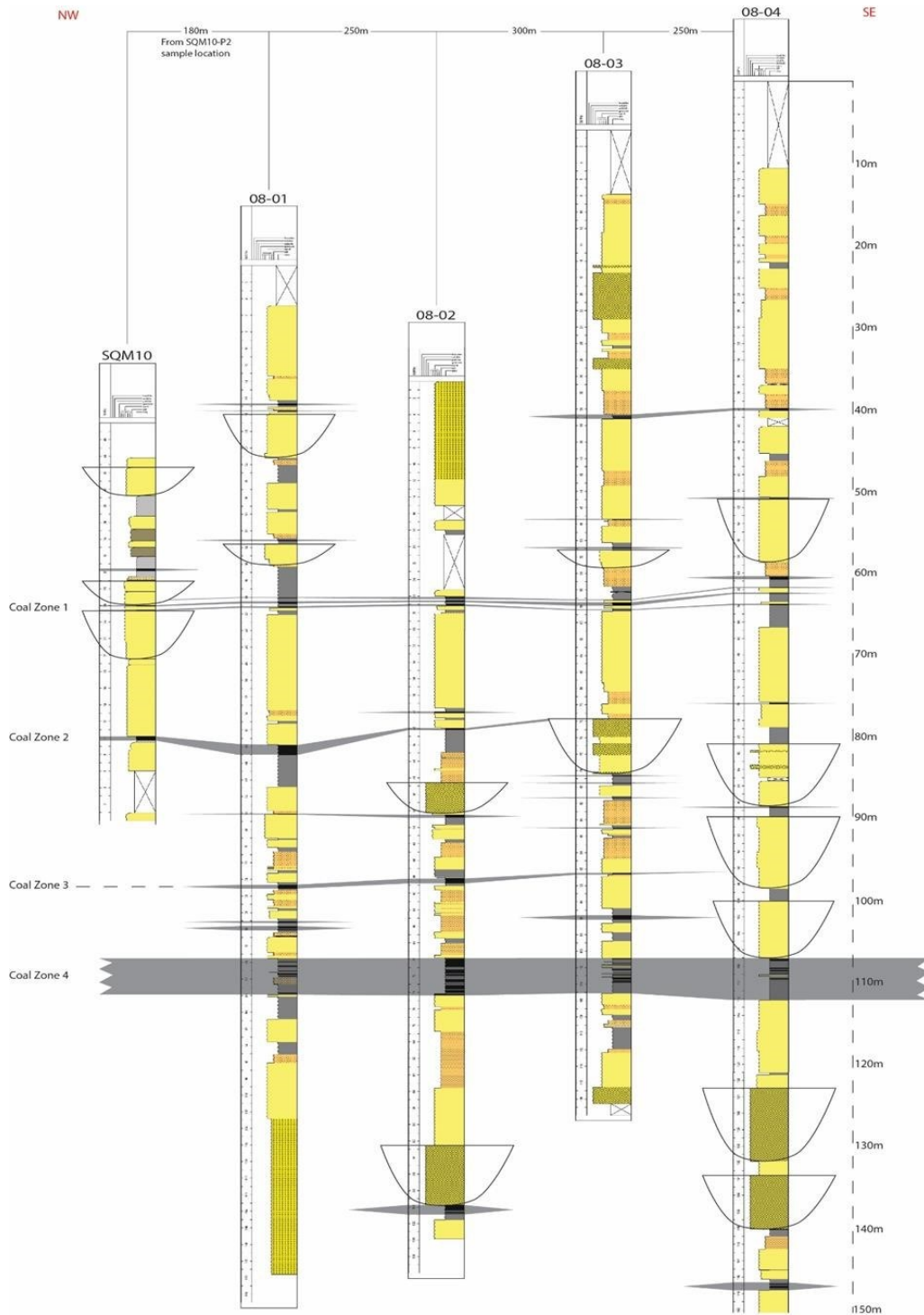


Figure 2.21. The ages of sedimentary strata at the Suquash Mine site and the methods used to derive them. Purple represents DZ YGC2 $\sigma$  MDAs along with uncertainties for SQM10-Z1 and SQM10-Z2 (Huang, pers. comm., 2024). Orange represents biostratigraphic ages based on work by Nixon et al. (2011), and green represents palynological ages based on pollen, spores, and dinocysts presented in Galloway et al. (2023).



**Figure 2.22. Stratigraphic cross section of the Suquash Mine Site. This cross section is flattened on the top of Coal Zone 4 (CZ4). Coal zones are numbered on the left side of the figure and relative depths and thicknesses are displayed on the right. Distances between wells are shown at the top. Interpreted channels within the cross section are shown as black polygons. SQM-SS04 is shown to only 150 m. See Figure 2.14 for outcrop and core positions.**

The third studied outcrop area of Upper Cretaceous and younger strata is located along the shoreline below and adjacent to the Orca Gravel Company's ship-loading facility (OGL; Figure 2.11, Figure 2.23). Three distinct outcrop locations are identified and two measured sections were generated: OGL-1 and OGL-3 (Figures 2.23, 2.24; Table 2.5). No measured section was constructed for OGL-2 because the strata are extensively weathered and are obscured by dense extant marine plant and animal life in the intertidal zone. The OGL outcrops comprise predominantly sandstone with abundant trough cross-stratification and planar tabular bedding (Figure 2.25A) and are dominated by trace fossils considered indicative of marine influence (e.g.. *Ophiomorpha* isp.; Figures 2.25B and C). OGL-3 bears a significant pebble/cobble conglomerate which is largely obscured by marine life. Both measured outcrops contained several pebble- and cobble-bearing sandstone beds (Figure 2.25A). A sample was taken from OGL-1 for detrital zircon (OGL1-Z1), and from OGL-3 for palynology (OGL3-P1, P2; Table 2.5).

**Table 2.5. List of measured outcrop sections and samples from the Orca Gravel Loader (OGL) site. Location data as well as bedding orientations for outcrop sections are included. Sample data include location as well as stratigraphic height within the relevant measured section.**

<b>Outcrop Name</b>	<b>Length</b>	<b>Dip/Dip Direction</b>	<b>Base of Section</b>	<b>Sample/Section Height</b>	<b>Sample Location</b>
OGL-1	6.6 m	3°/112°	50.61025° N, 127.152056° W	OGL1-Z1: 4 m	50.609889° N, 127.150389° W
OGL-3	5.75 m	9°/054°	50.609167° N, 127.149361° W	OGL3-P1, OGL3-P2: 5.75 m	50.608722° N 127.147194° W

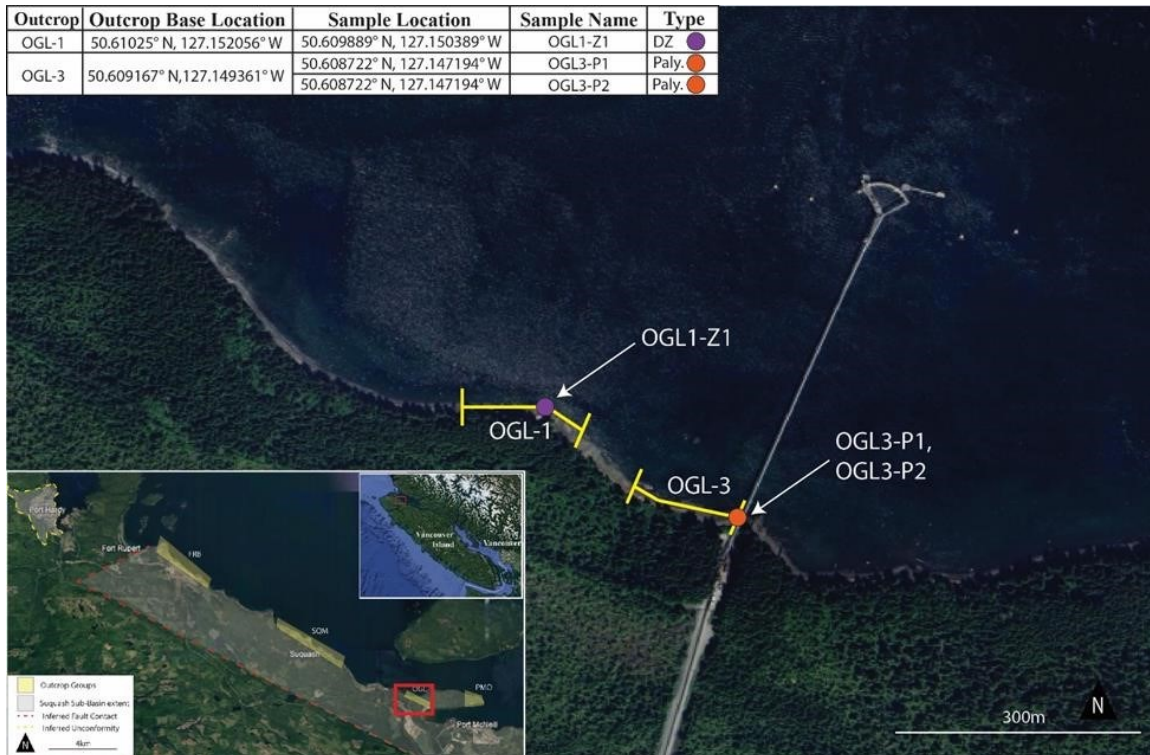
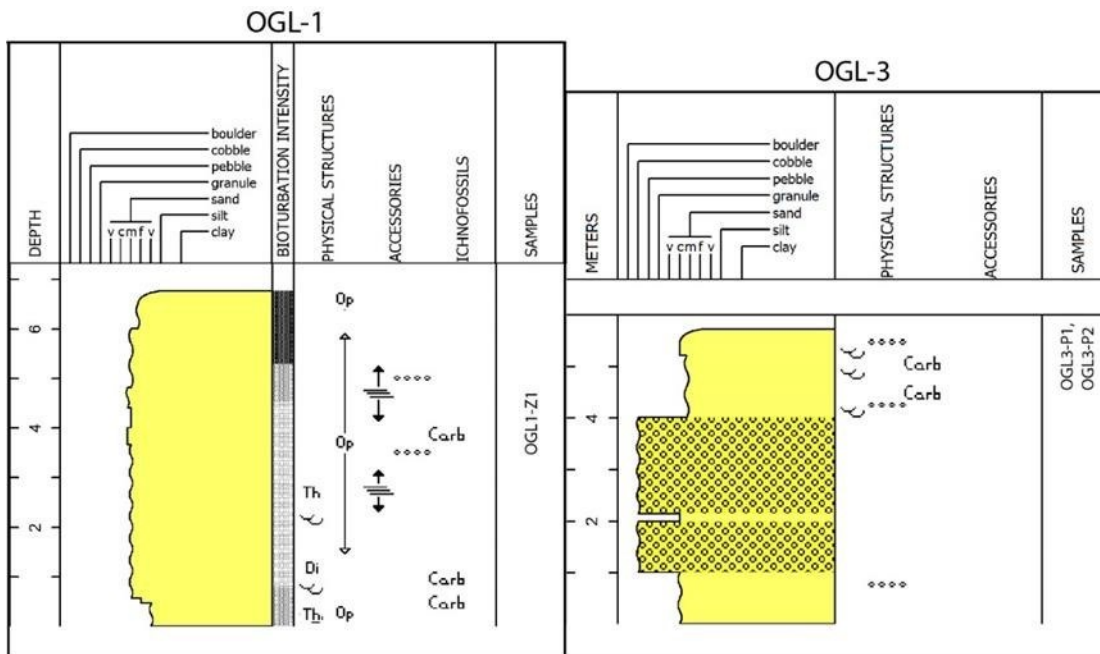
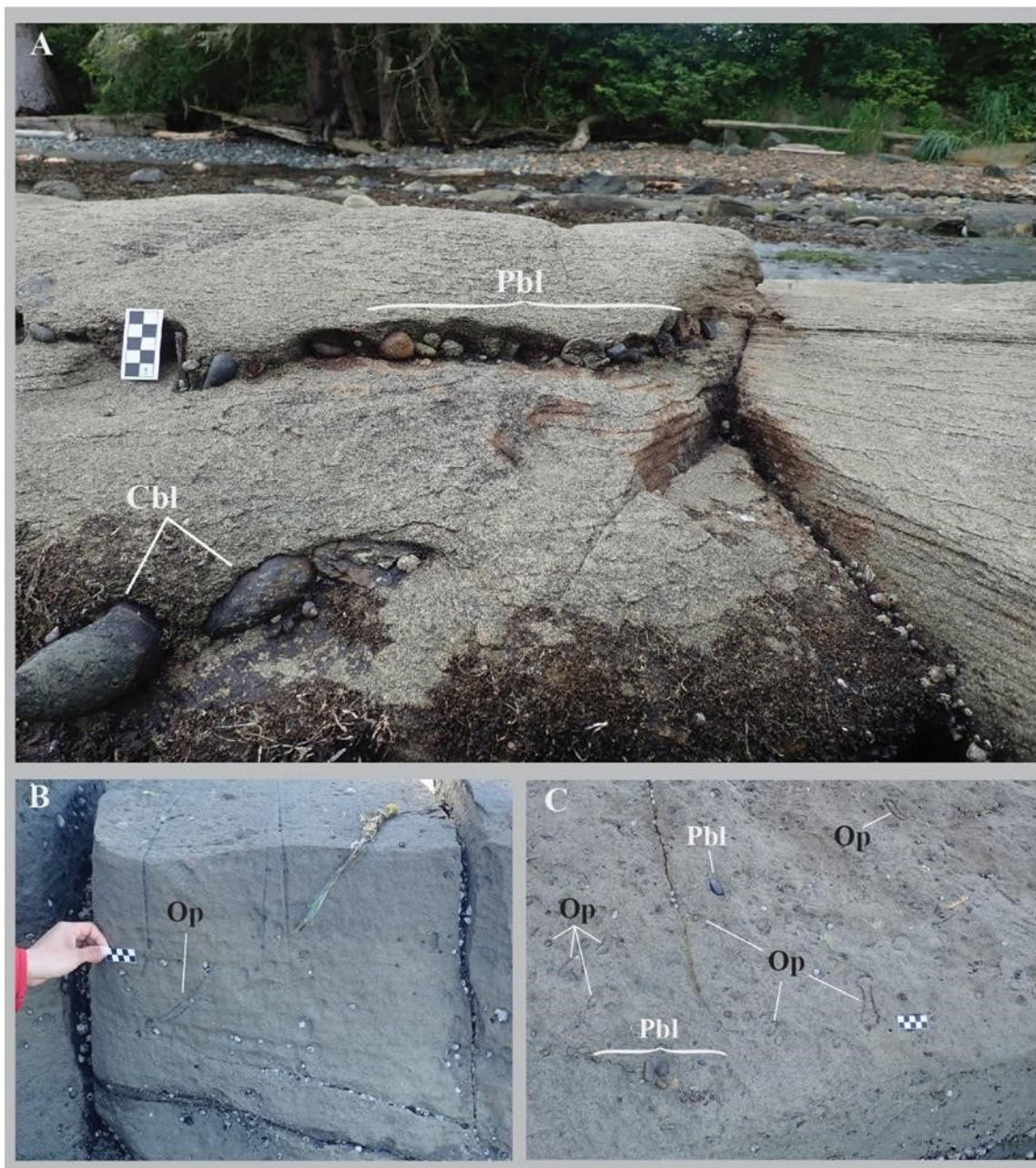


Figure 2.23. Aerial map of the Orca Gravel Loader (OGL) site with measured outcrops and sample locations shown. Inset map shows Figure 2.11 with the outcrop area highlighted and its relative position on Vancouver Island.

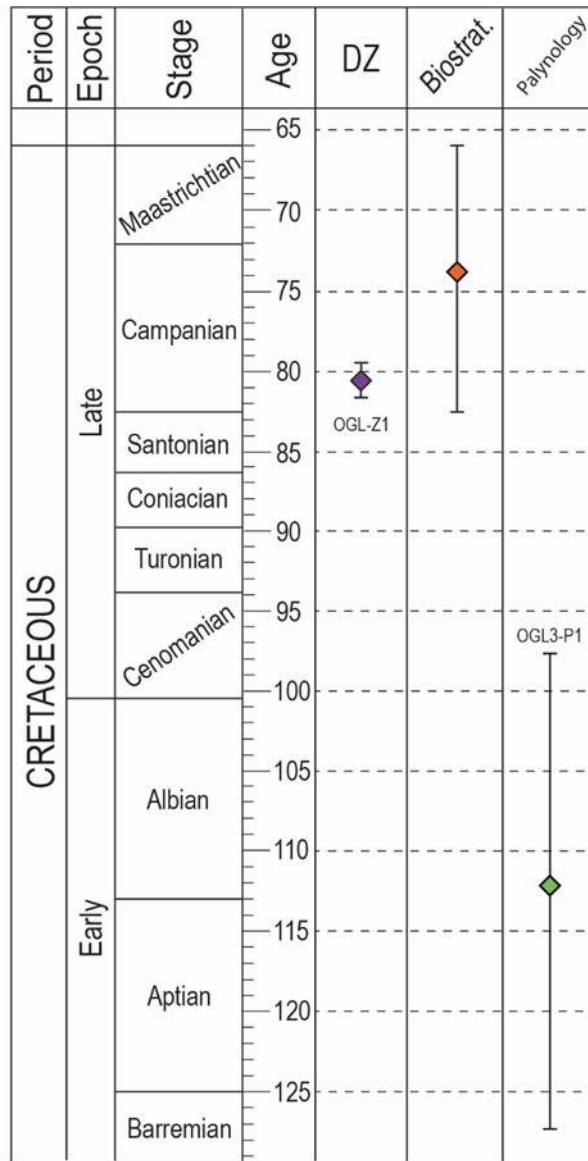


**Figure 2.24. Graphic lithologs of measured outcrops at the Orca Gravel Company loader site near Port McNeill. The location of these outcrops are shown in Table 2.5.**



**Figure 2.25. A) Planar tabular bedding containing pebbles (Pbl) and cobbles (Cbl) in OGL-1 at approximately 5 m. B) Vertical expression of *Ophiomorpha* isp. (Op) in OGL-1 outcrop between 0 and 1 m. C) Plan view of Pbl emplaced within sandstone and oblique views of *Ophiomorpha* isp. (Op) at approximately 3.5 m in OGL-1.**

Palynology sample OGL3-P1 (Table 2.1, 2.5) returns an estimated late Barremian to early Cenomanian age based on dinocysts (Table 2.1). Detrital zircon sample OGL-Z1 returned a YGC2 $\sigma$  MDA of  $80.5 \pm 1.1$  Ma (Table 2.2; C. Huang, pers. comm., 2024). A comparison figure for the age data from OGL outcrop samples is shown in Figure 2.26.



**Figure 2.26. The ages of sedimentary strata at the Orca Gravel Loader (OGL) outcrop area and the methods used to derive them. Purple represents DZ YGC2 $\sigma$  MDAs along with their associated uncertainties. Orange represents biostratigraphic age ranges based on work by Nixon et al. (2011). Green represents palynological age ranges based on dinocyst analysis from Galloway et al. (2023) (see Table 2.1).**

The final studied outcrop location of Upper Cretaceous and younger strata is located adjacent to Port McNeill (Figure 2.11). Two outcrops were described and measured in this area: PMO-1 and PMO-2 (Table 2.6; Figure 2.27). PMO-1 is



characterised primarily by thinly bedded heterolithic bedsets alternating between medium- to fine-grained sandstone and mudstone. These intervals are highly variable lithologically and contain flaser, wavy, and lenticular bedding. The majority of this measured section lies in the intertidal zone, wherein extant marine plant and animal life obscures the sedimentological and ichnological characteristics of the strata. PMO-2 outcrop predominantly consists of medium- to coarse-grained sandstone showing trough cross stratification and bioturbation with mainly *Ophiomorpha* isp. The measured dips and dip directions are consistent between the top of measured section PMO-1 and the base of PMO-2. The covered interval between the two is calculated and a combined graphic litholog of the two sections showing sample locations is shown in Figure 2.28.

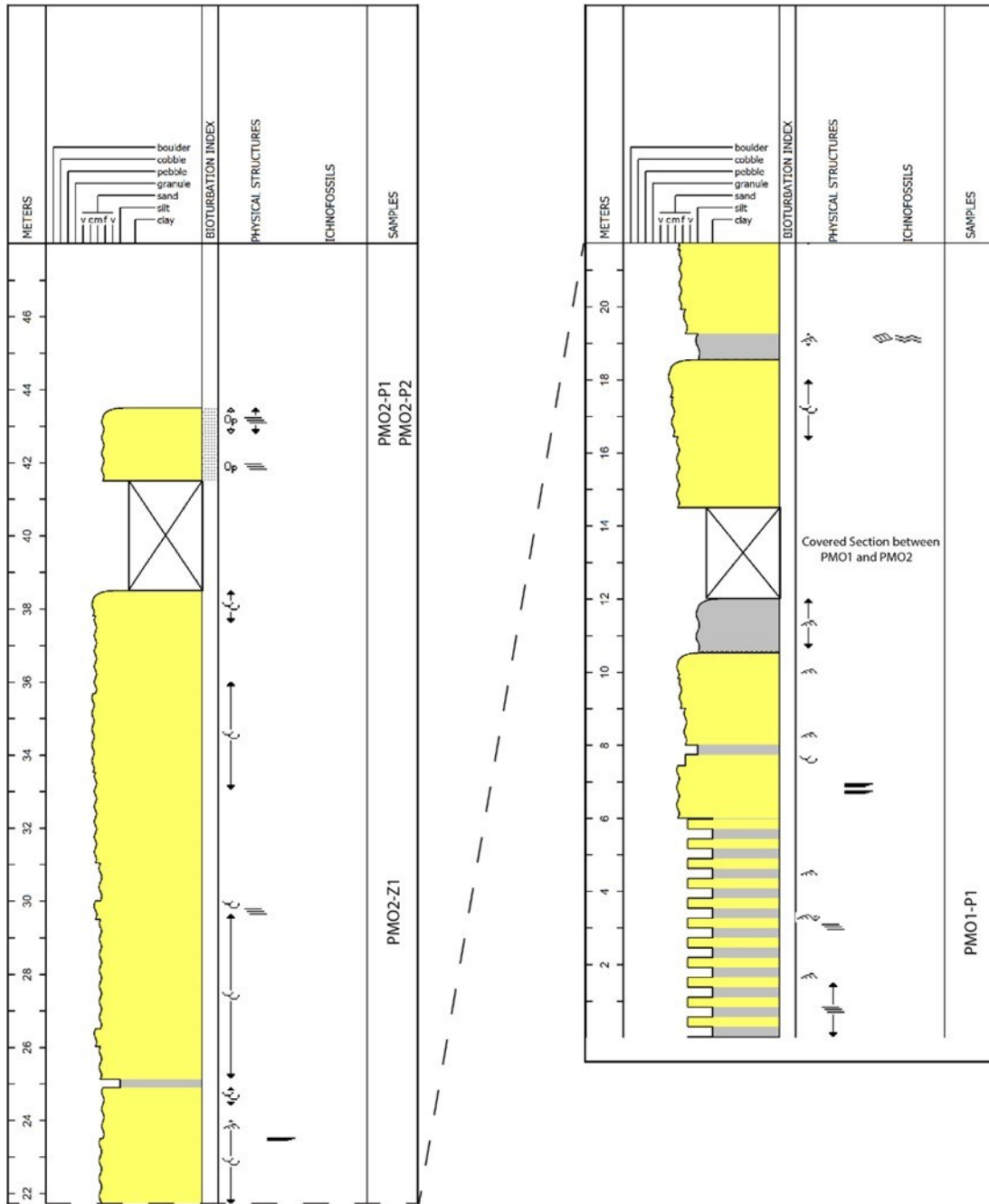
**Table 2.6. List of measured outcrop sections and samples from the Port McNeil (PMO) site. Location data as well as bedding orientations for outcrop sections are included. Sample data include location as well as stratigraphic height within the relevant measured section.**

Outcrop Name	Length	Dip/Dip Direction	Base of Section	Sample/Section Height	Sample Location
PMO 1	12 m	11°/317°	50.602889° N, 127.086556° W	PMO1-P1: 3.4 m	50.602880° N, 127.086561° W
PMO 2	28.75 m	6°/322°	50.602944° N, 127.087694° W	PMO2-P1, PMO2- P2: 43.5 m	50.602583° N, 127.092361° W
				PMO2-Z1: 30 m	50.60252° N, 127.08950° W

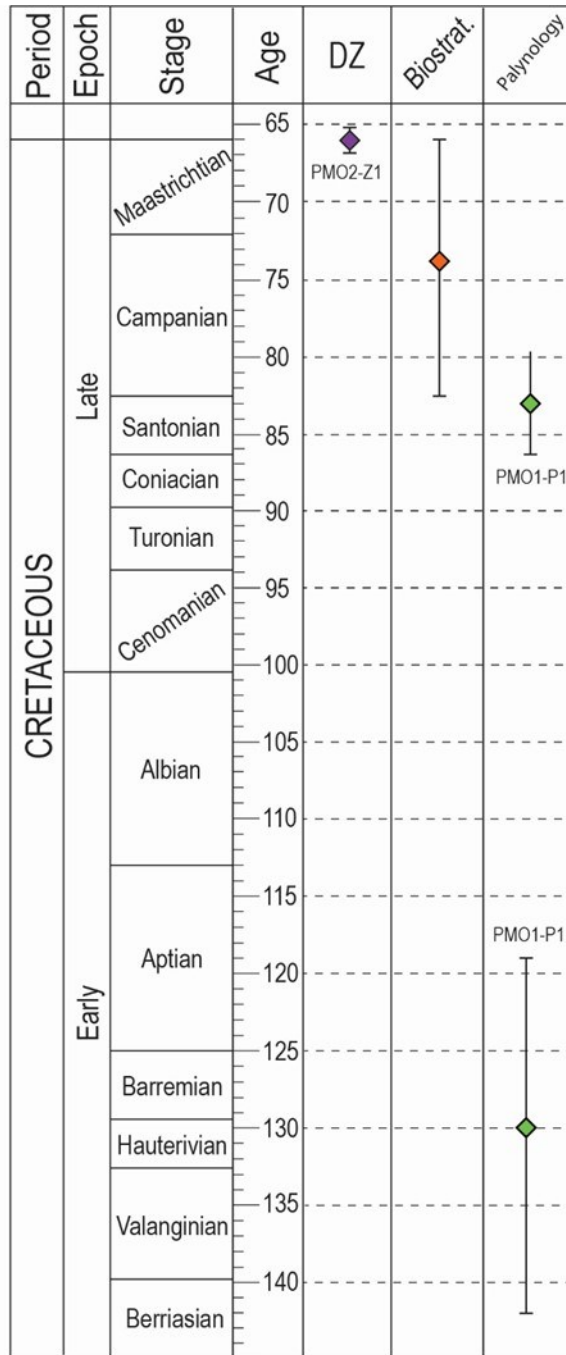
A DZ sample (PMO2-Z1; Table 2.2) was collected from PMO2 (50.60252° N, 127.08950° W; Figure 2.27) and returned a YGC2σ MDA of 66.1 ± 0.8 Ma (C. Huang, pers. comm., 2024). Samples for palynology were taken from both outcrops: PMO1-P1 contains pollen and spores suggestive of a Santonian or younger age, and dinocysts suggestive of a Barremian to Early Aptian age (Table 2.1). PMO2-P1 was contaminated by modern pollen rain and after reprocessing was found to be barren of pollen and spores (Galloway et al., 2023). PMO2-P2 was not analysed for this study. The PMO outcrop area lies within an area mapped by Nixon et al. (2011) as being Campanian to ?Maastrichtian. A comparative figure of age data from the PMO outcrops is shown in Figure 2.29.



**Figure 2.27. Aerial map of the Port McNeill outcrop area (PMO) with measured sections and sample locations highlighted (Image courtesy of Google Earth). Palynology samples (orange) and DZ sample (purple) are shown in their respective positions in the measured sections. The covered interval between PMO-1 and PMO-2 is represented by the dashed line segment. Inset map shows Figure 2.11, with outcrop location highlighted and its relative position on Vancouver Island.**



**Figure 2.28. Combined measured section PMO1 and PMO2. Stratigraphic heights of DZ sample PMO2-Z1 and palynology samples PMO1-P1, PMO2-P1 and P2 are indicated. The base of the combined section is located at 50.602880°N, 127.086561°W and the top of the section is at 50.602593°N, 127.092349°W. The legend for this measured section can be found in Figure 2.1.**



**Figure 2.29.** The ages of sedimentary strata at the Port McNeill Outcrop Area and the methods used to derive them. Purple represents DZ YGC2 $\sigma$  MDAs with their associated uncertainties calculated at the 2-sigma level. Orange represents biostratigraphic ages based on work by Nixon et al. (2011). Green represents palynological ages based on pollen and spores (Late Cretaceous) and dinocysts (Early Cretaceous) evaluated by Galloway et al. (2023).

## **Chapter 3. Discussion**

Chapter three discusses the various methods used to derive ages for north Vancouver Island (NVI) sedimentary strata and presents probable ages and age ranges for all strata investigated. Methods and ages are compared to assess the cogency of age-determining approaches and to support interpretations as to which method best approximates the true depositional ages of the studied strata. Chapter three also includes a discussion of the implications of interpreted ages in resolving the relation of NVI sedimentary strata to time-equivalent strata in nearby west-coast sedimentary basins.

The various age-determining methods employed include biostratigraphic ages derived from macrofossils and palynomorphs, and maximum depositional ages (MDAs) derived from detrital zircon (DZ). Biostratigraphic ages are derived from studies that compared fossils present in studied stratal intervals to known global holotypes and biozones, and age assessments are based on visual interpretations and the robustness of local, regional, and global biozone data. The validity of using DZ MDAs to establish stratigraphic relationships is determined by 1) the number of DZ grains incorporated into the MDA calculation; and 2) the perceived age-gap between true depositional age and the crystallization ages of the youngest DZ grains. As the number of DZ grains comprising the youngest source increases, MDA calculation methods such as  $YGC2\sigma$  become increasingly biased towards the young tail of the normal distribution and, hence, are a closer approximation of the true depositional age (Sharman and Malkowski, 2023).

### **3.1. Assessment and Discussion of Dating Techniques**

#### **3.1.1. Parsons Bay Formation**

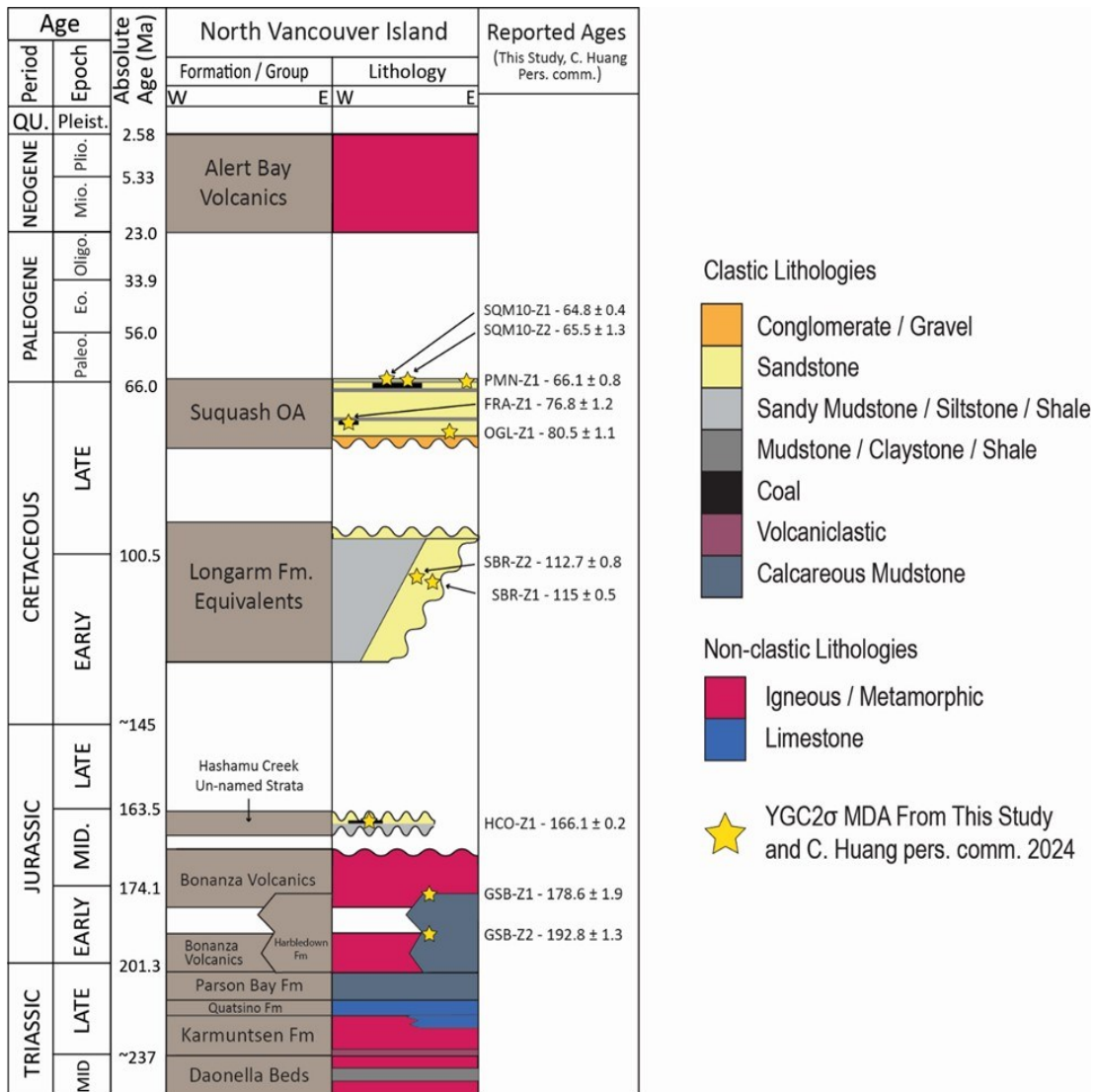
Strata at the Goodspeed fossil beds (GSB) consist of deep-water turbidites that were assigned previously to the Parsons Bay Fm (Figure 3.1; Crickmay, 1928; Nixon et al., 2011). The Parsons Bay Fm is assigned an Upper Triassic age (Carnian to Rhaetian) based on ammonite faunal zones (Muller and Rahmani, 1970; Tozer, 1967, 1994; Nixon et al., 2011).

The GSB site contains abundant specimens of the two bivalve species *Halobia alaskana* and *Monotis subcuricularis*, as well as common occurrences of the ammonite *Sympocyclus gunningi*? (identified through comparison with Ludvigsen and Beard, 1997) amongst other ammonites. The ammonite assemblage in the GSB represents the upper Carnian *Welleri* zone (Tozer, 1967) defined on Vancouver Island. These species are also present in the time-equivalent Kunga Group in Haida Gwaii.

Two detrital zircon samples (GSB-Z1 and GSB-Z2) were collected from GSB. GSB-Z2 was collected from strata containing the macrofossils described above and GSB-Z1 was collected from nearby non-fossiliferous strata. Detrital zircon MDAs were generated by taking the weighed average of the youngest DZ grains that overlap in age at  $2\sigma$  uncertainty (YGC $2\sigma$ ). The YGC $2\sigma$  MDA calculations of GSB-Z1 and GSB-Z2 are based on 6 and 9 DZ grains, respectively, and in the case of GSB-Z2, the 9 grains represent 90% of all recovered zircon. The exact stratigraphic relationship between GSB-Z1 and GSB-Z2 is unclear owing to the high-angle bedding and uncertain stratigraphic relationship of strata between the collection sites. The resulting YGC $2\sigma$  MDAs suggest that the fossiliferous strata from which GSB-Z2 was derived are Sinemurian ( $192.8 \pm 1.3$  Ma;  $n = 10$ ), and therefore stratigraphically below the nonfossiliferous strata from which GSB-Z1 was derived ( $178.6 \pm 1.9$  Ma;  $n = 286$ ; Toarcian). However, the low number of zircon in GSB-Z2 introduces significant uncertainty as to the reliability of this MDA as reflecting the true depositional age.

The low number of zircon in GSB-Z2 and the fact that nearly all zircon have the same age suggests that GSB-Z2 was derived from a single source. Between the Late Triassic and Late Jurassic, the Bonanza Arc situated on Vancouver Island was the main source of volcanic activity and remained active barring a period of quiescence from 190 to 182 Ma (Canil and Morris, 2023). The YGC $2\sigma$  MDA of GSB-Z2 suggests that the DZ grains crystallized just prior to the older limit of volcanic quiescence. The Bonanza Arc is the likely source of these zircon, however without a more robust population for analysis, assigning an age is difficult. The YGC $2\sigma$  MDA determined for GSB-Z1 is a statistically significant age and the MDA is younger than the period of volcanic quiescence and it is probable, therefore, that the Bonanza volcanism supplied near-depositional age grains to the strata hosting GSB-Z1.

There is uncertainty in the direct relation between the strata from which GSB-Z1 and GSB-Z2 are derived, although the two outcrops are close to one another. GSB-Z1 appears to be stratigraphically below GSB-Z2 based on field interpretation. The robust and statistically significant MDA derived for GSB-Z1 suggests that the GSB sedimentary strata are probably of Lower Jurassic (Toarcian) age or younger. This age would temporally equate these strata to the Harbledown Formation below the GB, and the Whiteaves Fm. of the Kunga Group, below the QCB. The fossil assemblage present in GSB-Z2 strata suggest they are a part of the Parson Bay Fm, but the DZ MDAs indicate these strata are significantly younger (Early Jurassic -Toarcian) than the first proposed Late Triassic (Carnian to Rhaetian) age based on ammonite faunal zones (Muller and Rahmani, 1970; Tozer, 1967, 1994; Nixon et al., 2011). Based on the younger age, these strata are temporally equivalent to the Harbledown Fm (Figure 1.2; Muller and Jeletzky, 1970; Nixon et al., 1992, 2011; Nixon and Orr, 2010), suggesting that the Harbledown and Parsons Bay formations are temporally equivalent.



**Figure 3.1. Updated stratigraphic column for strata in NVI, based on age determinations presented in Section 3.1. Detrital zircon MDAs are displayed as stars and are arranged from left-to-right in the Suquash OA to indicate geographic position from southeast to northwest.**

Figure 3.1 presents a stratigraphic column that incorporates all detrital zircon geochronology, palynology, and biostratigraphic age interpretations collected in this study, as well as the presently accepted chronostratigraphic positions of strata in NVI (Muller and Jeletzky, 1970; Nixon et al., 1992, 2011; Nixon and Orr, 2010). For GSB and HCO, where DZ MDAs do not overlap with current biostratigraphic zonation or the palynology is inconclusive, these strata are assigned ages as interpreted in Section 3.1. Stratal ages from the Suquash OA are shown left-to-right (northwest to southeast), corresponding to the four outcrop locations (see Figure 2.11).



### 3.1.2. Hashamu Creek Strata

Strata examined along Hashamu Creek (HCO, Figure 2.6) comprise bedsets with evidence of terrestrial deposition, based on the presence of coal seams and an absence of: 1) identifiable sedimentary structures indicative of depositional environment 2) marine trace fossils, and 3) marine palynomorphs (Table 2.1; Galloway et al., 2023). The Hashamu Creek strata crop out in several structurally dislocated sections between the mouth of Hashamu Creek and the location of HCO-Z1 (Figure 2.6), with outcrops displaying similar sedimentological characteristics, lithologies, and bed thicknesses. High-angle faults occur within sections of strata and may be present between outcrop locations, introducing uncertainty about direct stratigraphic relationships between outcrop sections.

Biostratigraphic interpretations from multiple mapping studies are presented in Chapter 2 (Figure 2.7) and show a discrepancy between reported ages. The Hashamu Creek strata and other outcrop sections mentioned in Jeletzky (1973), and Muller et al. (1974) lack any identifiable fossils and are correlated to the “uppermost Sinemurian argillite” (Crickmay, 1928) based solely on lithology. Jeletzky (1970, 1973) and Muller et al. (1974) correlate Quatsino Sound argillites (Hashamu Creek drains into Quatsino Sound) to “fossiliferous Sinemurian beds” (Crickmay, 1928) of the Harbledown Fm (in Haida Gwaii), based on the identification of *Paltechioceras* (Getty, 1973; changed from *Melanhippites*). Alternatively, Nixon et al. (2011) assign the Hashamu Creek strata to the Lower Cretaceous “Longarm Formation equivalents”, which are present in numerous outcrop locations in NVI (Figure 1.13). In the Quatsino Sound region, Nixon et al. (2011) describe numerous isolated outcrops that are typically confined to angular fault blocks. These strata were dated to the Early Cretaceous, based on the presence of coquinas containing *Buchia crassicolis*, although coquina beds were not identified along Hashamu Creek. The application by previous authors of diachronous biostratigraphic interpretations of Hashamu Creek strata is exacerbated by the lack of direct fossil evidence within these beds. No fossils were identified in these units as part of this study.

Palynology samples HCO4-P1 and HCO5-P1 did not yield an age for these strata, as they were both effectively barren of marine palynomorphs, and the pollen and

spore slides produced from these strata were contaminated by modern pollen rain (Table 2.1; Galloway et al., 2023). Resampling for and re-examination of palynomorphs may help to constrain the age of these strata.

One detrital zircon sample, HCO-Z1 (n=289; Table 2.2), was collected and analyzed, and returned a statistically viable YGC2 $\sigma$  MDA of 166.1  $\pm$  0.2 Ma. The age of this sample is coincident with volcanism in the Bonanza Arc on Vancouver Island (Canil and Morris, 2023) and active volcanism should have supplied abundant, neardeposition-aged zircon to these strata. The YGC2 $\sigma$  MDA for HCO-Z1 is based on 160 grains (55.4% of the total for the sample). This large unimodal population could impact the reliability of the MDA approximating the true depositional age (TDA). First, it is probable that the MDA incorporates numerous grains that crystallized before the TDA, and hence, the MDA may underestimate the TDA, however the unimodal nature of the MDA provides confidence that the weighted mean of the population is a close approximation of the TDA. Second, the ages of zircon within this sample (Figure 2.2) appear unimodal, which may indicate a single volcanic source for these grains. As such, the MDA does not reflect the age of the strata, but instead indicates the age of the volcanic source of zircon. In the former case, the strata are probably close to 166 Ma (with error), while in the latter case the strata could be any age younger than 166 Ma. Relative ages determined from both rock formations differ from the derived MDA, and further constraining the assigned age through macro-biostratigraphy, palynological analysis, and additional DZ MDAs may enable closer prediction of the TDA of these strata.

### **3.1.3. Lower Cretaceous Strata**

Lower Cretaceous strata include outcrops mapped as Longarm Formation equivalents by multiple authors (Muller and Jeletzky, 1970; Ludvigsen and Beard, 1997; Haggart, 2004; Dalby, 2009; Nixon et al., 2011). The Longarm Fm comprises one of the major units of the Cretaceous fill of the QCB and is assigned an age of upper Valanginian to at least the end of the Aptian (Figure 1.3; Dalby et al., 2009). The presence of these strata forms the basis for the possible extension of the southern terminus of the QCB to NVI (Wheeler et al., 1996; Nixon and Orr, 2010; Nixon et al., 2011). Direct correlation of stratigraphy has not been made due to the distance between the exposed outcrops, which is why these strata are referred to as “equivalents” rather

than as Longarm Fm *sensu stricto*. These strata were examined at two localities along the Strandby River and were characterized using sedimentological, biostratigraphic, and geochronological datasets.

The two outcrop areas of Lower Cretaceous strata contain abundant biostratigraphic evidence that support attributing them to the Longarm Fm equivalents. Both outcrop areas contain abundant fossil molluscs similar to *Inoceramus colonicus* (Figure 2.9B; Haggart, pers. comm., 2022). The first outcrop location, SBR1 (Figure 2.8), also contains an ammonite that appears similar to a Lower Cretaceous ammonite species (Figure 2.9C; Haggart, pers. comm., 2022). However, Global Boundary Stratotype Sections and Points (GSSPs) for Lower Cretaceous strata are based on European ammonite species not found in the North Pacific Biotic Province (Jeletzky, 1971; Haggart et al., 2009; Haggart and Graham, 2018; Huang et al., 2022). The biostratigraphic zonation scheme applied to these strata is based primarily on endemic mollusc, bivalve, and ammonite species (Jeletzky, 1971; Haggart and Graham, 2018). Correlation of these strata, therefore, is based primarily on co-occurring species within similar settings in the North Pacific Biotic province spanning North America, Alaska, Siberia, and parts of East Asia (Jeletzky, 1971; Huang et al., 2022). Sedimentary successions in the QCB are used as a standard reference for biostratigraphic correlation in the northeast Pacific (Dalby et al., 2009). The identification of *Inoceramus colonicus* (Figure 2.9B, D) in SBR strata, therefore, serves as a robust correlative tool to interpret these strata as being temporally equivalent to other Lower Cretaceous sedimentary strata in west-coast basins.

The two DZ samples SBR1-Z1 (n=279) and SBR2-Z1 (n=282) were taken from these outcrops. As discussed in Chapter 2, the direct stratigraphic relationship between the two outcrop areas is not known, nor is the orientation of strata within each outcrop. SBR1-Z1 returned a YGC2 $\sigma$  age of  $115.0 \pm 0.5$  Ma and SBR2-Z1 returned a YGC2 $\sigma$  age of  $112.7 \pm 0.8$  Ma, based on 33 and 9 grains, respectively. The number of grains utilised in each of these analyses shows no bias towards an extended young tail on the normal distribution of grains within each sample (Figure 2.2); hence, these grains seem to represent a single source that closely approximates the TDA of the strata. The probability density plots (PDP) for these samples show two distinct age populations in

each sample (Figure 2.2). The older of these populations most likely represents grains from sources that crystallized following the resumption of Bonanza Arc volcanism in NVI.

The source of the younger population of grains is likely volcanism from the developing western arc (Gehrels et al., 2009) of the Coast Mountains batholith (called CPC in this thesis). Volcanism in the western arc of the CPC occurred in three distinct pulses prior to 100 Ma. Specifically, the third pulse persisted from 118–100 Ma (Cecil et al., 2018) and is the probable source for near-depositional-aged zircon in SBR-Z1 and SBR-Z2. The robustness and similar ages of the two MDAs and the correlation to temporally equivalent strata based on biostratigraphy, suggest the strata are probably Longarm Fm equivalents and were deposited in the earliest Albian within NVI; this extends the depositional range for these strata by approximately 0.5 Ma (Figure 1.8; Haggart, 2004; Dalby et al., 2009).

### **3.1.4. Upper Cretaceous and Younger Strata**

Four outcrop areas mapped as Upper Cretaceous strata were investigated in this study, and these all occur in the Suquash Sub-Basin or Suquash Outcrop Area (Suquash OA; Muller and Jeletzky, 1970; Huang et al., 2022; Giroto et al., 2024). These strata were mapped as being Campanian to ?Maastrichtian based on macrofossil biostratigraphic evidence (Nixon et al., 2011). Ages presented herein are based on palynological analysis, DZ geochronology, and macrofossil biostratigraphy. The macrofossil biostratigraphy is derived from literature sources.

Thirteen palynological samples were collected from four sites in the Suquash OA (Table 2.1). Of the 13 samples, only four returned age data from dinocysts, with dinocyst preservation generally poor (Galloway et al., 2023). Only one dinocyst species was recognized in all 4 samples (*Pseudoceratium pelliferum*). All other dinocysts are identified to the genus level or higher. The paucity of dinocysts means that the resulting biostratigraphic interpretations are “broad and unreliable” (Galloway et al., 2023), and their poor preservation suggests that they were reworked prior to their incorporation into the sampled strata (Galloway et al., 2023).

Pollen and spore analysis of the 13 palynology samples returned ages for six samples. All six samples are assigned probable Late Cretaceous ages (Table 2.1), although these data do not preclude the inclusion of Paleocene or younger material in some samples (Galloway et al., 2023). Two common index taxa (*Aquilapollenites* sp. and *Woodehouseia* sp.) for dating Late Cretaceous-aged rocks in North America are absent in all samples. Galloway et al. (2023) suggest that the absence of these taxa could indicate an age that is either older than the Campanian or younger than the latest Cretaceous.

Detrital zircon samples were taken from all outcrop locations in the Suquash OA. From these samples, DZ dates were used to derive YGC2 $\sigma$  MDAs. Both Gehrels et al. (2009) and Cecil et al. (2018) identify widespread volcanism in the western CPC between 100 and 45 Ma. This volcanism provided a ready and proximal source of neardepositional-aged zircon for strata in the Suquash OA. The presence and abundance of near-depositional-aged zircon in samples are dictated by several factors related to the character of convergent-margin basins, including the depositional environment within which strata are deposited (Cecil et al., 2018; Huang et al., 2022). For example, in lower Nanaimo Group strata in the GB, Huang et al. (2022) demonstrate that sedimentary strata deposited in shallow- to deep-marine environments (*versus* fluvial and terrestrial environments) are better targets for DZ sampling, because of the higher probability of incorporating DZ from numerous active sources in the hinterland of the basin. Huang et al. (2022) showed that DZ derived from strata deposited in shallow- to deep-marine environments consistently aligned with biostratigraphic ages within the basin. Samples in the Suquash OA were taken preferentially from strata that showed ichnological evidence of deposition in marine influenced settings. Given this targeted sampling, the DZ MDAs are high confidence results for the Suquash OA.

### ***Fort Rupert Beach***

The Fort Rupert Beach (FRB) outcrops are close to the northwestern end of the Suquash OA. They were sampled for palynology and DZ, and the ages returned from these analyses are presented alongside the biostratigraphic age proposed by Nixon et al. (2011) (Figure 2.12). The YGC2 $\sigma$  age returned from these strata (FRB5-Z1, n=269) is

76.8 ± 1.2 Ma (n = 3), which indicates that they are mid-Campanian or younger. The palynology sample (FRB7-P1) processed for these strata was taken from an outcrop section approximately 1 km from FRB5-Z1 (Figure 2.12). This sample was barren of terrestrial pollen and spores but was assigned an age of late Berriasian to early Aptian from the dinocyst assemblage (Galloway et al., 2023). This age is deemed to be lowconfidence, as the dinocysts in the sample appear to be reworked from older strata and are very poorly preserved.

Fossiliferous beds in the FRB area (GSC loc. 82952; Jeletzky, 1969) have been referenced by numerous authors (Jeletzky, 1969; Muller and Jeletzky, 1970; Ward, 1987) and are described to contain inoceramid and trioniid fossil material similar to Sucia Island in Washington State, USA. These beds, however, could not be located during this study. *Baculites chicoensis* (elsewhere named *B. inornatus*; Ward, 1978) were identified by Muller and Jeletzky (1970) in beds stratigraphically below the fossiliferous beds mentioned above. Muller and Jeletzky (1970) also recognised placenticeratid ammonite material in the fossiliferous beds, which alongside more recent work (e.g., Ward, 1987; Nixon et al., 2011; Haggart and Graham, 2018) have been designated to the *Metaplacentieras cf. pacificum* zone (Figure. 1.9; Haggart and Graham, 2018). The macrofossil biostratigraphy places the FRB beds in either the upper part of the lower Campanian (equivalent to the Pender Fm of the Nanaimo Group), or to the lower part of the upper Campanian (equivalent to the Cedar District Fm of the Nanaimo Group) (Figure 1.9; Haggart and Graham, 2018). The combination of the MDA derived from FRB5-Z1 and its agreement with the upper-lower to lower-upper Campanian ages derived from the biostratigraphy combine to provide a robust midCampanian age for these outcrops.

### ***Suquash Coal Mine***

The Suquash coal mine area (SQM) comprises mostly short and dislocated discrete stratal sections. The most significant and continuous section of strata (SQM-10) was sampled for palynology and DZ, and a detailed measured section was produced (Figure 2.15). Measured section SQM-10 is correlated to numerous subsurface wells (Figure 2.22) drilled at this location. One well (SQM-SS04; Figure 2.20) penetrates the entire succession and has a total length of ~330 m. Well SQM-SS04 represents the most

significant continuous strata in the Suquash OA. These subsurface strata could not be described directly, as the cores were destroyed and no photographs of the interval exist. Lithologs were built using lithologic descriptions of the cored intervals made by the Electra Gold Company in 2008 (Figures 2.18, 2.19).

Biostratigraphic evidence from the Suquash OA has been collected and referenced by numerous researchers (e.g., Usher, 1952; Muller and Jeletzky, 1970; Nixon et al., 2011; Haggart and Graham, 2018). The oldest beds in the Suquash OA are attributed to the *Hoplitoplacenticeras vancouverense* zone (Figure 1.9; Muller and Jeletzky, 1970), now revised to belong to the upper part of the lower Campanian (Haggart and Graham, 2018). Additional fossil evidence of both *Metaplacenticeras cf. pacificum* and *Pachydiscus suciaensis* identified within the Suquash OA allows strata to be assigned to these faunal zones respectively (Figure 1.9; Muller and Jeletzky, 1970) in the middle upper Campanian (Haggart and Graham, 2018). The *P. suciaensis* zone previously spanned the upper Campanian and lower Maastrichtian, but this has since been constrained (Haggart and Graham, 2018; Figure 1.9) to only part of the upper Campanian. No macroscopic fossils were noted in SQM strata in this study.

Palynology samples collected from SQM-10 were examined by Galloway et al. (2023) with three samples returning ages for this section (SQM10-P1, -P2, -P6; Table 2.1). These samples indicate a Campanian or younger age, with SQM10-P2 specifically middle Campanian or younger. Angiosperm pollen *Tschudypollis* (+ *Proteacidites* noted by Muller and Jeletzky, 1970) found in these samples, for example, are useful for constraining the age of strata to the late Cretaceous-Early Paleocene. The timing of deposition is difficult to know precisely, however, as several taxa in these samples remain extant and therefore have no last appearance datum (J. Galloway, pers. comm., 2024).

DZ samples SQM10-Z1 (n=258) and SQM10-Z2 (n=145) returned statistically significant YGC2 $\sigma$  MDAs ( $64.8 \pm 0.4$  Ma and  $65.5 \pm 1.3$  Ma, respectively; Table 2.2), dating the outcrop section at SQM-10 to the earliest Paleocene (Danian) or Latest Cretaceous (Maastrichtian). Both samples were taken from strata that show some degree of marine influence during deposition. This evidence includes trace fossils with a marine association, as well as the presence of marine influenced sedimentary structures (Figures 2.15; 2.16). The evidence of marine influence and high-n numbers of analyzed

grains suggest the MDAs from SQM10-Z1 and SQM-Z2 are not erroneously young and incorporate multiple sources of near-depositional-aged zircon. The source of neardeposition-aged grains in these samples was likely ongoing volcanic activity in the CPC (Gehrels, 2009; Cecil et al., 2018). The ages for these samples have 100% overlap within uncertainty, possibly indicating that the OA was receiving sediment from the same source during the deposition of both samples.

### ***Orca Gravel Loader***

Orca Gravel Loader (OGL) outcrops (Figure 2.11) comprise two short sections for which measured sections were generated and which were sampled for palynology and detrital zircon. Biostratigraphic interpretation of these strata is based on fossils identified along the nearby Keogh River (Muller and Jeletzky, 1970), although no fossils were observed in the OGL sections. At the time of logging, both sections were largely obscured by extant intertidal plant and animal life. The OGL outcrops are assigned a Campanian to ?Maastrichtian age, based on fossil evidence presented in Muller and Jeletzky (1970).

Palynology sample OGL3-P1 did not return an age based on pollen and spores (Table 2.1). Dinocysts were recovered from the sample and were identified to the genus level, but of the four dinocysts identified, all were highly degraded (Galloway et al., 2023). A late Barremian to early Cenomanian age is assigned based on dinocyst analysis (Galloway et al., 2023; Table 2.1, Figure 2.24), but this age is deemed low confidence owing to the low number of dinocysts recovered and their poor preservation due to possible reworking.

A DZ sample (OGL-Z1, n=31) returned a lower Campanian YGC2 $\sigma$  MDA of 80.5  $\pm$  1.1 Ma based on eight grains. The source for near-deposition-aged zircon in this sample was likely ongoing volcanic activity in the CPC (Gehrels et al., 2009; Cecil et al., 2018). The population of grains within this sample is not statistically significant; however, the distribution of ages is similar to spectra in other samples collected from the Suquash OA (Figure 2.2). Further sampling for a larger population of zircon would increase the likelihood of a robust MDA.

The OGL sections contain significant pebble/cobble conglomerates that may correlate to conglomerates that were identified along the Keogh River by Muller and



Jeletzky (1970) and which were described as being in angular unconformity with the underlying Karmutsen Fm. However, Upper Cretaceous strata in the OGL section and nearby sites (Suquash Mine sites) also contain abundant conglomerate, and their correlation to those identified by Muller and Jeletzky (1970) could not be confirmed. The age derived from OGL-Z1 is a low confidence MDA due to the low number of grains, but if the MDA is an accurate representation of the true depositional age, then it supports the correlation of the OGL strata to the basal conglomerates of Muller and Jeletzky (1970) and by extension, the Cedar District Fm of the Nanaimo Group. Muller and Jeletzky (1970) assign these beds to the H. vancouverense zone, which was revised later and constrained to the upper part of the lower Campanian (Figure 1.9; Haggart and Graham, 2018). The MDA calculated for OGL-Z1 supports the biostratigraphic age.

### ***Port McNeill***

The final set of Upper Cretaceous outcrops are located near Port McNeill and were sampled for palynology and detrital zircon. These outcrops are situated near the southeastern extent of the Suquash OA and have been interpreted as Campanian to ?Maastrichtian (Nixon et al., 2011), based on biostratigraphic evidence presented in Muller and Jeletzky (1970). Muller and Jeletzky (1970) present two datasets to attribute an age to these strata. First, fossils of macro-flora from these strata were identified by Muller and Jeletzky (1970) and correlated to the Cedar District Fm, which is considered to have been deposited in the lower part of the Upper Campanian. Secondly, pollen and spores were used to assign a “post-Early Cretaceous” age.

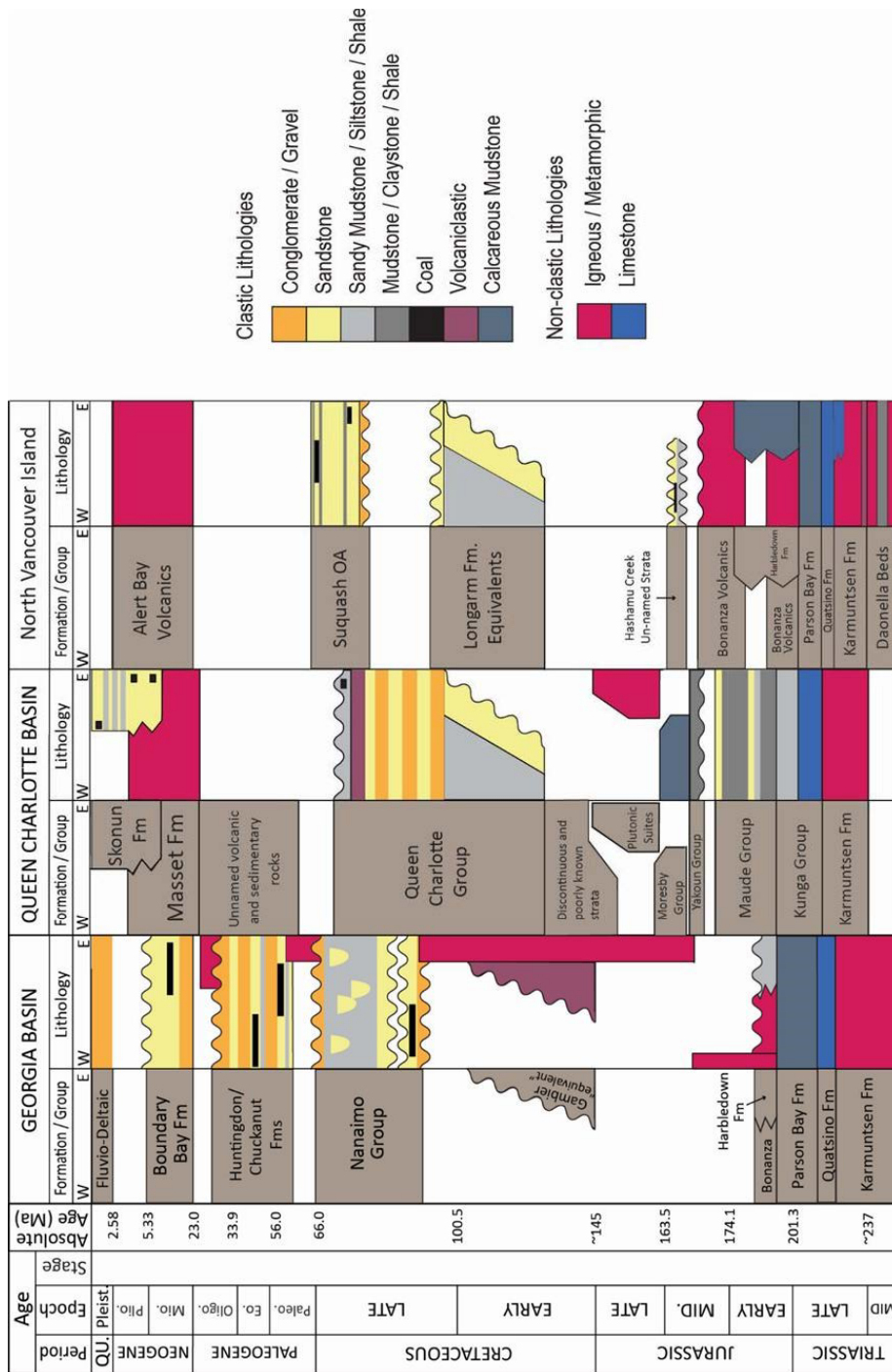
Two palynology samples (PMO1-P1 and PMO2-P1; Table 2.1) were collected from these strata. PMO2-P1 did not return a reliable age from the terrestrial palynomorphs due to modern pollen rain contamination, and were effectively barren of dinocysts (Table 2.1; Galloway et al., 2023). PMO1-P1 returned two ages (Figure 2.26), the first based on pollen and spores, and the second from dinocysts. Pollen and spores from PMO1-P1 returned an age of Santonian or younger. The constituent flora in the sample have a first appearance datum in the Santonian but may not have last appearance data due to the continuity of the taxa into the present (J. Galloway, pers. comm., 2024). A Berriasian to Early Aptian age was determined on the basis of dinocyst identification (Galloway et al., 2023). The dinocysts recovered from this sample have fair qualities of preservation but are highly fragmented. Only one recovered dinocyst could

be identified to the species level. All others could not be identified with certainty and are possibly long-ranging species. The possibility of reworking of the marine palynomorphs in these samples further reduces confidence in the reported age.

The DZ sample PMO-Z1 (n=22) returned a YGC2 $\sigma$  MDA of  $66.1 \pm 0.8$  Ma (Table 2.2; C. Huang pers. comm., 2024). The sample contained a statistically insignificant number of grains, of which five were used to calculate the MDA. This is not a robust MDA, although the population of grains presented in the age spectrum for PMO-Z1 does reflect a distribution of ages similar to other samples taken within the Suquash OA (Figure 2.2). Analysis of a larger number of zircon may reinforce the calculated age. No fossils were observed in these outcrops. The age data collected for these outcrops differ in their respective age interpretations. Further sampling of these sections for more biostratigraphically significant palynologic taxa and for a more statistically significant DZ MDA would help to better constrain the depositional age. Considering all datasets and not considering the dinocyst analysis, these strata were deposited at some point between the Santonian (Upper Cretaceous) and the Danian (early Paleocene).

### **3.2. Relation of NVI strata to West-Coast Sedimentary Basins**

Prior to this study, GSB strata within the Parsons Bay Fm were interpreted as being temporally equivalent to the lower Kunga Group in the QCB and were assigned an age of Late Triassic to Early Jurassic (Figure 3.2; Nixon et al., 2011). Detrital zircon MDAs calculated from GSB strata return middle to late Early Jurassic (Toarcian) ages that are younger than the lower Kunga Group (Table 2.2; Figure 3.1, 3.2), indicating that deposition of the Parsons Bay Fm extended into the late-Early Jurassic at least. While sedimentary strata of this revised age are present in Haida Gwaii in the Maude Group, possibly the mudstone and shale comprising the Whiteaves Formation (Haggart et al. 2009; Dalby et al., 2009), their biostratigraphic zonation differs in age to the zonation of species identified in GSB strata (Haggart et al., 1995; Ludvigsen and Beard, 1997). GSB strata may be equivalent to the younger Harbledown Fm in NVI based on the MDA from GSB-Z1. The evidence presented herein cannot directly correlate GSB strata to either the QCB or the GB.



**Figure 3.2.** Revised chronostratigraphic correlation of strata between the Georgia Basin, Queen Charlotte Basin, and NVI. Georgia Basin chronostratigraphy is modified after Hannigan et al. (2001) and Dashtgard (pers. comm., #####). Queen Charlotte Basin chronostratigraphy is modified after Haggart et al. (2009) and Dalby et al. (2009). Northern Vancouver Island chronostratigraphy is modified after Muller and Jeletzky (1970), Nixon et al. (1992, 2011) and Nixon and Orr (2010), with updated stratigraphic ranges from this study.

Hashamu Creek strata are assigned a Bathonian to Callovian age based on DZ MDAs. The Newcombe Fm of the Moresby Group comprises fossiliferous sandstone beds (Cameron and Tipper, 1985; Hannigan et al., 2001) that are temporally equivalent to HCO. The age of the Newcombe Fm is based on ammonite species (Cameron and Tipper, 1985) dated to the Bathonian and early Callovian. Moresby Group strata are interpreted as broadly marine with paleocurrent measurements suggesting sediment routing from northeast to southwest (Cameron and Tipper, 1985). The distance between the QCB and Hashamu Creek strata is a limiting factor in correlating the two outcrop areas, and the possible single zircon source for HCO suggests the strata may be of limited areal extent. There are no sedimentary strata of this age below or in the Georgia Basin.

Lower Cretaceous Longarm Fm “equivalents” are mapped across NVI (Figure 1.13; Nixon et al., 2011). These strata have been correlated to strata of similar lithologic composition and age of the actual (Longarm Fm) within the QCB (Bustin, 1997; Haggart et al., 2009), and this interpretation is supported by fossils identified in the Strandby River outcrops (Figure 2.9B, C, D). Robust DZ MDAs (SBR1-Z1, SBR2-Z2; Table 2.2) from the Strandby River outcrops support the interpretation that deposition of Longarm Fm “equivalents” in NVI occurred coincidentally with the Longarm Fm in QCB, and the two datasets (fossils and DZ MDAs) indicate an Aptian to Albian age.

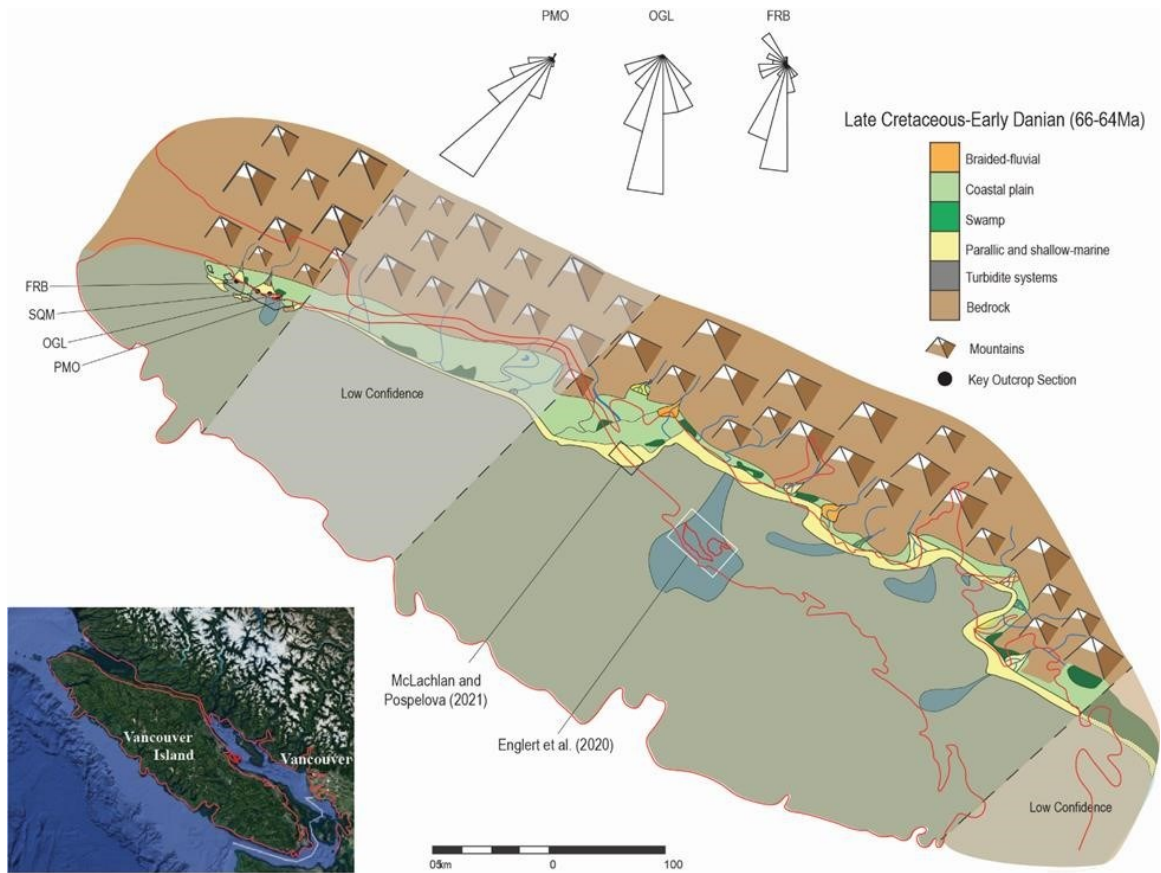
Muller and Jeletzky (1970) used faunal and floral macrofossils and palynology to assign a Campanian – ?Maastrichtian age for Suquash OA strata. This age was reaffirmed later with further macrofossil biostratigraphic evidence identified by Hannigan et al. (2001) and Nixon et al. (2011). Detrital zircon MDAs of Suquash OA strata provide three robust ages for units at FRB and SQM (Table 2.2). FRB5-Z1 supports the biostratigraphic interpretation of FRB strata as Campanian, and DZ MDAs from SQM provide a robust latest Maastrichtian to early Danian age. While statistically significant, the ages returned from Suquash OA strata juxtapose Campanian and Danian outcrops with limited spatial separation within a succession with a maximum of 326 m thickness. Two separate possibilities for explaining this Suquash OA stratal architecture are presented in Section 3.3.

### 3.3. Suquash Outcrop Area Stratal Architecture

The architecture of the Suquash OA is complex and appears to juxtapose outcrops of Danian strata at SQM with Campanian strata at FRB. The most significant continuous section in the Suquash OA is provided by cores drilled at SQM by the Electra Gold Company, and the longest cored interval has a maximum stratal thickness of 326 m after correcting for dip (329 m uncorrected length). Descriptions of lithology in these cores (Figure 2.19, 2.20) are compared to measured section SQM-10 (Figure 2.15) and based on this comparison there does not seem to be variation in depositional environments between what is interpreted at the surface and what can be inferred from core descriptions of lithology in the subsurface. The thickness of strata across the Suquash OA may be significantly impacted by topographic relief on the basal nonconformity. Disconformities also may be present within the SQM succession, and these could significantly impact the ages and correlation of strata therein.

Two models are proposed to explain the juxtaposition of outcrops of Campanian and Danian strata within the Suquash OA. The first model (Model 1) shows that sedimentary strata within the Suquash OA represent two topographically restricted, marine-influenced depositional environments within a broader coastal plain setting in the Danian (Figure 3.3). Model 1 proposes that FRB outcrops are located within an isolated embayed region, protected from the open ocean. The three remaining outcrop areas (SQM, OGL, and PMO) are similarly contained within an adjacent but restricted embayed area. In Model 1, the true depositional age of both FRB and SQM strata is Danian, and the different MDAs reflect different catchments. Specifically, short distance variations in topography and volcanism at the time of deposition impacted sediment routing in such a way that near-depositional-aged zircon present in SQM and PMO samples (Figure 2.2) are absent in the FRB MDA sample. This is supported by paleocurrent measurements taken in the Suquash OA (Figures 3.3 and 3.4A; S. Dashtgard, pers. comm., 2024) showing that sediment was sourced from the northeast in three of the outcrop locations (FRB, OGL, PMO). This routing could indicate distinct sources of sediment for both the northern and southern parts of the Suquash OA. The population of grains comprising the OGL sample is not statistically significant, in that the population may not represent all sources of zircon for these strata, and therefore an early Danian MDA cannot be ruled out without further investigation.

The Danian paleogeographic reconstruction in Figure 3.3 also incorporates studies demonstrating Paleogene strata within the bounds of the Georgia Basin. McLachlan and Pospelova (2021) conducted palynological analyses of strata comprising the Oyster Bay Fm and identified a conformable Cretaceous-Paleogene (K-Pg) boundary, based on well-preserved marine taxa spanning the Maastrichtian to the Selandian. This is the first study to demonstrate a conformable K-Pg boundary in the northeast Pacific and is evidence of time-equivalent shallow- marine strata to the Suquash OA in the early Danian. Englert et al. (2020) utilised DZ MDAs from samples of Upper Nanaimo Group strata on Denman and Hornby Islands to, in-part, demonstrate a long-lived, deep-marine slope-channel system spanning the middle Campanian to Paleocene.



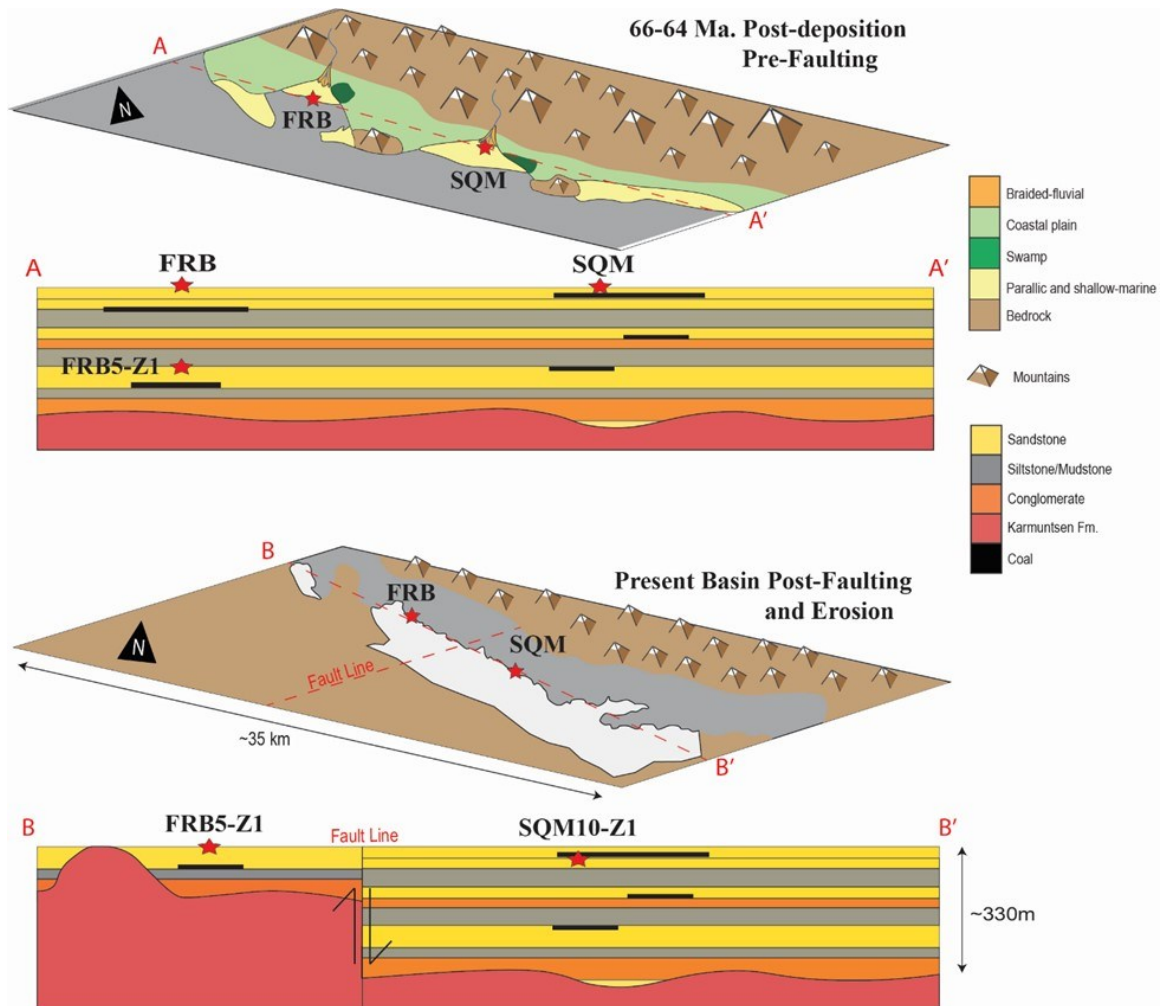
**Figure 3.3. Paleogeographic reconstruction of the Suquash OA and Georgia Basin from 66–64 Ma. This interpretation presents the Suquash OA as two distinct and restricted depocenters. Compiled paleocurrent directions are from S. Dashtgard (pers. comm., 2024) and general directions are displayed as rose diagrams. Paleoenvironmental reconstruction of the Georgia Basin to the southeast are based on facies interpretations presented in Englert et al. (2020; white polygon) and McLachlan and Pospelova (2021; black polygon).**

The second model (Model 2) invokes a hitherto unknown thrust (or less likely, normal) fault that crosscuts the Suquash OA and separates FRB strata from outcrop areas to the southeast (Figure 3.4). In Model 2, the northwestern part of the Suquash OA is thrust up relative to the southeast, and this exposes older strata at FRB. Strata situated in the southeastern part of the Suquash OA preserve a greater stratal succession including younger, Danian-aged strata. In Model 2, the sedimentary succession at SQM represents the entire thickness of the Suquash OA, and Campanian strata at FRB correlates to deeply buried subsurface strata at the SQM site. SQM strata are 326 m thick, and the gently dipping strata at FRB, if continuous, should be situated at approximately 190 m depth in the SQM succession (Figure 2.12). The interpretation of a

thrust fault in Model 2 is speculative as no fault has been identified in the Suquash OA that would facilitate the uplift and erosion required in this model. As well, there is no evidence available to indicate the preservation of Campanian-aged strata below SQM. However, the interpretation of post-depositional faulting is consistent with the Late Mesozoic–Early Cenozoic history of deformation (Monger et al., 1982; Monger and Price, 2002) in the western Canadian Cordillera. Model 2 also implies that the Suquash OA is a long-ranging, low-accommodation depocenter wherein sedimentary strata record at least 15 million years of deposition over the 326 m thickness, and this implies that at least one disconformity is present in the succession.

When weighing both interpretations of the development of the Suquash OA stratal architecture, the author considers the first interpretation as being the more likely. Considering the variance seen along strike in convergent margin basin settings, and the modern topographical changes along the North American west coast, it seems likely that conditions existed historically for multiple, isolated depocenters to exist coincidentally in the region. The data collected for DZ analysis also lend support for the model 1 interpretation. The difference in statistically valid zircon populations taken from both FRB and SQM suggest that short, along strike variance existed in the Suquash OA from the Late Cretaceous through to the Early Paleocene. With further sampling, it may be shown that the OGL and PMO zircon populations reflect a similar provenance of zircon as SQM, reinforcing the model 1 interpretation. Further, the author believes it more likely that the zircon populations for the statistically invalid DZ samples (OGL and PMO) do not contain zircon of all constituent sources, than for a Suquash OA spanning thrust or normal fault to have not been identified by any previous author or in this study.





**Figure 3.4.** Proposed development of the Suquash OA from Late Cretaceous/early Paleogene to present-day, invoking the presence of a thrust fault spanning the Suquash OA from southwest to northeast. Generalised stratigraphic cross sections are shown below the surface topography images. Historical depositional environments are shown in the first panel, the second panel shows the present basin architecture with the removal of overlying strata at FRB and the full sedimentary sequence preserved at SQM. Depositional environments and lithology are indicated on the right. Suquash OA outline from Nixon et al. (2011).

## Chapter 4. Conclusions

The main objectives of this thesis are to: 1) assess Mesozoic sedimentary strata across NVI using multiple means of sedimentological and geochronological investigation; and 2) relate these strata to sedimentary successions within Canadian west-coast sedimentary basins and investigate possible correlations to strata therein.

Two questions were proposed to achieve these aims:

1) Do Northern Vancouver Island Mesozoic strata lying stratigraphically below the Suquash outcrop area reflect a history of sedimentation within one or more of the west-coast sedimentary basins?

2) What is the depositional history of Upper Cretaceous to Danian strata in the Suquash outcrop area, and do those strata share a basin evolutionary history with either the Georgia Basin or Queen Charlotte Basin?

Chapter 4 summarizes the findings of this research and how each question is addressed.

### **4.1. Do Northern Vancouver Island Mesozoic Strata Lying Stratigraphically Below the Suquash Outcrop Area Reflect a History of Sedimentation Within One or More Sedimentary Basins?**

Goodspeed Fossil Bed strata were previously assigned to the Upper Triassic (Carnian to Rhaetian), Parsons Bay Fm based on macrofossils identified within the succession (Figure 2.4). However, a DZ MDA from GSB indicates that these strata were deposited during the Early Jurassic (Toarcian) (Table 2.2; Figures 2.5 and 3.1).

The GSB-Z1 MDA shows that the non-fossiliferous strata at GSB are younger than the Parsons Bay Fm. and that these younger strata are equivalent in age to the Harbledown Fm below the GB and potentially the Whiteaves Fm of the Maude Group in the QCB. The Harbledown Fm occurs below the GB and crops out across NVI (Figures 3.1–3.2). The second DZ MDA, GSB-Z2, which was taken from the fossiliferous beds at GSB, which have been assigned to the Parsons Bay Fm. based on the biostratigraphic assemblage therein, is not a statistically valid MDA and therefore cannot supersede the

current biostratigraphic zonation of these strata. Given the uncertain relationship between these two outcrop areas, and based on the data presented here, the strata likely represent distinct geological formations juxtaposed in close proximity. More careful sampling for DZ may produce a statistically valid population of grains to more confidently assess an MDA and assign an age to the fossiliferous strata at GSB. As the Harbledown Fm. crops out across NVI, it is more likely that the non-fossiliferous beds at GSB represent further outcrop of this formation, and therefore are associated with strata below the GB.

Strata at Hashamu Creek have been correlated to both the Harbledown Fm (Jeletzky, 1974) and to Longarm Fm equivalents in NVI (Nixon et al., 2011) based largely on lithological characteristics. No biostratigraphic evidence has been presented to correlate the Hashamu Creek strata with sedimentary strata elsewhere in NVI, Gb, or QCB, and palynology samples collected from Hashamu Creek did not return useful age data due to modern pollen contamination due to sampling from weathered surfaces (Galloway et al., 2023). Age data for Hashamu Creek strata comprise a single statistically viable DZ MDA (Table 2.2; Figure 2.7) and indicates a Bathonian age. However, the DZ ages are unimodal (Figure 2.2), and the significant (55.4%) proportion of young zircon in this sample probably includes grains that crystallized significantly prior to deposition. The unimodal distribution of the zircon dates from this sample may represent the age of the volcanic source, rather than the TDA of the strata, however the unimodal distribution does support that the weighted mean of the dates approximate the TDA. Further, a single volcanic source for zircon may indicate a limited spatial extent of the strata, rendering it difficult to correlate Hashamu Creek strata to temporally equivalent strata elsewhere. Resampling and using multiple chronostratigraphic datasets may help constrain and refine the age of these strata.

Based on the DZ MDA ( $166.1 \pm 0.2$  Ma), time equivalent strata to Hashamu Creek exist in QCB in the fully marine Moresby Group (Figure 3.2). The DZ MDA is the only correlative link, however, as the Hashamu Creek strata record deposition in terrestrial environments and are situated over 400 km away from the Moresby Group strata (Figure 3.1). Given the distances between locations and their discrete depositional settings, the DZ MDA is insufficient to confidently correlate the Hashamu Creek strata to

that of the Moresby Group. There are no known temporally equivalent strata to Hashamu Creek underlying the Georgia Basin.

Strata along the Stranby River are assigned to the Longarm Fm “equivalents” (Figure 3.2; Muller and Jeletzky, 1970; Jeletzky, 1976; Nixon et al., 2011), and multiple datasets including macrofossil biostratigraphy and DZ chronostratigraphy indicate that these strata are Lower Cretaceous (Valanginian to Albian; Figures 2.10 and 3.1). Cooccurring fossil species identified in SBR outcrop sections are similarly identified in the QCB (on Haida Gwaii) in the Longarm Fm (Figure 2.9B–D). Two statistically valid DZ MDAs (Table 2.2) indicate that the Stranby River strata are temporally equivalent to strata in the QCB, but no direct correlation has been made due to the distance between Stranby River and the QCB (Muller and Jeletzky, 1970). Lower Cretaceous strata situated below the GB comprise volcanoclastic Gambier equivalents (Figure 3.2; Hannigan et al., 2001) in which there is no biostratigraphic, or palynological evidence which can be correlated to NVI.

In summary, the correlation of GSB strata with time-equivalent units below the GB and in the QCB uncertain. Fossiliferous strata at GSB cannot be correlated confidently to units in either west-coast sedimentary basin based on DZ MDAs produced in this study and the biostratigraphic data suggest that these strata are part of the Triassic Parsons Bay Fm. Non-fossiliferous strata at GSB are shown to be temporally equivalent to the Jurassic Harbledown Fm. which crops out across NVI. Given the proximity and age data, it is likely that these strata represent further exposure of this formation. Middle Jurassic (Bathonian) strata at Hashamu Creek show a limited spatial extent, but there are time-equivalent strata in the QCB (and not in the GB). However, the distance between Hashamu Creek and the QCB do not allow for confident correlation of these strata. Finally, Lower Cretaceous Strandby River strata are time equivalent with the Longarm Fm deposited in the QCB, and this is corroborated by numerous datasets (Table 2.1; Figures 2.10 and 3.1). No strata of this age exist below the GB. Given the absence of strata that is time equivalent to Hashamu Creek and Strandby River in the GB, and the presence of time-equivalent units in the QCB, there is a higher probability that NVI pre-Upper Cretaceous strata are the southern extent of the QCB rather than an independent basin or the northern extent of the GB.

## **4.2. What is the Depositional History of Upper Cretaceous to Danian Strata in the Suquash Outcrop Area, and do those Strata Share a Basin Evolutionary History with Either the Georgia Basin or the Queen Charlotte Basin?**

The Suquash OA has historically been included as a sub-basin of the Georgia Basin (Muller and Jeletzky, 1970; Nixon et al., 1992, 2011; Hannigan et al., 2001; Girotto et al., 2024) with strata therein being temporally equivalent to parts of the Nanaimo Group. Late Cretaceous stratal ages (Campanian to ?Maastrichtian; Nixon et al., 2011) are based on both macrofossil biostratigraphic evidence from multiple locations in the Suquash OA and from palynological analyses (Muller and Jeletzky, 1970). In this study, dinocyst analyses returned four ages that are deemed low confidence because of palynomorph reworking prior to deposition (Galloway et al., 2023). Six Late Cretaceous ages are defined based on pollen- and spore-assigned ages, but these ages do not include an upper (younger) boundary due to the continuance of extant species beyond the Late Cretaceous.

Three DZ samples returned MDAs that are considered robust approximations of the TDAs of Suquash OA strata (Table 2.2; Figure 3.1). FRB5-Z1 returned a midCampanian age which coincides with previous biostratigraphic interpretations (Jeletzky, 1969; Muller and Jeletzky, 1970; Ward, 1987). Both SQM10-Z1 and SQM10-Z2 returned ages from the latest Maastrichtian or early Danian, and three DZ samples returned ages that are deemed low confidence due to the small population of zircon grains in each sample.

The FRB5-Z1 MDA equates Suquash OA strata to deposition of either the Protection or Cedar District formations of the lower and upper Nanaimo Group (Georgia Basin), respectively. In the QCB, the FRB5-Z1 MDA equates the strata to the Tarundl Fm of the Queen Charlotte Group. SQM10-Z1 and SQM10-Z2 returned ages that are equivalent to the deposition of the very uppermost Gabriola Fm (Englert et al., 2020) and Oyster Bay Fm (MacLachlan and Pospelova, 2021), both in the GB. There are no strata of equivalent age in the QCB. Although Campanian strata equivalent to FRB5-Z1 occur in both the QCB and the GB, the Nanaimo Group in the GB contains strata that is temporally equivalent to all DZ MDAs from the Suquash OA, suggesting the Suquash

OA is either a northwest extension of the GB, or at least contains strata that are time equivalent to deposition in the GB.

Two models are proposed to explain the architecture of Suquash OA strata (Figures 3.3 and 3.4). Model 1 proposes that all Suquash OA strata are Danian in age and are hosted in two distinct but adjacent embayed regions. Along depositional strike variations in paleotopography and volcanism are hypothesized to have isolated the northwest extent of the Suquash OA (Fort Rupert Beach) from the source of neardepositional, Danian-aged zircon that occur in strata exposed in the southeast at SQM. Suquash OA strata in Model 1 are deposited coincidentally with strata found in both the Oyster River Fm (MacLachlan and Pospelova, 2021) and in the Upper Nanaimo Group on Hornby and Denman Islands (Englert et al., 2020). This allows for a broad paleogeographic reconstruction of Canada's west coast in the Danian (Figure 3.3). Englert et al. (2020) established a Paleogene upper boundary ( $63.0 \pm 1.7$  Ma) for deposition of the Nanaimo Group, and MacLachlan and Pospelova (2021) identified the first conformable K-Pg boundary within the GB, based on palynological analysis.

Variations in paleotopography may have isolated the Suquash OA, and therefore a shared depositional history with the GB is speculative and difficult to establish without more data. No temporally equivalent sedimentary strata (Danian) have been described from the QCB, and hence, no shared history can be established between the Suquash OA strata and QCB strata.

Model 2 proposes that strata represent periodic, but spatially continuous deposition across the Suquash OA between the Campanian through to the Danian. Major disconformities are probably present within the succession (but were not identified in this study), and a thrust (or normal?) fault separates outcrops of older strata in the northwest (e.g., FRB) from younger strata exposed at SQM, OGL, and PMO (Figure 3.4). The age interpretation of strata in Model 2 equates Suquash OA strata temporally to deposition of the upper part of the lower Nanaimo Group and the upper Nanaimo Group in the GB (Figure 3.2; Haggart and Graham, 2018; Kent et al., 2020; Englert et al., 2020; MacLachlan and Pospelova, 2021; Huang et al., 2019, 2022; Giroto et al., 2024). As well, Suquash OA strata are temporally equivalent with the Tarundl Fm in the QCB and correlation to the Tarundl Fm is supported by the presence of *Pachydiscus suciaensis* in

both locations. The Tarundl Fm (Figure 3.2) comprises predominantly shelf mudstone, marking the end of the transgression of the QCB (Haggart et al., 1991; Lewis et al., 1991).

Evidence that was collected from limited core descriptions from the SQM site does not indicate variations in depositional environment for the entire succession (Figures 2.19–2.20 and 2.22). Deposition is interpreted to have occurred in terrestrial, coastal plain, and shallow-marine environments based on outcrop and core descriptions. In convergent margin settings, such as that hosting the Suquash OA, rates of subsidence, variations in sediment routing length, and volcanism can create highly variable rates of sedimentation. These factors may result in variable stratal architecture (Cawood et al., 2012; Gong et al., 2016; Giroto et al., 2024). From the Campanian to the Danian, during deposition of Suquash OA strata, both the GB (Pacht, 1980; Katnick and Mustard, 2003; Bain and Hubbard, 2016; Coutts et al., 2020; Mahoney et al., 2021) and QCB (Haggart et al., 1991; Lewis et al., 1991) were undergoing basin-wide transgression and experienced deep-marine clastic sedimentation. Contrasting this, deposition in the Suquash OA records seemingly consistent deposition within terrestrial through shallow-marine settings (Figures 2.19–2.20). This may indicate that the Suquash OA is situated in a hinge point between the GB and the QCB, which resulted in long periods of sediment bypass and shorter periods of subsidence and sediment accumulation. In this case, significant disconformities may exist in the stratigraphic succession, marking significant periods of exposure, sediment bypass, and erosion. Alternatively, regional tectonism could have driven subsidence through normal faulting, such that the Suquash OA is a fault-bound graben.

Finally, based on the age data collected for Lower Cretaceous and older strata, and the interpretations made regarding the Suquash outcrop area and its relationship to the Georgia Basin, it is possible that NVI constituted part of the QCB during sedimentation of older units, and became a depocenter for the Georgia Basin in the Upper Cretaceous and Paleogene. This is a reasonable possibility as variations in basin architecture (during amalgamation of Wrangellia to the west coast of North America), and along strike differences in topography, subsidence, and sedimentation are common in convergent-margin settings, and this would enable reconfiguration of NVI to contain sedimentary strata deposited in two distinct basins throughout the Mesozoic.

### 4.3. Future Work

This study has worked to build a stratigraphic interpretation of Mesozoic sedimentary strata hosted in northern Vancouver Island (NVI). Where possible, strata have been correlated to, or shown to be temporally equivalent to sedimentary successions hosted within and below sedimentary basins on Canada's west coast. Many avenues for future study of NVI sedimentary strata remain open.

First, there remain opportunities to further corroborate the age data presented in this thesis using multiple geochronological datasets. More complete and careful sampling for palynological analysis would help to constrain ages for all strata investigated herein. For example, many samples from Suquash OA strata returned palynomorph ages that lack a definitive last appearance datum. As well, numerous samples collected as part of this study did not return age data either due to a lack of identifiable pollen, spores or dinocysts, or to contamination of the samples by modern pollen rain (Table 2.1). More careful sampling of unexposed rocks and from multiple heights within identified stratigraphic sections may aid in providing more robust age data for these strata. Analysis of additional DZ samples would help further to constrain ages.

Second, additional sedimentological data can be collected to build a more complete genetic stratigraphic interpretation of NVI sedimentary strata. Preliminary work in making detailed descriptions of outcrop sections could be complemented by detailed facies analyses and collection of additional paleocurrent measurements. These datasets, coupled with DZ and biostratigraphic ages would help to constrain stratigraphic relationships between strata, particularly within the Suquash OA, and help to better relate these strata to other west-coast sedimentary basins. Completion of this work would also allow for the construction of better constrained paleogeographic models of North America's west coast.

Third provenance studies conducted in NVI may utilize DZ data to assess and interpret the relative position of NVI to the QCB, the GB, and North America throughout the Mesozoic. Deeper insight may also be gleaned into the tectonic history of North Vancouver Island. By determining the sources of sediment to this area, hypotheses such as 'Baja BC' (Garver and Brandon, 1994; Irving et al., 1995; Enkin et al., 2001) have the potential to be resolved. A full provenance study within the Suquash OA may also help



to constrain the stratal architecture of the area and provide insight(s) into the viability of the two proposed models for the basin's development (Figures 3.3 and 3.4).

## References

- Alberts, D. Gehrels, G.E., and Nelson, J. (2021) U-Pb and Hf analyses of detrital zircons from Paleozoic and Cretaceous strata on Vancouver Island, British Columbia: Constraints on the Paleozoic Tectonic evolution of Southern Wrangellia. *Lithosphere*, 1, 1–20.
- Bain, H.A., and Hubbard, S.M. (2016) Stratigraphic evolution of a long-lived submarine channel system in the Late Cretaceous Nanaimo Group, British Columbia, Canada. *Sedimentary Geology*, 337, 113–132.
- Bickford, C.G.C. and Kenyon, C. (1988) Coalfield geology of eastern Vancouver Island (92F). BC Ministry of Energy and Mines, *Geological Fieldwork*, 441-450.
- Bustin, R.M. (1997). Petroleum source rocks, organic maturation and thermal history of the Queen Charlotte Basin, British Columbia. *Bulletin of Canadian Petroleum Geology*, 45, 255-278.
- Butler, R. F., Gehrels, G. E., Baldwin, S. L., & Davidson, C. (2002). Paleomagnetism and geochronology of the Ecstall pluton in the Coast Mountains of British Columbia: Evidence for local deformation rather than large-scale transport. *Journal of Geophysical Research: Solid Earth*, 107, EPM-3.
- Cameron, B.E.B. and Tipper, H.W. (1985) Jurassic Stratigraphy of the Queen Charlotte Islands, British Columbia. Geological Survey of Canada. 45 p.
- Canil, D. and Morris, R. A. (2023) Continentalization of an intra-oceanic arc as exemplified by the Jurassic Bonanza arc of Vancouver Island, Canada. *GSA Bulletin* 2023; 136 (1-2), 880–892.
- Carter, E.S., Haggart, J.W., Enkin, R.J. and Monger, J.W.H. (2006) Radiolarian biogeography of the Pacific region indicates a mid-to high-latitude (> 30) position for the Insular superterrane since the late Early Jurassic. *Paleogeography of the North American Cordillera: evidence for and against large-scale displacements. Geological Association of Canada Special paper* 46, 109-132.
- Cathyl-Bickford, C.G. (1991): Coal geology and coalbed methane potential of Comox and Nanaimo coalfields; Rocky Mountain Association of Geologists, in *Coalbed Methane of Western North America*. 155-162.
- Cecil, M. R., Rusmore, M. E., Gehrels, G. E., Woodsworth, G. J., Stowell, H. H., Yokelson, I. N. (2018) Along-strike variation in the magmatic tempo of the Coast Mountains batholith, British Columbia, and implications for processes controlling episodicity in arcs. *Geochemistry, Geophysics, Geosystems*, 19, 4274–4289.
- Clapp, C.H. (1914) Geology of the Nanaimo Map-area. Geological Survey of Canada, *Memoir*, 56, 232 p.

- Clapp, C.H. and Cooke, H.C. (1917) Sooke and Duncan map areas, Vancouver Island. Geological Survey of Canada, Memoir, 96, 105 p.
- Copeland, P. (2020) On the use of geochronology of detrital grains in determining the time of deposition of clastic sedimentary strata. *Basin Research* 32, 1532-1546.
- Coutts, D.S., Matthews, W.A., and Hubbard, S.M. (2019). Assessment of widely used methods to derive depositional ages from detrital zircon populations. *Geoscience Frontiers*, 10, 1421-1435.
- Coutts, D.S., Matthews, W.A., Englert, R.G., Brooks, M.D., Boivin, M-P., and Hubbard, S.M. (2020) Along-strike variations in sediment provenance within the Nanaimo basin reveal mechanisms of forearc basin sediment influx events. *Lithosphere*, 12, 180-197.
- Cowan, D.S., Brandon, M.T., and Garver, J.L., (1997), Geologic tests of hypotheses for large coastwise displacements—A critique illustrated by the Baja British Columbia controversy: *American Journal of Science*, 297, 117–173.
- Crickmay, C. H. (1928) The stratigraphy of Parson Bay, British Columbia. University of California Geological Sciences Bulletin Paper No. 18, 51-70.
- Dalby, A., Patterson, R.T. and Haggart, J.W. (2009) Distribution of Albanian- Cenomanian foraminifera from the Queen Charlotte Islands, British Columbia, Canada: Constraints on the northward migration of Wrangellia Terrane. *The Journal of Foraminiferal Research*, 39, 231-245.
- Dorsey, C. (2019) Detrital Zircon Geochronology of the Queen Charlotte Group, Haida Gwaii, British Columbia. Masters Thesis, University of Calgary. 82 p.
- England, T. (1989) Late Cretaceous to Paleogene evolution of the Georgia Basin, Southwestern British Columbia. PhD Thesis, Memorial University of Newfoundland. 303 p.
- England, T., and Bustin, R. (1998) Architecture of the Georgia Basin southwestern British Columbia. *Bulletin of Canadian Petroleum Geology*, 46, 288-320.
- Englert, R.G., Hubbard, S.M., Coutts, D.S., and Matthews, W.A. (2018) Tectonically controlled initiation of contemporaneous deep-water channel systems along a Late Cretaceous continental margin, western British Columbia, Canada. *Sedimentology*, 65, 2404-2438.
- Englert, R. G., Hubbard, S. M., Matthews, W. A., D.S. Coutts, D. S. and Covault, J. A. (2020) The evolution of submarine slope-channel systems: Timing of incision, bypass, and aggradation in Late Cretaceous Nanaimo Group channel-system strata, British Columbia, Canada. *Geosphere* 16, 281–296.

- Enkin, R., Baker, J. and Mustard, P.S.. (2001). Paleomagnetism of the Upper Cretaceous Nanaimo Group, southwestern Canadian Cordillera. *Canadian Journal of Earth Sciences*, 38, 1403-1422.
- Galloway, J.M., McLachlan, S.M.S., Sproule, A., Dashtgard, S.E., Bringué, M. (2023) Palynological analyses of samples from the Comox Sub-Basin, Suquash SubBasin, and Lower Cretaceous of Northern Vancouver Island, British Columbia. Geological Survey of Canada, Open File 9071, 87 p.
- Garver, J.I., and Brandon, M.T. (1994) Fission-track ages of detrital zircons from Cretaceous strata, southern British Columbia: Implications for the Baja BC hypothesis. *Tectonics*, 13, 401-420.
- Gehrels, G., Rusmore, M., Woodsworth, G., Crawford, M., Andronicos, C., Hollister, L., Patchett, J., Ducea, M., Butler, R., Klepeis, K. and Davidson, C., (2009) U-Th-Pb geochronology of the Coast Mountains batholith in north-coastal British Columbia: Constraints on age and tectonic evolution. *Geological Society of America Bulletin*, 121 (9-10), 1341-1361.
- Getty, T. A. (1973) A revision of the generic classification of the family Echioceratidae (Cephalopoda, ammonoidea) (Lower Jurassic): Kansas University Paleontology Control Paper, 63, 1-32.
- Girrotto, K., Dashtgard, S.E., Huang, C. MacEachern, J. A., Gibson, H. D., Cathyl-Huhn, G. (2024) Tectono-stratigraphic model for the early evolution of the Late Cretaceous Nanaimo Group, Georgia Basin, Canada. *Basin Research*. 36, 1-31.
- Haggart, J.W. (1987) On the age of the Queen Charlotte Group of British Columbia. *Canadian Journal of Earth Sciences*, 24, 2470-2476.
- Haggart, J.W. (1991) A new assessment of the age of the basal Nanaimo Group, Gulf Islands, British Columbia. Geological Survey of Canada, Current Research Paper (part E), 91, 1E-77.
- Haggart, J.W. and Smith, P.L. (1991) Biostratigraphy of the Upper Cretaceous Nanaimo Group, Gulf Islands, British Columbia. A field guide to the paleontology of southwestern Canada. University of British Columbia, Vancouver, 223-256. Haggart, J.W. and Carter, E.S. (1993) Biogeography of latest Jurassic and Cretaceous mollusc and radiolarian faunas of the Insular belt, British Columbia, suggests minimal northward displacement [abstract]: *Geological Society of America, Abstracts with Programs*, 26, 148 p.
- Haggart, J.W. (1994) Turonian (Upper Cretaceous) strata and biochronology of southern Gulf Islands, British Columbia. *Current research*, 42, 159-164.

- Haggart, J. W. Jakobs, G, K, and Orchard, M. (1995) Mesozoic stratigraphy and paleontology of Haida Gwaii (Queen Charlotte Islands). Geological Association of Canada, Fieldtrip Guidebook. B4. 1-123.
- Haggart, J.W., Ward, P.D., and Orr, W. (2005) Turonian (Upper Cretaceous) lithostratigraphy and biochronology, southern Gulf Islands, British Columbia, and northern San Juan Islands, Washington State. *Canadian Journal of Earth Sciences*, 42, 2001-2020.
- Haggart, J.W. (2009), Molluscan Biostratigraphy and Paleomagnetism of Campanian Strata, Queen Charlotte Islands, British Columbia: implications for Pacific coast North America biochronology. *Cretaceous Research*, 30, 939-951.
- Haggart, J.W., and Graham, R. (2018) The crinoid Marsupites in the Upper Cretaceous Nanaimo Group, British Columbia: Resolution of the Santonian–Campanian boundary in the north Pacific Province: *Cretaceous Research*, 87, 277-295.
- Hamblin, A. (2012) Upper Cretaceous Nanaimo Group of Vancouver Island as a potential bedrock aquifer zone: summary of previous literature and concepts. Geological Survey of Canada, Open File, 7265, 20 p.
- Hannigan, P.K., Dietrich, J.R., Lee, P.J., and Osadet, K.G. (2001) Petroleum resource potential of sedimentary basins on the Pacific margins of Canada. *Bulletin of the Geological Survey of Canada* No. 564, 1-62.
- Housen, B.A., and Beck, M.E. (1999) Testing Terrane Transport: An Inclusive Approach to the “Baja-BC” Controversy, *Geology*, 27, 1143-1146.
- Huang, C., Dashtgard, S., Kent, B., Gibson, D., and Matthews, W. (2019) Resolving the architecture and early evolution of a forearc basin (Georgia Basin, Canada) using detrital zircon. *Scientific Reports*, 9, 15360.
- Huang, C., Girrotto, K.,B and Dashtgard, S.E. (2022) Synthesis of chronostratigraphic data and methods in Georgia Basin, Canada, with implications for convergentmargin basin chronology. *Earth-Science Reviews*, 231, 1-25.
- Irving, E., Woodsworth, G.J., Wynne, P.J., and Morrison, A. (1995) Paleomagnetic evidence for displacement from the south of the Coast Plutonic Complex, British Columbia. *Canadian Journal of Earth Sciences*, 22, 584-598.
- Jeletzky, J., and Muller, J. (1970) Geology of the Upper Cretaceous Nanaimo Group, Vancouver Island and Gulf Islands, British Columbia. Department of Energy, Mines and Resources, Ottawa, 77. 77 p.
- Jeletzky, J.A. (1970) Cretaceous macrofaunas. In: Bamber, E.W. (1987) *Biochronology: Standard of Phanerozoic Time*. Geological Survey of Canada, Economic Geology Report No. 1, Part B, 649–662.

- Jeletzky, J.A., (1971) Marine Cretaceous biotic provinces and paleogeography of western and Arctic Canada: Geological Survey of Canada Paper 70, 92 p.
- Jeletzky, H.A. (1976) Mesozoic and Tertiary rocks of Quatsino Sound, Vancouver Island, British Columbia. Geological Survey of Canada Bulletin, 242, 318 p.
- Johnstone, P., Mustard, P., and MacEachern, J. (2006) The basal unconformity of the Nanaimo Group, southwestern British Columbia: a Late Cretaceous storm-swept rocky shoreline. Canadian Journal of Earth Sciences, 43, 1165-1181.
- Jones, M.T., Dashtgard, S.E., and MacEachern, J.A. (2018) A conceptual model for the preservation of thick, transgressive shoreline successions: examples from the forearc Nanaimo Basin, British Columbia, Canada. Journal of Sedimentary Research, 88, 811-826.
- Katnick, D.C., and Mustard, P.S., 2003. Geology of Denman and Hornby islands, British Columbia: implications for Nanaimo Basin evolution and formal definition of the Geoffrey and Spray formations, Upper Cretaceous Nanaimo Group. Canadian Journal of Earth Sciences 40, 375-392.
- Kent, B.A.P., Dashtgard, S.E., Huang, C., MacEachern, J.A., Gibson H.D., and Cathyl-Huhn, G. (2018) Early Evolution of a forearc basin: Georgia Basin, Vancouver Island, Canada. Basin Research, 32, 163-185.
- Kenyon, C. and Bickford, C.G. (1989) Vitrinite Reflectance Study of Nanaimo Group Coals of Vancouver Island (92F); B.C. Ministry of Energy, Mines and Petroleum Resources; Geological Fieldwork, Paper 1989.1, 543-552.
- Lewis, P.D., Haggart, J.W., Anderson, R.G., Hickson, C.J., Thompson, R.I., Dietrich, J.R., and Rohr, K.M.M. (1991) Triassic to Neogene geologic evolution of the Queen Charlotte region. Canadian Journal of Earth Sciences, 28, 854-869.
- Lowe, C., Best, M.E., Bobrowsky, P.T. and Seemann, D.A. (2002) Integrated geophysics for mineral exploration in drift-covered volcanic terrains: examples from northern Vancouver Island. Geophysical Prospecting, 46, 201-225.
- Ludvigsen, R., and Beard, G. (1997) West Coast Fossils: A Guide to the Ancient Life of Vancouver Island, 2nd Edition, Madeira Park, BC, Harbour Publishing, 216 p.
- Mahoney, J.B., Mustard, P.S., Haggart, J.W., Friedman, R.M., Fanning, C.M., and McNicoll, V.J. (1999) Archean zircons in Cretaceous strata of the western Canadian Cordillera: The "Baja B.C." hypothesis fails a "crucial test": Geology, 27, 195-198.
- Matthews, W.A., Guest, B., Coutts, D., Bain, H., and Hubbard, S. (2017) Detrital zircons from the Nanaimo basin, Vancouver Island, British Columbia: An independent test of Late Cretaceous to Cenozoic northward translation. Tectonics, 36, 854–876.

- McLachlin, S.M.S., Pospelova, V., and Hebda, R.J. (2018) Dinoflagellate cysts from the upper Campanian (Upper Cretaceous) sedimentary rocks of Hornby Island, British Columbia, Canada, with implications for Nanaimo Group biostratigraphy and paleo-environmental reconstructions. *Marine Micropaleontology*, 145, 1-20.
- McLachlan, S.M.S., Pospelova, V. , and Hebda, R.J. (2019) Areoligeracean dinoflagellate cysts from the upper Campanian (Upper Cretaceous) of Hornby Island, British Columbia, Canada. *Palynology*, 43, 669-689.
- McLachlan, S. M. S., and Pospelova, V. (2021) Dinoflagellate cyst-based paleoenvironmental reconstructions and phytoplankton paleoecology across the Cretaceous–Paleogene (K/Pg) boundary interval, Vancouver Island, British Columbia, Canada, *Cretaceous Research*, 126, 104878.
- McLearn, F.H. (1972) Ammonoids of the Lower Cretaceous Sandstone member of the Haida Formation, Skidegate Inlet, Queen Charlotte Islands, western British Columbia. *Geological Survey of Canada Bulletin No. 188*, 78 p.
- McGugan, A. (1962) Upper Cretaceous foraminiferal zones, Vancouver Island, British Columbia, Canada. *Bulletin of Canadian Petroleum Geology*, 10, 585-592.
- McGugan, A. (1979) Biostratigraphy and paleoecology of Upper Cretaceous (Campanian and Maestrichtian) foraminifera from the Upper Lambert, Northumberland, and Spray Formations, Gulf Islands, British Columbia, Canada. *Canadian Journal of Earth Sciences*, 16, 2263-2274.
- McGugan, A. (1981) Late Cretaceous (Campanian) foraminiferal faunas, Charter et al. Saturna No. 1, Gulf Islands, British Columbia. *Bulletin of Canadian Petroleum Geology*, 29, 110-117.
- McGugan, A. (1982) Upper Cretaceous (Campanian and Maestrichtian) foraminifera from the upper Lambert and Northumberland formations, Gulf Islands, British Columbia, Canada. *Micropaleontology*, 28, 399-430.
- Monger, J.W.H. and Ross, C.A. (1971). Distribution of fusulinaceans in the western Canadian Cordillera. *Canadian Journal of Earth Sciences*. 8. 259-278.
- Monger, J.W.H., Price, R.A., and Tempelman-Kluit, D.J. (1982) Tectonic accretion and the origin of the two major metamorphic and plutonic belts in the Canadian Cordillera. *Geology*, 10, 70–75.
- Monger, J. and Price, R. (2002) The Canadian Cordillera: Geology and Tectonic Evolution. *CSEG Recorder*. 17. 17-36.
- Mustard, P.S., (1994) The Upper Cretaceous Nanaimo Group, Georgia Basin, in Monger, J.W.H., ed., *Geology and Geological Hazards of the Vancouver Region, Southwestern British Columbia*, Geological survey of Canada Bulletin, 481, 2795.

- Muller, J. and Jeletzky, J. A. (1970) Geology of the Upper Cretaceous Nanaimo Group, Vancouver and Gulf Islands, British Columbia. Geological Survey of Canada Paper 69 (25), 77 p.
- Muller, J.E. and Rahmani, R.A. (1970): Upper Triassic sediments of northern Vancouver Island. Geological Survey of Canada, Paper 70-1B, 11–18.
- Nixon, G.T., Hammack, V. M., Koyanagi, G. J., Payie, A., Pantelejev, N. W. D., Massey, J. V., Hamilton, B.C. (1993) Preliminary geology of The Quatsino - Port McNeill map areas, northern Vancouver Island (92U12,LI). BCGS Geological Fieldwork 1993. 63-85.
- Nixon, G.T., and Orr, A. (2010) Recent revisions to the Early Mesozoic stratigraphy of northern Vancouver Island (NTS 102I; 092L) and metallogenic implications, British Columbia. Geologic Fieldwork, 1, 163-178.
- Nixon, G.T., Hammack, J.L., Hamilton, J.V., Jennings, H., Larocque, J.P., Orr, A.J., Friedman, R.M., Archibald, D.A., Creaser, R.A., Orchard, M.J., Haggart, J.W., Tipper, H.W., Tozer, E.T., Cordey, F., and McRoberts, C.A. (2011) Geology, geochronology, lithogeochemistry, and metamorphism of the Mahatta Creek area, northern Vancouver Island (092L/5). British Columbia Ministry of Energy and Mines, British Columbia Geological Survey Geoscience Map 2011-3, 1:50,000 scale.
- Nixon, G., Hammack, J. L., and Konyanagi, V.M. (2011) Geology, geochronology, lithogeochemistry, and metamorphism of the Holberg-Winter Harbour area, North Vancouver Island. British Columbia Geological Survey. Map 02 1:50000 scale.
- Nordsvan A.R., Kirscher U., Kirkland C.L., Barham M., and Brennan D.T. (2020) Resampling (detrital) zircon age distributions for accurate multidimensional scaling solutions, *Earth-Science Reviews*, 204, 103-149.
- Pacht, J.A., (1980). Sedimentology and petrology of the Late Cretaceous Nanaimo Group in the Nanaimo Basin, Washington and British Columbia: Implications for Late Cretaceous tectonics. Ph.D. thesis. Ohio State University. 206 p.
- Reineck, H.-E. (1963) Reineck H-E (1963) Sedimentary structure in the southern North Sea. *Abh Senckenberg Naturforsch Gesellschaft* 505, 1–138.
- Sharman, G.R. and Malkowski, M.A. (2023) Modeling apparent Pb loss in zircon U-Pb geochronology. *Geochronology Discussions* 2023, 1-25.
- Shellnutt, J.G., and Dostal, J. (2019) Haida Gwaii (British Columbia, Canada): a Phanerozoic analogue of a subduction-unrelated Archean greenstone belt. *Sci. Rep.*, 9, 3251.
- Sliter, W. V. (1973) Upper Cretaceous foraminifers from the Vancouver Island area, British Columbia, Canada: *Journal of Foraminiferal Research*, 3, 167-186.



- Stacey, R.L. (1975) The Structure of the Queen Charlotte Basin, Canada's Continental Margins and offshore Petroleum Exploration, Memoir 4, 723-741.
- Sutherland-Brown, A. (1968) Geology of the Queen Charlotte Islands: B.C. Ministry of Mines and Petroleum Resources, Bulletin no. 5, 226 p.
- Taylor, A.M., and Goldring, R. (1993), Descriptions and analysis of bioturbation and ichnofabric: *Journal of the Geological Society (London)*, 150. 141-148.
- Tozer, E. T. (1967) A standard for Triassic time. *Geological Survey of Canada, Bulletin* 156, 103 p.
- Tozer, E. T. (1994) Canadian Triassic Ammonoid Faunas. *Geological Survey of Canada, Bulletin* 467. 669 p.
- Traverse, A. (2007). Differential sorting of palynomorphs into sediments: Palynofacies, palynodebris, discordant palynomorphs. *Paleopalynology. Topics in Geobiology*, 28, 543-579.
- Usher, J.L. (1952) Ammonite faunas of the Upper Cretaceous rocks of Vancouver Island, British Columbia: E. Cloutier, Queen's Printer, Ottawa 182 p.
- Vellutini, D. and Bustin, R.M. (1990) Organic maturation of Mesozoic and Tertiary strata, Queen Charlotte Islands, British Columbia. *Bulletin of Canadian Petroleum Geology*, 38, 452-474.
- Vellutini, D., Bustin, R.M., and Goodarzi, F. (1990) Source rock potential of Mesozoic and Tertiary strata, Queen Charlotte Islands, British Columbia. *Bulletin of Canadian Petroleum Geology*, 38, 440-451.
- Vermeesch, P. (2004) How many grains are needed for a provenance study? *Earth and Planetary Science Letters*, 224, 441-451.
- Vermeesch, P. (2013) Multi-sample comparison of detrital age distributions. *Chemical Geology*, 341, 140-146.
- Vermeesch, P. (2021) Maximum depositional age estimation revisited. *Geoscience Frontiers*, 12 (2), 843-850.
- Ward, P.D. (1987) Revisions to the stratigraphy and biochronology of the Upper Cretaceous Nanaimo Group, British Columbia and Washington State. *Canadian Journal of Earth Sciences*, 15, 405-423.
- Ward, P.D., Haggart, J.W., Mitchell, R., Kirschvink, J.L., and Tobin, T. (2012) Integration of macrofossil biostratigraphy and magnetostratigraphy for the Pacific Coast Upper Cretaceous (Campanian-Maastrichtian) of North America and implications for correlation with the Western Interior and Tethys. *Geological Society of America Bulletin*, 124, 957-974.

Wheeler, J.O., Hoffman, P.F., Card, K.D., Davidson, A., Sanford, B.V., Okulitch, A.V., Roest, W.R. (Compilers), 1996. Geological Map of Canada. Geological Survey of Canada Map 1860A, 1:5 000 000 scale.

Williams, T.B. (1924) The Comox Coal Basin. Unpublished Ph. D. Thesis, University of Wisconsin. 143 p.

Wyld, S.J., Umhoefer, P.J. and Wright, J.E., (2006) Reconstructing northern Cordilleran terranes along known Cretaceous and Cenozoic strike-slip faults: Implications for the Baja British Columbia hypothesis and other models, in Haggart, J.W., Enkin, R.J. and Monger, J.W.H., eds., Paleogeography of the North American Cordillera: Evidence For and Against Large-Scale Displacements: Geological Association of Canada, Special Paper 46, 277-298.

# Appendix A.

## Logged Outcrop Sections

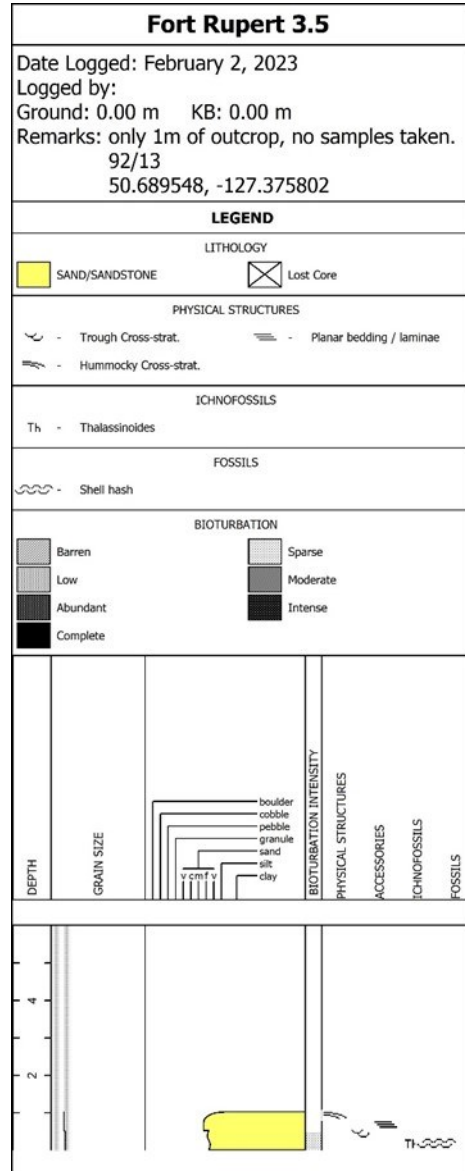


Figure A. 1. Logged section FRB-3.5. Section location details are located in Table 2.3 Outcrop section produced using Applecore.

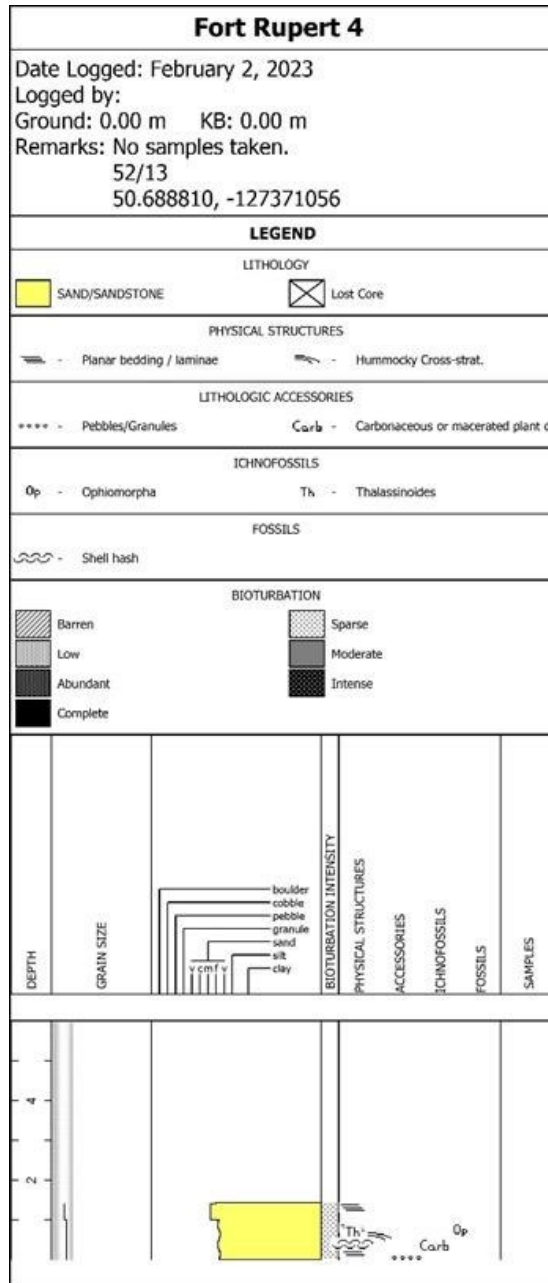
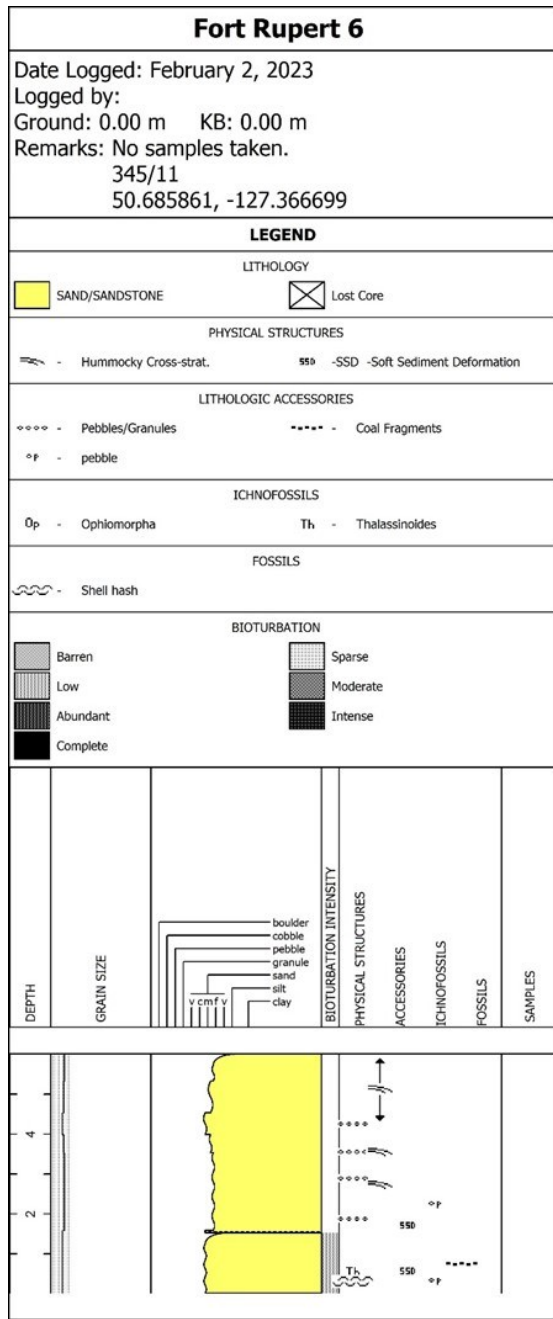
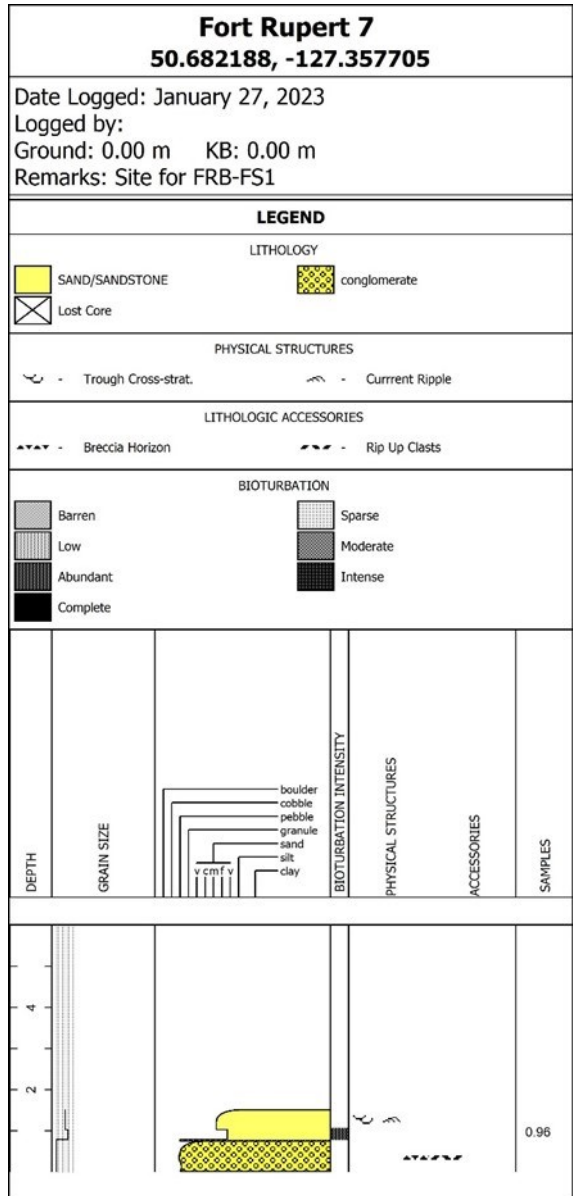


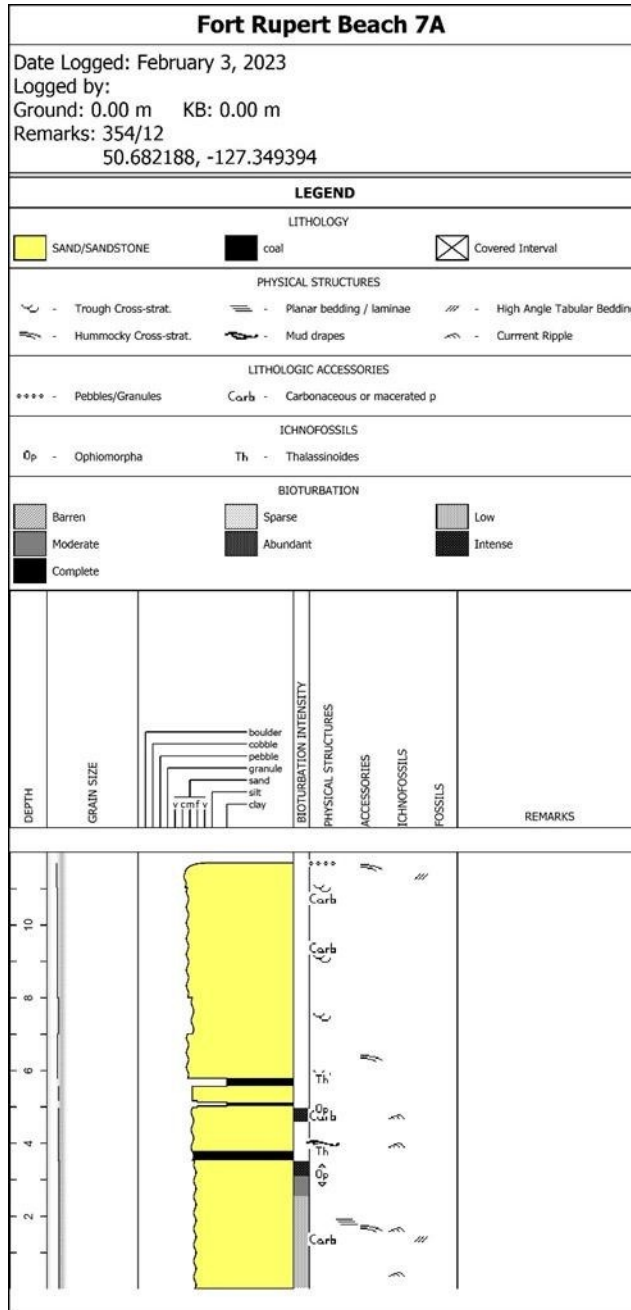
Figure A. 2. Logged section FRB-4. Section location details are located in Table 2.3. Section produced using Applecore.



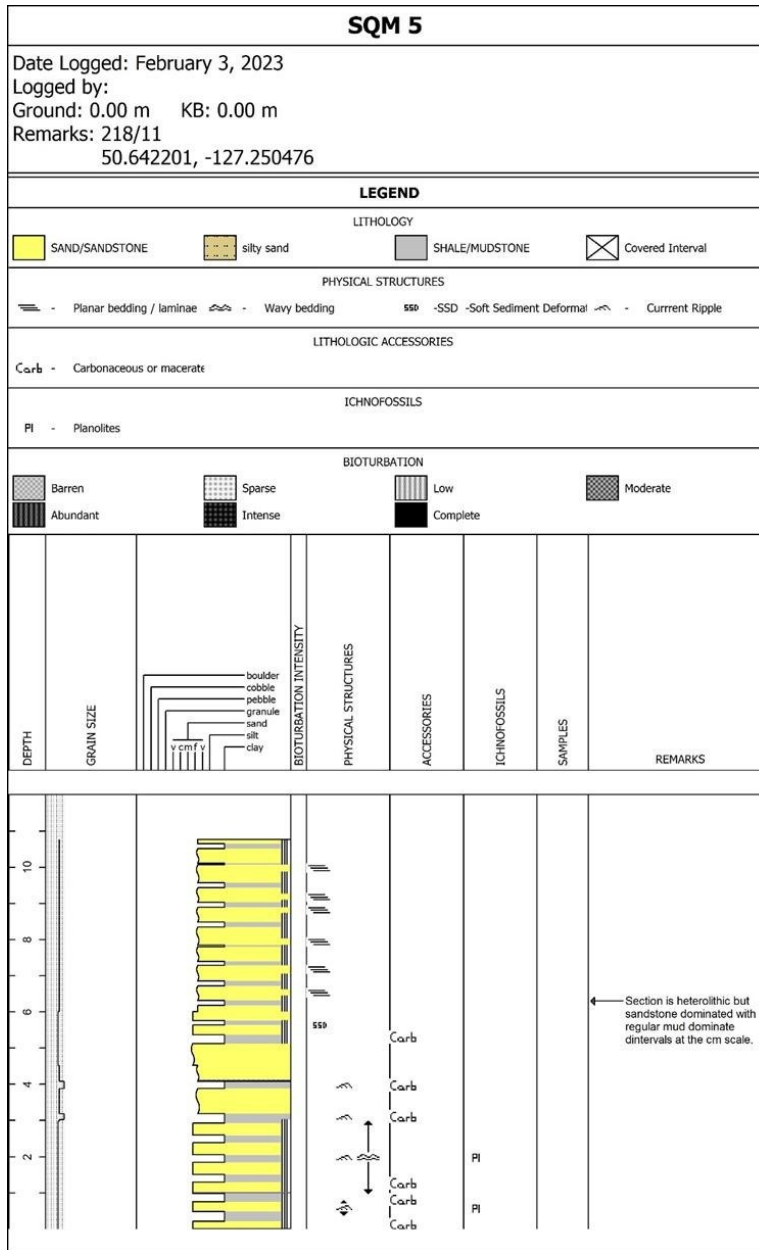
**Figure A. 3. Logged section FRB-6. Location details for this section are located in Table 2.3. Section produced using Applecore.**



**Figure A. 4. Logged section FRB-7. Section location details are located in Table 2.3. Section produced using Applecore.**

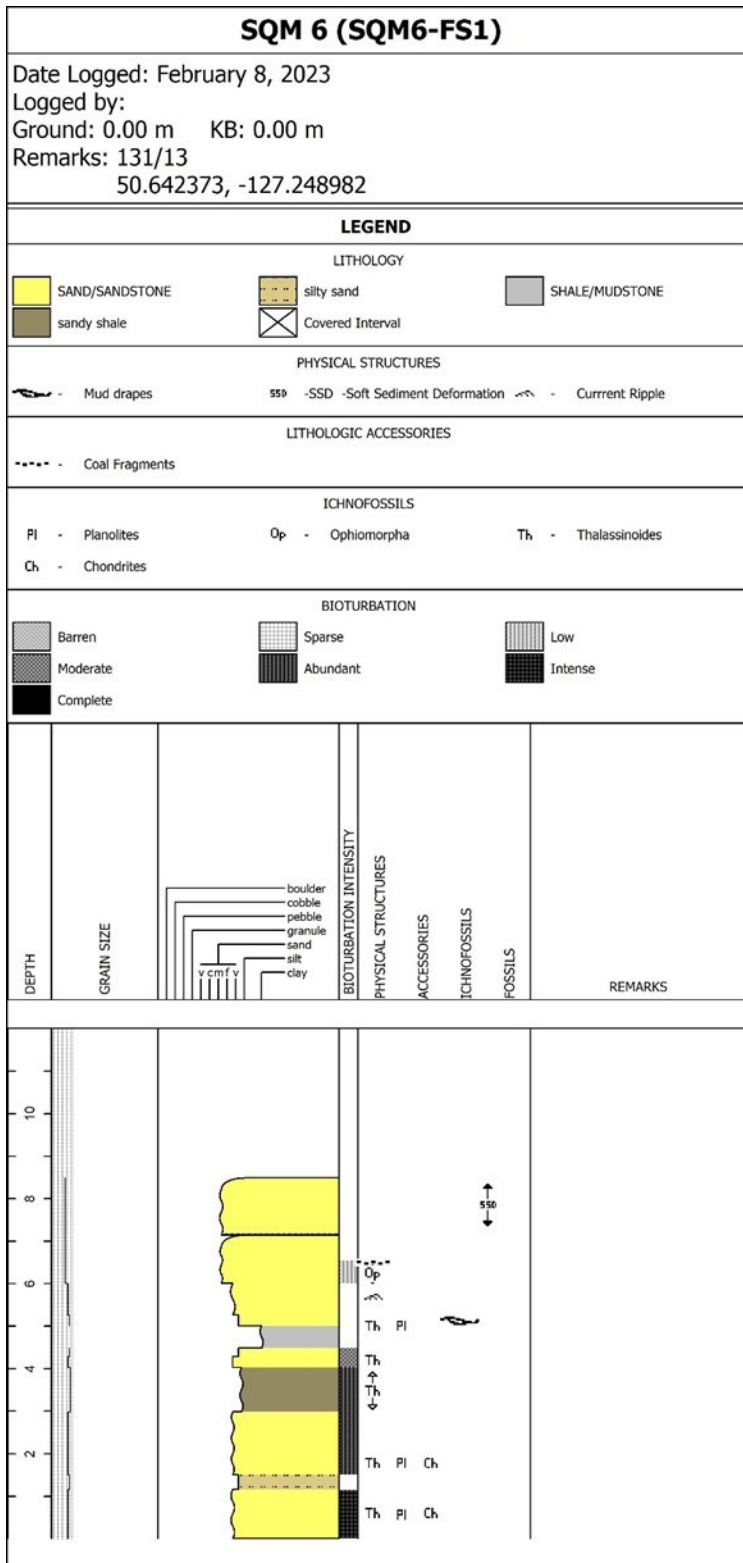


**Figure A. 5. Logged section FRB-7A. Section location details are located in Table 2.3. Section produced using Applecore.**



**Figure A. 6. Logged section SQM-5. Section location details are located in table 2.4. Section produced using Applecore.**





**Figure A. 7. Logged section SQM-6. Section location details are located in Table 2.4. Section produced using Applecore.**

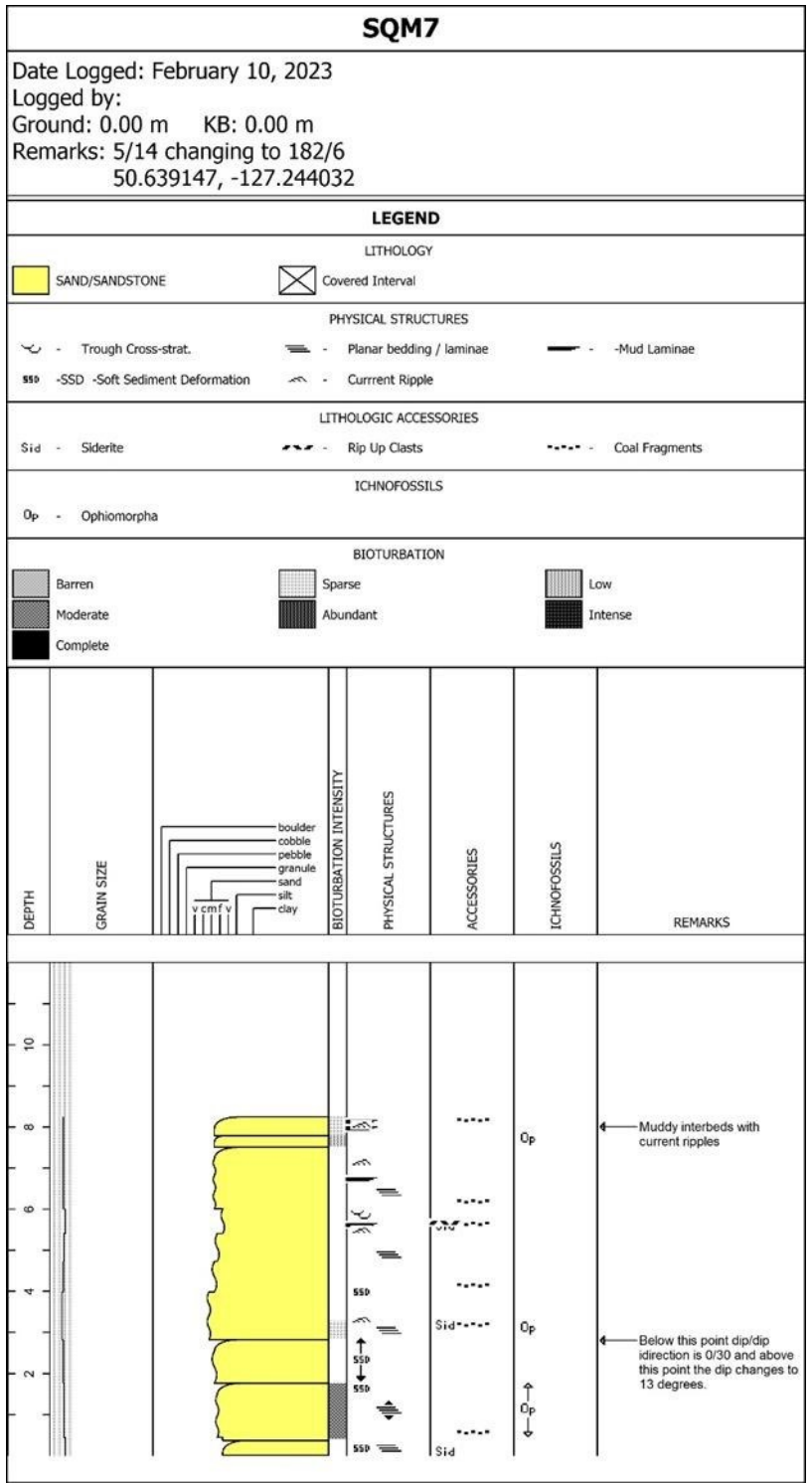


Figure A. 8. Logged section SQM-7. Section location details are located in Table 2.4. Section produced using Applecore.